TEST TECHNOLOGY TECHNICAL COUNCIL (TTTC) OF THE IEEE COMPUTER SOCIETY
MINISTRY OF EDUCATION AND SCIENCE OF UKRAINE

KHARKOV NATIONAL UNIVERSITY
OF RADIOELECTRONICS

ISSN 1563-0064

RADIOELECTRONICS & INFORMATICS

Scientific and Technical Journal **Founded in 1997**

№ 1 (68) 2015 **Published 4 times a year**

Certificate of the State Registration КВ № 12097-968 ПР 14.12.2006

Address of journal edition: Ukraine, 61166, Kharkiv, Lenin avenu, 14, KNURE, Design Automation Department, room 321, ph. (0572) 70-21-326, d-r Hahanov V.I.
E-mail: ri@kture.kharkov.ua; hahanov@kture.kharkov.ua,
http://www.ewdtest.com/ri/

CONTENTS

Optimal Placement Problem in Printing Production

I. Grebennik, D. Grytsay and S. Shekhovtsov

***Abstract* — In the article we deal with the optimal placement problem in manufacturing printing products. A special set of two-dimensional geometric objects bounded by circular arcs and line segments are introduced as mathematical models of real-life printing objects. We derive phi-functions, as well as normalized and pseudo-normalized phi-functions to describe the relations (non-overlapping, containment and distance constraints) between the geometric objects. A mathematical model of the optimal placement of printing objects is constructed and a solution strategy is proposed.**

***Index Terms* – cutting, phi-functions, printing objects, mathematical model, solution strategy**

I. Introduction

Book-and-magazine editions are the main product type printing houses deal with. Although printing houses print not only books but also handouts, business cards, beer coasters, stickers, promo materials etc., the shape of those printing products types usually differs from the rectangle and generally their printrun is small. A variety of materials (cardboard of various types and density, coated paper of various density, different types of plastic and so on) is used for printing those printing products. Depending on the shape, the type of material, the printrun and other aspects of each printing product, the printing house chooses one of the two following variants of work: a) it can pick the cutting ticket (object layout on the template sheet) out of the existing set of object layouts or b) it can approximate the printing objects by rectangles and place them on a layout template sheet as ordinary rectangles. Hereinafter, we shall refer to parts of printing products which are placed on the printing sheet as printing objects.

Printing objects are always printed using the standard material sheet formats. Depending on the material type and the product binding it is possible to use different placement rules to place the objects on the printing sheet. For example, the book which consists of several printing objects collected from separate pages or which uses the spring as the binding can be printed without keeping to the folding rules.

The current problem in its statement relates to the cutting and packing problems [1]. The problem of placing such printing objects is relevant because printing objects are placed into the rectangular area (printing sheet) using the rectangular placing methods but the objects do not have a rectangular shape in most cases. The more the shape of the printing object differs from the rectangle the bigger blank spaces are and correspondently the more material is wasted. The next problem is to fill the remaining blank spaces of the existing layout using other printing objects (in other words it is necessary to place other printing objects into blank spaces of the existing layout sheet) to reduce material waste.

If printing objects are of the same material type, density, printrun, the printing house could place it in one combined printing sheet. It makes it possible to print products using fewer plates for printing, having cheaper printing cost and saving energy. It increases profit of the printing house and reduces environmental pollution due to saving material.

First, generally the printing objects mentioned above have the shape of a rectangular with “rounded corners”; second, a great part of the objects having complicated shapes can be approximated by simple objects. Figure 1 shows some examples of printing objects.

Fig.1. Shapes of printing objects and their approximation: printing objects (a); shape approximation (b)

It is obvious that the shape approximation by a “rectangle” with a “rounded corner” shown in Figure 1 is better than approximation by a regular rectangle. If we

Manuscript received January 11, 2015.

I. Grebennik is with the Kharkov National University of Radioelectronics, Lenin Ave, 14, Kharkov, 61166, Ukraine (corresponding author, e-mail: grebennik@kture.kharkov.ua).

D. Grytsay is with the Kharkov National University of Radioelectronics, Lenin Ave, 14, Kharkov, 61166, Ukraine.

S. Shekhovtsov is with the Kharkov National University of Internal Affairs

place these shapes instead of the rectangle we save material.

The problem is that prepress centers place the printing objects as ordinary rectangles even when the printing objects do not have a rectangular shape.

Lets us consider only those types of printing objects which have the shapes presented in Figure 2 (e.g. business cards, promotional handouts, stickers, brochures etc.).

The article [2] considers a multi-stock cutting problem of a collection of arbitrary-shaped two-dimensional objects in order to maximize usable space or, in other words, minimize waste of manufacturing material. The frontiers of the objects are formed by circular arcs and line segments.

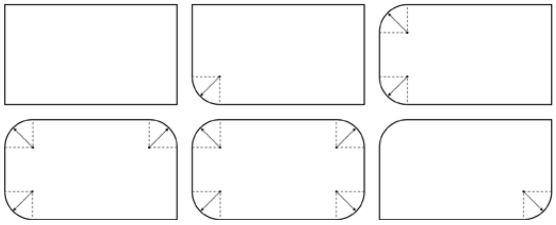

Fig. 2. Shapes used in printing

Today the printing products which have the proposed shapes are printed in small printruns and using the standard layout template sets. Typically each printing sheet collects the same type of the printing objects several times in the form of the array. After that if it is necessary to print several types of the printing objects in one time (using the same printrun and the same material for each printing object), different standard layout templates with array form should be used. It is useful if the printing objects have rectangular shapes. If it is necessary to round the corners for these objects then it has to be done in the end of the production cycle.

Generally when the curving radii are small enough it is useful to approximate these shapes by rectangles. At that the problem reduces to the standard problem of placing rectangles into a rectangular area [3-6]. In some cases if the rounded radii are compared to the edges length of the objects, there is a need for material saving (and what is the most important it is possible). Figure 3 shows the situation when the rectangular approximation can not be used.

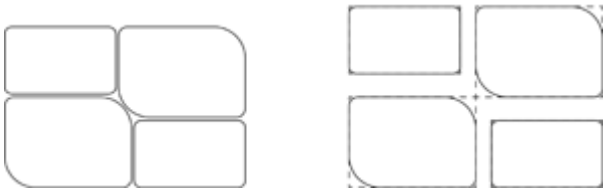

(a) (b)

Fig. 3. Placement of printing objects: a) without approximations; b) with rectangular approximations

Figure 3 shows that the alternate version a) is more compact, therefore it is more material-saving. The placement problem for the proposed printing objects can be formulated as follows: 1) place all printing objects on the printing sheets of the standard format; 2) place as many objects as possible on printing sheets of a standard format; 3) place all printing objects using as few printing sheets of a standard format as possible; 4) determine the optimal printing sheet format to place the given printing objects set.

All mentioned alternatives can be formulated using sheet packing factor which also allows to economize by using fewer plates, saving the material, reducing the final product cost. Let us consider the shape of the objects in a more precise way.

As the mathematical models for the printing objects we consider a collection of phi-objects bounded by circular arcs and line segments [7]. We note the collection by $\Re$. The phi-function technique [7, 8] is used to describe the relations (non-intersection, containment, minimum allowable distances) between the geometric objects in the analytical form.

The aim of the paper is to construct a mathematical model and develop the solution strategy for the problem of determining the optimal printing sheet format to place the given printing objects.

II. Placement Objects

Let us consider a set of basic objects $\Im = \{C,\ R,\ D,\ K\}$, which are described in details in [7]. Figure 4 shows the basic objects.

Here C: is a circle of radius r, i.e. $m_C = (r)$; R: is the rectangle of a and half-height b, i.e. $m_R = (a,\ b)$; D: is a circular segment of radius r and height h, i.e. its metric characteristics is given by $(r,\ h)$, $D = T \cap C$, $O \notin D$, where T is a triangle which is constructed using two tangents and the chord that is drawn through the tangency points of the circle C; K: is a convex polygon with the vertices $v_1, \ldots, v_m$ which are given anticlockwise with the respect to the eigen coordinate system, i.e. $m_K = (v_1,\ \ldots,\ v_m)$.

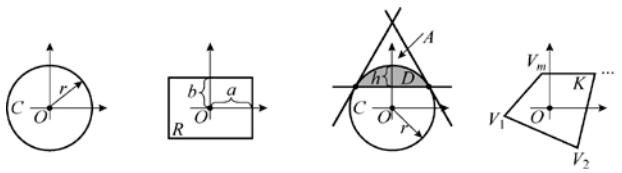

Fig.. 4. Basic objects $C,\ R,\ D,\ K$

Let us make the objects shape classification which comes to the phi-function technique. These shapes are composed phi-objects (hereinafter referred to as "the objects").

1) If the rectangle corner curvings are equal then it is possible to construct the object using rectangle R determined by $(a,\ b)$ and circle C determined by radius r (Fig. 5,a). So the metric characteristics of type

a object $m_a = (a, b, r)$. Therefore the first object type can be defined as

$$A_a = R(0) \oplus C(0), \quad (1)$$

where $\oplus$ is the Minkovsky sum symbol.

2) If the rectangle corner curvings are different and all radii are less then the half-length of the rectangle after that it is possible to construct the object using polygon K with vertices v_i, $i = 1, \ldots, 8$, and four circles C_1, C_2, C_3, C_4 which are determined by different radii r_1, r_2, r_3, r_4 where the longest radius length is shorter than the half-height and half-width of the rectangle that circumscribes about the object A_b ($r_i \le \min\{a, b\}$, see Fig. 5,b). The metric characteristics of type b object are $m_b = (v_1, \ldots, v_8, r_i, \ldots, r_4)$. Therefore the second object type can be defined as

$$A_b = K \cup \left(\bigcup_{i=1}^{4} C_i \right). \quad (2)$$

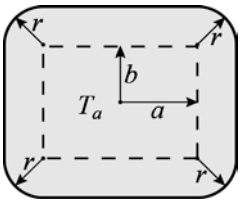

(a)

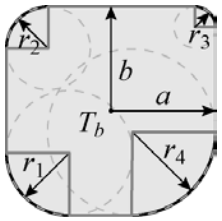

(b)

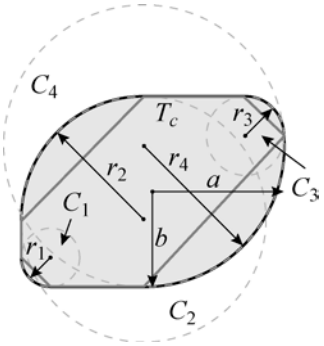

(c)

Fig.5. Types of object shapes from collection $\mathfrak{R}$: the first type object (a) ; the second type object (b) ; the third type object (c)

3) If each corner of the rectangle has the arbitrary curving radius, it is possible to construct the objects as the union of the polygon K with the vertices v_i, $i = 1, \ldots, 8$, and four circular segments D_1, D_2, D_3, D_4, which are constructed using the tangents, the chord, the radii with unrestricted length whose the metric characteristics are (r_j, h_j), $j = 1, \ldots, 4$ (see Fig. 5,c). The metric characteristics of type c object are $m_c = (v_1, \ldots, v_8, (r_1, h_1), \ldots, (r_4, h_4))$. Therefore the third object type can be defined as

$$A_c = K \cup (\bigcup_{i=1}^{4} D_i). \quad (3)$$

Let us note that the rectangle is degenerate case of object of type a, the type a object can be formulated like object of type b and all of the recommended objects can be formulated like a type c object. Depending on the problem requirements you can us all of this types without fail.

We provide a type c object that shows possible shapes depending on the metric characteristics.

The possible shapers of the type c object are given in the Figure 6.

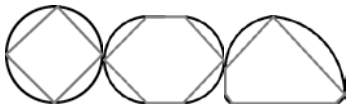

Fig.. 6. Possible shapers of the type c object

It has been proved in [7] that any phi-object bounded by circular arcs and line segments can be represented as a union of basic objects of four types.

Since A is a particular case which is described in [7] the following is true:

$$A = (A_1 \cup A_2 \cup \ldots \cup A_k),$$

where $A_i \in \Im$.

Let translation vectors $u_A = (x_A, y_A)$, $u_B = (x_B, y_B)$ be placement parameters of objects A and B respectively. We denote the vector of variables of both objects A and B by $u_{AB} = (x_A, y_A, x_B, y_B)$.

III. Placement Area

Taking into account the specific character of printing industry we note that the placement area is a printing sheet (or several printing sheets) which is always a rectangle $\Omega = R$. We set the pole $u_\Omega = (0, 0)$ of R in the bottom left corner (see Fig. 7) .

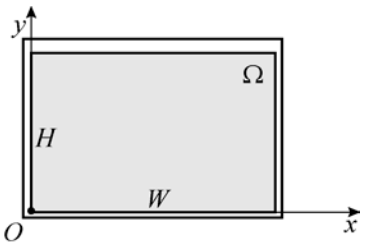

Fig.. 7. The placement area

According to the problem formulation defined in Section 1 each component of vector $P = (h,\ w)$, may be variable, where $h,\ w$ are the height and the width of R.

Now we introduce the possible additional constraints on $h,\ w$ for placement area R:

$$h_{\min} \le h \le h_{\max},\ w = \text{const}, \quad (3)$$

$$h = \text{const},\ w_{\min} \le w \le w_{\max}, \quad (4)$$

$$h = \text{const},\quad w = \text{const}, \quad (5)$$

$$h_{\min} \le h \le h_{\max},\ w_{\min} \le w \le w_{\max}, \quad (6)$$

where n is the number of the allowable printing sheet formats, $h_{\min}$, $h_{\max}$, $w_{\min}$, $w_{\max}$ are the minimal and maximal allowable values of $h,\ w$ respectively. For example, if we need to find the optimal printing sheet format to place the printing objects, the variables of the problem are h and w.

IV. Mathematical Modeling of The Relations of Printing Objects

The printing objects placement has its specific. It is clear that business cards, stickers, the handouts etc. can not be placed overlapping each other. It is also impossible to place the objects in such a way that any of the placed objects partially belong to the placement area (printing sheet) so any of the objects can not intersect the placement area boundary, all of the objects must be contained in the placement area completely. Sometimes, if it is necessary to place some specific kinds of printing objects, it is necessary to keep the minimal distance between the objects or between the frontier of placement area and the objects. For example, if we need to place stickers, the minimal allowed distance between the objects (depending on the equipment) can be 3 mm, which is due to engineering constrains of the knifes.

Taking into account all these object placement features the considered constraints can be formulated as follows.

1) The non-overlapping constraint, i.e. the objects do not overlap each other

$$\text{int}\, A \cap \text{int}\, B = \varnothing. \quad (7)$$

2) The containment constraint, i.e. each printing object has to be arranged within the placement area

$$A \subset \Omega \Leftrightarrow \Omega^* \cap A = \varnothing, \quad (8)$$

where $\Omega^* = R^2 \setminus \text{int}\,\Omega$.

3) The minimal allowed distances, i.e. the distance between the objects has to be greater than or equal to the minimal allowable distance:

$$\text{dist}(A,\ B) \ge \rho^-_{AB},\quad \text{dist}(\Omega^*,\ A) \ge \rho^-_{A}, \quad (9)$$

where $\text{dist}\,(A,\ B) = \min\limits_{a \in A,\ b \in B} \rho\,(a,\ b)$ is the Euclidian distance between objects A and B, $\rho(a,b)$ – distance between two points $a \in A$ and $b \in B$; $\text{dist}(\Omega^*,\ A)$ is the Euclidian distance between object A and object Ω^*.

We apply the Stoyan phi-function technique [9, 10] in order to formalize constraints (8)-(10). As is known [11] within the field of Packing and Cutting the technique is the most powerful tool of mathematical modeling of relations between arbitrary shaped geometric objects in an analytical form. It should be noted that the algorithm of the constructing the No-Fit Polygon for the objects bounded by circular arcs proposed in [12] can be used only for heuristics solution methods.

V. Phi-Functions

According to the definition given in [9] continuous function $\Phi(u_A, u_B)$ defined everywhere is called a phi-function if it has the following characteristic properties:

$$\begin{aligned} &\Phi\,(u_A,\ u_B) > 0, \text{ if } A \cap B = \varnothing \\ &\Phi\,(u_A,\ u_B) = 0, \text{ if } \text{int}\, A \cap \text{int}\, B = \varnothing, \\ &\qquad\qquad \text{fr}\, A \cap \text{fr}\, B \ne \varnothing \\ &\Phi\,(u_A,\ u_B) < 0, \text{ if } \text{int}\, A \cap \text{int}\, B \ne \varnothing. \end{aligned} \quad (11)$$

Fig. 8 shows arrangements of objects A and B.

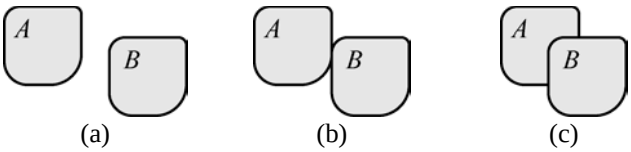

Fig. 8. Arrangement of objects A and B non-overlapping (a), contact (b), overlapping (c)

When the distance between the objects or the distance between the objects and the frontier of placement area is important we use the normalized phi-function (Fig. 9,a) or pseudo-normalized phi-function (Fig. 9,b).

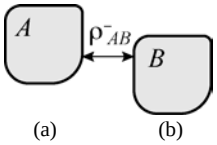

Fig.9. The arrangement of A (a) and B (b) taking into account minimal allowable distance ρ^-_{AB}, $\Phi\,(u_A,\ u_B) = \rho^-_{AB}$, $\Phi\,(u_A,\ u_B) = 0$

The phi-function $\Phi(u_A,\ u_B)$ is said to be normalized [9] if its values are equal to the Euclidian distance $\rho(A,\ B)$ between two objects A and B, subject to $(u_A,\ u_B) \in D$,

$$D = \left\{(u_A,\ u_B) \in R^6 :\ \operatorname{int} A(u_A) \cap \operatorname{int} B(u_B) = \varnothing\right\}.$$

The pseudo-normalized phi-function [8] is called the continuous, everywhere defined function $\Phi(u_A,\ u_B)$ for which:

$$\begin{aligned} &\Phi(u_A,\ u_B) > 0, \text{ if } \operatorname{dist}(A,\ B) > \rho_{AB}^{-} \\ &\Phi(u_A,\ u_B) = 0, \text{ if } \operatorname{dist}(A,\ B) = \rho_{AB}^{-}. \\ &\Phi(u_A,\ u_B) < 0, \text{ if } \operatorname{dist}(A,\ B) < \rho_{AB}^{-} \end{aligned} \quad (12)$$

Let $\hat{A} = A \oplus C(\rho)$, where $C(\rho)$ is the circle the radius of which is equal to the minimal allowed distance ρ_{ij}^{-} between two objects, the symbol $\oplus$ is the Minkovsky sum operation sign of object A and circle C, then $\Phi(u_A,\ u_B) = \Phi^{AB} = \Phi^{\hat{A}B}$, where $\Phi^{\hat{A}B}$ is the phi-function for a couple of objects $\hat{A}$ and B. Note that object $\hat{A}$ is an equidistant object, ρ_{ij}^{-} is radius of circle $C(\rho)$.

However, we note that the pseudo-normalized phi-function doesn't have radicals, it makes the function use in the modeling easier in the sense the effective local optimisation methods.

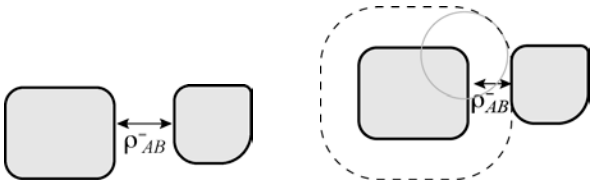

Fig..10. Minimal allowable distance ρ_{AB}^{-} between objects A and B: normalized phi-function $\Phi = \rho_{AB}^{-}$ (a), pseudo-normalized phi-function $\Phi^{AB} = 0$ (b)

The problem constraints in terms of phi-functions

Constraints (9)–(11) described in Section IV can be formulated in the terms of phi-functions as follows:

1) Non-overlapping constraint:

$$\Phi^{AB} \geq 0, \quad (13)$$

where Φ^{AB} is a phi-function of objects A and B.

2) Containment constraint:

$$\Phi^{\Omega^* A} \geq 0, \quad (14)$$

where $\Phi^{\Omega^* A}$ is a phi-function for Ω^* and object A.

3) Distance constraints:

$$\begin{aligned} &\Phi^{AB} \geq \rho_{AB}^{-} \Leftrightarrow\ \Phi^{AB} \geq 0, \\ &\Phi^{\Omega^* A} \geq \rho_{A}^{-} \Leftrightarrow \Phi^{\Omega^* A} \geq 0, \end{aligned} \quad (15)$$

where Φ, Φ are the normalized and pseudo-normalized phi-functions respectively [7].

4) Based on additional constraints on metric characteristics of the placement area the vector can be given in the form:

$$u = (h,\ u_1,\ u_2,\ \ldots,\ u_m) \in R^{2m+1},$$
$$h_{\min} \leq h \leq h_{\max} \quad (16)$$

$$u = (w,\ u_1,\ u_2,\ \ldots,\ u_m) \in R^{2m+1},$$
$$w_{\min} \leq w \leq w_{\max} \quad (17)$$

$$u = (u_1,\ u_2,\ \ldots,\ u_m) \in R^{2m}, \quad (18)$$

$$u = (h,\ w,\ u_1,\ u_2,\ \ldots,\ u_m) \in R^{2m+2},$$
$$h_{\min} \leq h \leq h_{\max},\ w_{\min} \leq w \leq w_{\max} \quad (19)$$

where n is the number of the feasible printing sheet formats, m is the number of the objects which it is necessary to place on the printing sheet, h, w are the height and the width of the placement area respectively.

The phi-function constructing

For all object types which are mentioned in Fig. 5 we construct the phi-function that simulate the arrangement of a pair of objects.

Phi-functions for the arbitrary shaped and basic oriented objects bounded by circular arcs and line segments are proposed in works [7, 8]. Let us consider phi-functions for all combinations of pairs of objects from set A.

Non-overlapping constraints

Let there be objects A and B of type A_a given by (1) with placement parameters $u_A = (x_A,\ y_A)$, $u_B = (x_B,\ y_B)$ and metric characteristics $m_A = (a_A,\ b_A, r_A)$, $m_B = (a_B,\ b_B, r_B)$ respectively. Then, assuming $x = x_B - x_A$, $y = y_B - y_A$, the phi-function for the objects is defined as follows:

$$\Phi^{AB} = \max\left\{\chi_i,\ \min\{\omega_i,\ \psi_i\},\ i = 1,\ \ldots,\ 4\right\}, \quad (20)$$

where $\chi_1 = -x - A'$, $\chi_2 = y - B'$, $\chi_3 = x - A'$, $\chi_4 = -y - B'$,

$$\omega_1 = (x + A')^2 + (y + B')^2 - R^2,$$
$$\omega_2 = (x + A')^2 + (y - B')^2 - R^2,$$
$$\omega_3 = (x - A')^2 + (y - B')^2 - R^2,$$

$$\omega_4 = \left(x - A'\right)^2 + \left(y + B'\right)^2 - R^2,$$

$$\psi_1 = -x - y - A' - B' - R,\ \psi_2 = -x + y - A' - B' - R,$$

$$\psi_3 = x + y - A' - B' - R,\ \psi_4 = x - y - A' - B' - R.$$

Here $A' = a_A + a_B + R$; $B' = b_A + b_B + R$, $R = r_A + r_B$.

Let the objects $A = \bigcup_{i=1}^{5} A_i$, $A_i \in \{A_b\}$ and $B = \bigcup_{j=1}^{5} B_j$, $B_j \in \{A_b\}$ (2) with $u_A = \left(x_A,\ y_A\right)$ and $u_B = \left(x_B,\ y_B\right)$ as the placement parameters respectively then the phi-function for the pair of the objects is defined as follows:

$$\Phi^{AB} = \min\left\{\Phi^{A_i B_j},\ \ i = 1,\ \ldots,\ 5,\quad j = 1,\ \ldots,\ 5\right\}, \quad (21)$$

where $\Phi^{A_i B_j}$ is the phi-function of the basic objects pair which form objects A_b and B_b.

A phi-function for the objects may be derived in the form (20), where $x = x_2 - x_1$, $y = y_2 - y_1$, $\chi_1 = -x - A'$, $\chi_2 = y - B'$, $\chi_3 = x - A'$, $\chi_4 = -y - B'$,

$$\omega_i = \left(x + A' - R_i\right)^2 + \left(y + B' - R_i\right)^2 - {R_i}^2,$$

$$\psi_i = x + y + A' + B' - R_i,\ i = 1, \ldots, 4,\ A' = a_A + a_B,$$

$$B' = b_A + b_B,\ a_A,\ \ a_B,\ \ b_A,\ \ b_B$$

are the length parameters which characterize the phi-objects A and B respectively.

Let us consider objects $A = K' \bigcup (\bigcup_{i=1}^{4} D_i')$, $A \in \{A_c\}$ and $B_c = K'' \bigcup (\bigcup_{i=1}^{4} D_i'')$, $B \in \{A_c\}$ (3) which have $u_A = \left(x_A,\ y_A\right)$ and $u_B = \left(x_B,\ y_B\right)$ as the placement parameters respectively. In this case the phi-function is defined as follows:

$$\Phi^{AB} = \min\{\Phi^{K'K''},\ \ \Phi^{K'D_i''},\ \ i = 1,\ \ldots,\ 4,$$

$$\Phi^{K''D_j'},\ \ j = 1,\ \ldots,\ 4\}, \quad (22)$$

where $\Phi^{K'K''}$ is a phi-function for $K' \subset A_c$ and $K'' \subset B_c$; $\Phi^{K'D_i''}$ is a phi-function for convex polygon $K' \subset A_c$ and circular object $D'' \subset B_c$; $\Phi^{K''D_j'}$ is a phi-function for convex polygon $K'' \subset B_c$ and circular object $D' \subset A_c$.

Containment constraints

According to the object classification given in Section II of this work let us construct the phi-functions describing relation of the containment the objects in the placement area for all mentioned objects.

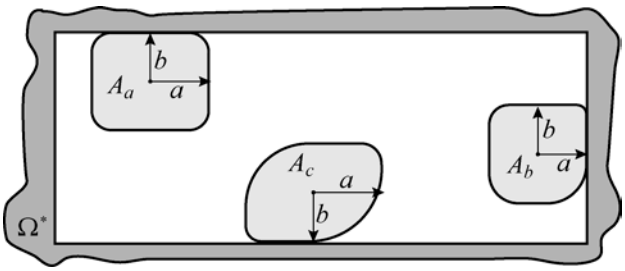

Fig. 11. The placement of the three types of printing objects

In view of the domain area specifics we note that the placement area is always a rectangle. As Figure 11 shows all of the objects have the half-width and the half-height as their parameter. Thus, based on the object of set A and placement area $\Omega^* = R^2 / \operatorname{int}\Omega$ have the placement parameters $u_A = \left(x_A,\ y_A\right)$ and $u_{\Omega^*} = \left(0,\ 0\right)$ then the following is true for all phi-object types of set A:

$$\Phi^{\Omega^* A} = \min\left\{\chi_i,\ \ i = 1,\ \ldots,\ 4\right\}, \quad (23)$$

where H, W are the height and the width of the placement area respectively;

$\chi_1 = x - a$, $\chi_2 = w - b - x$, $\chi_3 = y - b$, $\chi_4 = h - b - y$, $x = x_A$, $y = y_A$.

Distance constraints

If the problems need the constraints (15), it should be taken using the normalized or pseudo-normalized phi-function (see Fig. 10 a, b).

The normalized phi-function for the type objects (1) can be defined by (20), assuming $x = x_B - x_A$, $y = y_B - y_A$, $\chi_1 = -x - A'$, $\chi_2 = y - B'$, $\chi_3 = x - A'$, $\chi_4 = -y - B'$, $\omega_1 = \sqrt{\left(x + A'\right)^2 + \left(y + B'\right)^2} - R$,

$$\omega_2 = \sqrt{\left(x + A'\right)^2 + \left(y - B'\right)^2} - R,$$

$$\omega_3 = \sqrt{\left(x - A'\right)^2 + \left(y - B'\right)^2} - R,$$

$$\omega_4 = \sqrt{\left(x - A'\right)^2 + \left(y + B'\right)^2} - R,$$

$$\psi_1 = -x - y - A' - B' - R,\ \psi_2 = -x + y - A' - B' - R,$$

$$\psi_3 = x + y - A' - B' - R,\ \psi_4 = x - y - A' - B' - R,$$

$$A' = a_A + a_B + R;\ B' = b_A + b_B + R.$$

Here a_A, a_B, b_A, b_B are the metric characteristics of objects A and B respectively, $R = r_A + r_B$; r_A, r_B are the radii of the circles which are characterized the corner curving for the objects A and B.

The normalized phi-function for the type objects (2) can be defined by (20), assuming $x = x_2 - x_1$, $y = y_2 - y_1$, $\chi_1 = -x - A'$, $\chi_2 = y - B'$, $\chi_3 = x - A'$, $\chi_4 = -y - B'$,

$$\omega_i = \sqrt{\left(x + A' - R_i\right)^2 + \left(y + B' - R_i\right)^2} - R_i\ ,$$

$$\psi_i = x + y + A' + B' - R_i,\ i = 1,\ 2,\ 3,\ 4;\ A' = a_A + a_B$$

$B' = b_A + b_B$. Here a_A, a_B, b_A, b_B are the metric characteristics of objects A and B respectively.

The limitation of the determining the distances using the normalized phi-function is associated with the radicals that makes normalized phi-function use more complex in the local and the global optimization methods. Therefore it should be used the pseudo-normalized phi-function (12) to determine the distances between the objects.

V. Mathematical Model And Solution Strategy

Let us consider the printing objects placement problem of the given shape on the printing sheet in the following statement.

Let a rectangular region $P = \left\{ (x,\ y) \in R^2 \mid \ 0 \le x \le w,\ \ 0 \le y \le h \right\}$ of variable length w and height h, and objects $A_i \subset R^2$, $i \in I_m = \{1, \ldots, m\}$ be given. Also the minimal distance constraints are given: between objects A_i and A_j, i.e. $\rho\left(A_i,\ \ A_j\right) \ge \rho_{ij}^-$, $i \ne j$, $\ i, j \in I_m$, as well as between object $A_i \subset R^2$ and the frontier of placement area Ω i.e. $\rho\left(\Omega^*,\ \ A_i\right) \ge \rho_i^-$, $\ i \in I_m$.

Placement problem. Place objects A_i, $i \in I_m$ within placement area Ω taking into account distance constraints so that

$$\operatorname{int} A_i\left(u_i\right) \cap \left(\Omega^* \oplus S_i\right) = \varnothing,$$

$$\operatorname{int} A_i \cap \left(A_j \oplus S_{ij}\right) = \varnothing,\ i \ne j,\ \ i, j \in I_m,$$

where S_i, $\ S_{ij} \subset R^2$ are circles of radii ρ_i^- and ρ_{ij}^- respectively.

In the phi-function terms the constraints can be described by the inequalities (13)-(15) and the placement problem can be formulated as the following optimisation problem:

$$\min F\left(u\right), \text{ s.t. } u \in W \subset R^{2m+2} \qquad (24)$$

where $u = \left(h,\ w,\ u_1,\ u_2,\ \ldots,\ u_m\right)$, $F\left(u\right) = h \cdot w$,

$$W = \begin{cases} u \in R^{2m+2} : \Phi_{ij}\left(u_i,\ u_j\right) \ge 0,\ i < j = 1, 2, \ldots, m; \\ \Phi_i\left(0,\ u_i\right) \ge 0,\ i = 1, 2, .., m; \end{cases}$$

$h_{\min} \le h \le h_{\max}$, $w_{\min} \le w \le w_{\max}$.

The problem (24) is the nonlinear mathematical programming problem with the linear objective function, a solution space (a feasible region) W is described using $\frac{1}{n}(n-1)$ inequalities in the form $\Phi_{ij}(u_i, u_j) \ge 0$ and n inequalities in the form $\Phi_i(0, u_i) \ge 0$; phi-inequality $\Phi_{ij}(u_i, u_j) \ge 0$ provides non-overlapping of objects $A_i\left(u_i\right)$ and $A_j\left(u_j\right)$, $i < j = 2, \ \ldots, n$; the condition $\Phi_i(0, u_i) \ge 0$ provides the containment of objects $A_i\left(u_i\right)$ to placement area P, $i = 1,\ 2,\ \ldots,\ n$; m makes it possible to determine the number of objects which are placed in the area.

It is well known that feasible region W of problem (24) can be represented as a union of subregions W^k, $i = 1,\ 2,\ \ldots, \eta$, because each phi-function is a superposition of the finite number of the minimum or the maximum functions.

Therefore to solve the problem (24) it is always possible to construct a solution tree. Each terminal node there corresponds to a non-linear inequality system which describe subregion W^k.

The problem (24) can be reduced to the following problem:

$$F\left(u^{*k}\right) = \min\left\{F\left(u^k\right), k = 1, 2, \ldots, \eta\right\}, \qquad (25)$$

where

$$F\left(u^{*k}\right) = \min F\left(u\right), \text{ s.t. } u \in W^k. \qquad (26)$$

Based on the characteristics of problem (24) we conclude that the problem is a multiextremal and NP-hard. We propose the solution strategy based on [13] which involves: construction of starting points from the feasible region; searching for a local minima of subproblems (26); searching for a good local optimal placement of problem (24).

This algorithm finds good solutions with reasonable computation times that do not increase significantly with the complexity of the objects. In order to obtain a good starting solution $u^0 \in W$ the algorithm employs a fast and the efficient heuristic given in [8]. The heuristic is based on searching for an approximate solution of problem (24) provided that the placement parameters of objects take discrete values. Then the algorithm applies IPOPT [14] search for local minima. Below we give a description of the algorithm.

Let us define function $\Lambda(u) = \min\{\Phi_{ij}(u_i, u_j), i < j = 1, ..., n, \Phi_i(0, u_i), i = 1, ..., n\}$. Our aim is to extract from $\Lambda(u^0) \ge 0$ an inequality system, which describes subregion $W_s \subset W$, such that $u^0 \in W_s$, using the solution tree strategy proposed in [13]. We form the subregion W_s as follows.

Each basic phi-function Φ_k may be given in the form:

$$\Phi_k = \max_{i=1,..,\eta_k} f_i^k = \max_{i=1,..,\eta_k} \min_{j=1,...,J_i^k} f_{ij}^k,$$

where f_{ij}^k are infinitely-differentiable functions. Since $\min\limits_{j=1,\dots,J_i^k} f_{ij}^k \ge 0$ is equivalent to $f_{ij}^k \ge 0$ for all j, and $\max\limits_{i=1,\dots,\eta_k} f_i^k \ge 0$ means at least one of the inequalities, say $f_{i_0}^k \ge 0$ has to be fulfilled, each of these terms can be considered as a system of (in general non-linear) inequalities. Then for each inequality $\Phi_k \ge 0$ we may construct a tree, called a *basic phi-tree* and noted by $\Im_k$, and η_k means the number of terminal nodes of the basic phi-tree. Each terminal node of $\Im_k$ corresponds to a system of inequalities $f_i^k \ge 0$, $i = 1, 2, \dots, \eta_k$.

The solution tree $\Im$ describes feasible region W of problem (24). We realise an exhaustive search of nodes v_s^1, $s = 1, \dots, \eta_1$, of the first level of the solution tree $\Im$ sequentially and search for the number s_1 such that

$$f_{s_1}^1(u^0) = f^1(u^0) = \max\{f_1^1(u^0),\ f_2^1(u^0), \dots,\ f_{\eta_1}^1(u^0)\}$$

Then we realize an exhaustive search of offsprings v_s^2, $s = 1, \dots, \eta_2$, of node $v_{s_1}^1$ and search for the number s_2 such that

$$f_{s_2}^2(u^0) = f^2(u^0) = \max\{f_1^2(u^0),\ f_2^2(u^0), \dots,\ f_{\eta_1}^2(u^0)\}$$

and so on.

On the *n*-th level of our solution tree $\Im$ we realise an exhaustive search of nodes v_s^n, $s = 1, \dots, \eta_n$ which are offsprings of node $v_{s_{n-1}}^{n-1}$ and search for the number s_n such that

$$f_{s_n}^n(u^0) = f^n(u^0) = \max\{f_1^n(u^0),\ f_2^n(u^0), \dots,\ f_{\eta_n}^n(u^0)\}$$

Then we form inequality system which corresponds to s-*th* terminal node of our solution tree $\Im$ in the form: $W_s = \{u \in R^\sigma : f_{s_1}^1 \ge 0,\ f_{s_2}^2 \ge 0, \dots,\ f_{s_n}^n \ge 0, \lambda \ge 0\}$. To each sequence of numbers $s_1, s_2, \dots, s_k, \dots, s_n$ there corresponds the number s.

Finally, we solve problem $\min\limits_{u \in W_s} F(u)$ starting from point u^0.

VI. Conclusion

The proposed mathematical model and solution strategy allow us to employ the local and the global optimisation methods for solving the optimisation placement problem of printing objects.

The real placement problem of printing objects can be applied in the publishing-printing houses. Using the mathematical model allows us to get the layout templates for printing the different objects from several clients in one time reducing the time for processing the order and saving the material, which can be used for order group printing. Due to the involvement the proposed solution strategy to the production the publishing-printing houses can reduce the material waste by saving the material and this will influence to the environment pollution reduction.

References

[1] Wascher, G., Hauner, H. and Schumann, H., An improved typology of cutting and packing problems, European Journal of Operational Research, Volume 183, Issue 3, 16, 2007, pp. 1109-1130.

[2] Grebennik, I.V. Mathematical modeling of cutting material in the printed products production / I.V. Grebennik, D.V. Gritsay, T.E. Romanova, S.B. Shekhovtsov // Journal of Computational and Applied Mathematics. Kiev National University named after Taras Shevchenko. 2009, 3 (99), p. 38-47.

[3] Hamiez Jean-Philippe. A Tabu Search Algorithm with Direct Representation for Strip Packing. / Jean-Philippe Hamiez, Julien Robet, Jin-Kao Hao // Springer-Verlag Berlin Heidelberg.— 2009.— с. 61—72.

[4] R. Alvarez-Valdes, F. Parreño, J. M. Tamarit Reactive GRASP for the strip-packing problem. / // Computers & Operations Research.— 2008.— №35(4).— с. 1065—1092.

[5] K. Fleszar, C. Charalambous Average-weight-controlled bin-oriented heuristics for the one-dimensional bin-packing problem. // Computers & Operations Research.— 2011.— №210(2).— с. 176—184.

[6] Jens Egeblad and David Pisinger. Heuristic approaches for the two- and three-dimensional knapsack packing problems / DIKU Technical-report no. 2006-13, Department of Computer Science, University of Copenhagen. 2006.

[7] N. Chernov ,Y. Stoyan, T. Romanova. Mathematical model and efficient algorithms for object packing problem // Computational Geometry: Theory and Applications, vol. 43:5 (2010), pp. 535-553.

[8] Chernov N, Stoyan Y, Romanova T and Pankratov A, "Phi-Functions for 2D Objects Formed by Line Segments and Circular Arcs, "Advances in Operations Research, 2012, doi:10.1155/2012/346358.

[9] Stoyan Y. Phi-functions and their basic properties // Dokl. National Academy of Sciences of Ukraine. Ser. A. 2001. № 8. P. 112-117.

[10] J. Bennell, G. Scheithauer, Yu. Stoyan, and T. Romanova. Tools of mathematical modeling of arbitrary object packing problems. // J. Annals of Operations Research, Publisher Springer Netherlands: V 179, Issue 1 (2010), pp. 343-368.

[11] J.A. Bennell and J. F. Oliveira, The geometry of nesting problems: A tutorial, European J. Operational Research, 184 (2008), pp. 397-415.

[12] E.K. Burke, R. Hellier, G. Kendall, and G. Whitwell. Irregular packing using the line and arc no-fit polygon, Operations Research, 58(4) (2010) pp.948–970.

[13] Bennell J., Scheithauer G., Stoyan Y., Romanova T., Pankratov A. (2015) Optimal clustering of a pair of irregular objects. – Journal of Global Optimization 61, 497-524.

[14] Wachter, A., Biegler, L.T.: On the implementation of an interior-point filter line-search algorithm for large-scale nonlinear programming. Math. Program. 106 (1), 25–57, (2006).

Igor V. Grebennik received Doctor of Technical Sciences degree in Mathematical Modeling and Computational Methods (2007) from Institute for Problems in Machinery of National Academy of Sciences of Ukraine (Kharkov). From 2007 he is a professor at the Department of Systems Engineering, Kharkiv National University of Radio Electronics. His current research interests include mathematical modeling, operational research, combinatorial optimisation, packing and cutting.

Sergey B. Shekhovtsov received Candidate of Technical Sciences degree in Mathematical Modeling and Computational Methods (1989) from Kharkov National University of Radioelectronics (Kharkov). From 1994 he is a associate professor at the Department of Applied Mathematics, Kharkov National University of Internal Affairs. His current research interests include mathematical modeling, operational research, computational geometry, optimisation, packing and cutting.

Applications of Multipath Routing for Energy Balancing in Sensor Networks

I.S. Shostko, Ye. Kulia

***Abstract* — When designing a wireless sensor network (WSN) with autonomous nodes there emerges an issue how to provide the maximum duration of its life. For this purpose the use of multipath routing with support of the regime of energy balancing nodes is proposed in the article. The model for study of algorithms, multipath routing considering redressing the imbalance of power consumption in WSN transit nodes is developed.**

Keywords: **wireless sensor network, routing, power, imbalance.**

I. Introduction

Autonomous wireless sensor networks (WSN) are a special direction of development of telecommunication networks (TCS). The load on the communication lines WSN can fluctuate significantly over time: from the formation of a constant flow of information to rare, short signals or packets. In some cases, transmission of information from the sensor occurs only as a result of occurrence of certain events. Information signals may be analog or digital, and data to transfer, image, speech, etc. Unlike traditional TCS where by routing methods the maximum volume of traffic in the WSN is achieved, this task is usually not necessary. Is not important and the order of the nodes participating in the routing process. What is important is the accuracy of the transmitted commands or messages with a maximum length of the lifetime WSN. To increase duration of time the network operation saving power both of the sensor and other network nodes operating independently is of particular importance. This imposes a restriction on the choice of FSU routing protocols on the topology of the network and the strategy of nodes relationship.

Manuscript received February 8, 2015.

Igor Shostko is with the Kharkov National University of Radio Electronics, Department of Telecommunication Systems, Ukraine, 61166, Kharkov, Lenin Prosp., 14, e-mail: igor-shostko@yandex.ru.

Julia Kulia is with the Kharkov National University of Radio Electronics, Department of Telecommunication Systems, Ukraine, 61166, Kharkov, Lenin Prosp., 14, e-mail: sosedka.27@mail.ru

II. Analysis of published data and problem statement

Improving the energy efficiency of nodes WSN is a hot topic for many researchers. The following is an analysis of the number of publications devoted to reducing energy consumption and optimization modes WSN.

Energy balancing of data transfer route is considered in Y. Chen [1]. The proposed new approach to routing EBMR (Energy-Balancing Multipath Routing), is based on the account of the energy sources of supply constraints for nodes with WSN energy balancing route. The method of dynamic reconfiguration of WSN described in [2], allows to optimize traffic flow on the criterion of maximizing the time of its life. With the help of a set of programs developed by the author the proposed methods and algorithms for dynamic reconfiguration of the existing network are compared, and the dependence of the lifetime of a possible increment of the parameters of operation of the network sensor nodes and mobile runoff is investigated. In the work [3] the author noted that when the energy parameters and the level of signal / noise ratio of the sensor network topology changes for each cycle of the network. Moreover, since the choice of the headend is based on residual energy, each node can be selected mainly in a cluster, and thus the life of the sensor network can be extended in general. The large number of scientific papers on the development of methods to reduce energy consumption WSN suggests that research questions are relevant. Each of the considered methods has its advantages and disadvantages and is well suited for a particular situation.

III. Problem Formulation

The object of study is the process of functioning of the autonomous wireless sensor network. The purpose of work is the increase of lifetime of the autonomous WSN through the use of algorithms for routing support of the regime of nodes energy balancing. To achieve the goal the task is defined: - development of model for the study of algorithms, multipath routing considering redressing the imbalance of power consumption in the transit nodes WSN.

IV. Statement of the problem of routing considering redressing the imbalance of power consumption in the transit nodes of wireless sensor network

Let us consider a network consisting of m routing nodes. As part of the basic model network configuration is described by a graph $G_s = (V_s, E_s)$, where $V_s = \{\alpha_1, \alpha_2, \alpha_3, ..., \alpha_m\}$ – a plurality of network routing nodes, $E_s = \{\beta_1, \beta_2, \beta_3, ..., \beta_n\}$ – a plurality of communication channels (Fig. 1). For each communication channel $(i, j) \in E_S$ given its carrying capacity $c_{i,j}$. Magnitude $x_{i,j}$ describes the proportion of the incoming traffic flowing in the duct $(i, j) \in E_S$.

If the role of nodes is dynamically changed and the network topology is reconstructed, it is possible to bring the lifetime of the network to the terminal device (TD) lifetime. This may increase the lifetime due to the fact that most of the time each of the nodes will be in the role TD. In addition the set of concurrent routing nodes (RN) cyclically follow each other. Decisions on how to rebuild the topology are taken at the level of the network coordinator.

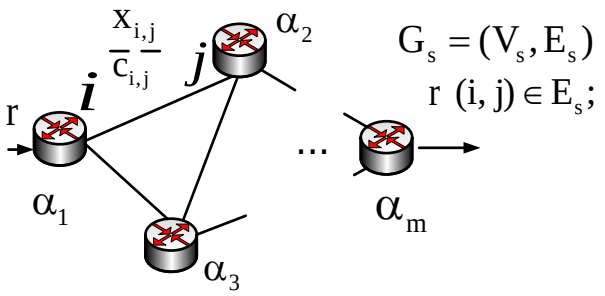

Fig. 1. An example of a graph for describing the network model

We solve the problem of maximizing the lifetime of the network. We construct all related subgraphs T_k, $k \in \overline{1,K}$ graph G_s, it is a tree with a root element containing all vertices G_s. R_k - set of all RNs of the graph T_k. Consider an arbitrary subset $\{R_{k_s}\}_{s=1}^{S}$ of a plurality $\{R_k\}_{k=1}^{K}$. We have S independent sets of plurality $\{R_{k_s}\}_{s=1}^{S}$ each comprising S_u RNs and $S - S_u$ TDs. Then the average current in the node α_j is expressed by the formula

$$I_j = I_R\left(\frac{S_u}{S}\right) + I_E\left(\frac{S - S_u}{S}\right) = I_E + (I_R - I_E)\frac{S_u}{S}, \quad (1)$$

where I_R — an average current strength in BI time (Beacon Interval — interval between beacons) at a node located as RN; I_E — an average current strength in BI for a node which currently plays the role of TD. The lifetime of the device is determined by WSN with the shortest lifetime

$$T_{WSN} = \min_j \frac{Q_{bat\ j}}{I_j} \to \max, \quad (2)$$

where $Q_{bat\ j}$ — battery charge of the node α_j. For simplicity, we assume that at the initial time all devices have the same battery charge $Q_{bat\ j} = Q_{bat}$. Then the condition (2) becomes

$$\max_j I_j = I_E + (I_R - I_E)\frac{\max_u S_u}{S} \to \min. \quad (3)$$

If sets $\{R_{k_s}\}_{s=1}^{S}$ are independent, $\forall s \in \overline{1,S} \to S_u \in \{0;1\}$, therefore $\max S_u = 1$ and there remained only one condition

$$S \to \max. \quad (4)$$

This is the required condition. Thus, in order to achieve a maximization of network life time it is necessary to find the maximum number of independent sets of routers.

Statement of the problem of routing in view of redressing the imbalance of power consumption in the transit nodes WSN:

Given:

- number of communication channels in the network (n);
- number of nodes in the network (m);
- the sending node packages α_j;
- the recipient node packages α_j;
- network bandwidth ($c_{i,j}$);
- metric of communication channels ($f_{i,j}$);
- traffic intensity incoming in the network (r).

It is necessary to define:

- the way (ways) from the sending node to the recipient node, that passes along the channels of the simulated network and are "optimal" in the framework of the selected metrics;
- the dependence of the number of ways which are used during routing, as a function of the intensity of the traffic entering the network;
- the dependence of energy consumption on the number of engaged nodes.

V. Model of multipath routing using Traffic Engineering technology in the form of the quadratic programming problem

Let the network structure and the capacities of its of communication channels are shown in Fig. 2. Then the total number of nodes in the network is equal to five (m = 5), and the total number of links is ten (n = 10). Let the sending node packages be the unit 1 and unit-recipient – the unit 5.

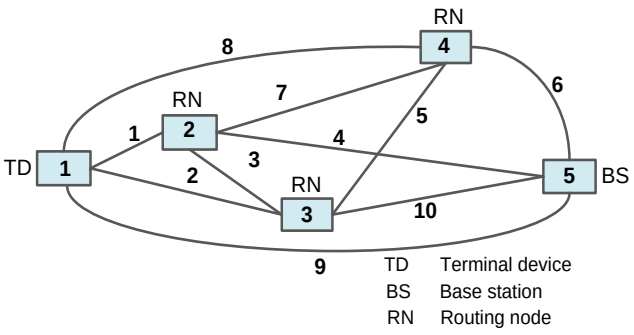

Fig. 2. The structure of the simulated network

The number of communication channels in the network (n) defines the dimension of the vector x, variables $x_{i,j}$ of which characterizes the share of traffic in the channel of communication between the i-th and j-th nodes. The dimension of the vector metrics f corresponds to the number of communication channels in the network (n), variables $f_{i,j}$ which characterize metric communication channel between i-th and j-th nodes. To implement multipath routing coordinates of the vector x the following restrictions are imposed

$$0 \le x_{i,j} \le 1,\ i,\ j = \overline{n,m};\ i \ne j, \qquad (5)$$

where the variables $x_{i,j}$ can take values in the interval from zero to one. The physical meaning of the variables (5) determines the possibility of branching into several flow paths in the network, i.e. traffic may be transmitted as one or a plurality of ways. In this case, each communication channel will be assigned to the metric,

$$f_{i,j} = \frac{10^7}{c_{i,j}},$$

where $c_{i,j}$ - bandwidth connections between i - th and j - th nodes (1/s).

In the course of solving the problem of routing is important to prevent packet loss at the network nodes in the network as a whole, it is necessary to ensure that the conditions of conservation of flux:

$$\begin{cases} \sum\limits_{j:(i,j)} x_{i,j} - \sum\limits_{j:(j,i)} x_{j,i} = 1, & \text{for sender node} \\ \sum\limits_{j:(i,j)} x_{i,j} - \sum\limits_{j:(j,i)} x_{j,i} = 0, & \text{for transit nodes} \\ \sum\limits_{j:(i,j)} x_{i,j} - \sum\limits_{j:(j,i)} x_{j,i} = -1, & \text{for recipient node} \end{cases} \qquad (6)$$

In addition, it is necessary to ensure fulfillment of the conditions in the channels to prevent overloading the network:

$$r \cdot x_{i,j} \le c_{i,j}, \quad \left(i, j = \overline{n,m};\ \ i \ne j\right). \qquad (7)$$

To solve the problem we use the model of multipath routing using the technology of Traffic Engineering where as the objective function to be minimized the quadratic form is used:

$$\min_x \left[x^t H x + f^t x\right],$$

where H - additionally defined diagonal matrix of $n \times n$ size, coordinates of which (like the vector f) characterize metric of communication channels.

Thus, the solution to the problem of multipath routing using the technology of Traffic Engineering is reduced to solving the optimization problem of quadratic programming using the tool «Optimization Toolbox» of MatLab package v.14.b, which is represented by subroutine «quadprog»:

[x,fval]=quadprog(H,[],A,b,Aeq,beq,lb,ub) – decision,

$fval = \min_x \left[x^t H x + f^t x\right]$ при $Aeq \cdot x = beq$, $A \cdot x \le b$ и

$lb \le x \le ub$,

where $H = \mathrm{diag}(f)$, that is, the main diagonal matrix H are located metrics of communication channels;

f, x, b, beq - vectors, A and Aeq - matrix, lb и ub – column vectors of size n, and in accordance with the expression (5), all coordinates of the vector lb zero, and all the coordinates of the vector ub equate units. To describe the routing problem in the formalism of the conditions of preservation of the environment MatLab flow (6) should be submitted in vector-matrix form: $Aeq \cdot x = beq$. Thus, the matrix Aeq has dimension $m \times n$, the coordinates of which take numerical values {-1,0,1} at $\left(j = \overline{1,m}, i = \overline{1,n}\right)$:

$a_{j,i} = 1$, if i-th communication channel exits from j-th node;

$a_{j,i} = -1$, if i-th communication channel enters in j-th node;

$a_{j,i} = 0$, if i-th communication channel is not incident j-th node.

The dimension of the vector beq It corresponds to the number of nodes in the network (m), and its coordinates are formed as follows $\left(j = \overline{1,m}\right)$:

$beq_j = 1$, if i-th is the node-sender;

$beq_j = -1$, if i-th node is receiving packets;

$beq_j = 0$, if i-th is transit node.

Condition (7) must also be to submitted in vector-matrix form of inequality $A \cdot x \le b$.

Example of routing and address problems in Matlab. Form the unknown vector x and the vector of metrics f:

$$x = \begin{bmatrix} x_{1,2} \\ x_{1,3} \\ x_{1,4} \\ x_{1,5} \\ x_{2,5} \\ x_{3,2} \\ x_{3,4} \\ x_{3,5} \\ x_{4,2} \\ x_{4,5} \end{bmatrix}, \quad f = \begin{bmatrix} f_{1,2} \\ f_{1,3} \\ f_{1,4} \\ f_{1,5} \\ f_{2,5} \\ f_{3,2} \\ f_{3,4} \\ f_{3,5} \\ f_{4,2} \\ f_{4,5} \end{bmatrix} = \begin{bmatrix} 10^7/250/4 \\ 10^7/250/4 \\ 10^7/250/4 \\ 10^7/0 \\ 10^7/250/4 \\ 10^7/250/4 \\ 10^7/250/4 \\ 10^7/250/4 \\ 10^7/250/4 \\ 10^7/250/4 \end{bmatrix}. \quad (8)$$

Formalize the preservation of flow in the network nodes (6):

$$\begin{cases} x_{1,2} + x_{1,3} + x_{1,4} + x_{1,5} = 1 \\ -x_{1,2} - x_{3,2} - x_{4,2} + x_{2,5} = 0 \\ -x_{1,3} + x_{3,2} + x_{3,4} + x_{3,5} = 0 \\ -x_{3,4} - x_{1,4} + x_{4,2} + x_{4,5} = 0 \\ -x_{1,5} - x_{2,3} - x_{3,5} - x_{4,5} = -1 \end{cases}.$$

We form a matrix Aeq and vector beq:

$$Aeq = \begin{bmatrix} 1 & 1 & 0 & 0 & 0 & 0 & 0 & 1 & 1 & 0 \\ -1 & 0 & -1 & 1 & 0 & 0 & -1 & 0 & 0 & 0 \\ 0 & -1 & 1 & 0 & 1 & 0 & 0 & 0 & 0 & 1 \\ 0 & 0 & 0 & 0 & -1 & 1 & 1 & -1 & 0 & 0 \\ 0 & 0 & 0 & -1 & 0 & -1 & 0 & 0 & -1 & -1 \end{bmatrix}, \quad beq = \begin{bmatrix} 1 \\ 0 \\ 0 \\ 0 \\ -1 \end{bmatrix},$$

formalize conditions to prevent overloading of communication channels (7):

$$\begin{cases} r \cdot x_{1,2} \le c_{1,2} \\ r \cdot x_{1,3} \le c_{1,3} \\ r \cdot x_{1,4} \le c_{1,4} \\ r \cdot x_{1,5} \le c_{1,5} \\ r \cdot x_{2,5} \le c_{2,5} \\ r \cdot x_{3,2} \le c_{3,2} \\ r \cdot x_{3,4} \le c_{3,4} \\ r \cdot x_{3,5} \le c_{3,5} \\ r \cdot x_{4,2} \le c_{4,2} \\ r \cdot x_{4,5} \le c_{4,5} \end{cases}.$$

Form the matrix A and the vector b:

$$A = \begin{bmatrix} L & 0 & 0 & 0 & 0 & 0 & 0 & 0 & 0 & 0 \\ 0 & L & 0 & 0 & 0 & 0 & 0 & 0 & 0 & 0 \\ 0 & 0 & L & 0 & 0 & 0 & 0 & 0 & 0 & 0 \\ 0 & 0 & 0 & L & 0 & 0 & 0 & 0 & 0 & 0 \\ 0 & 0 & 0 & 0 & L & 0 & 0 & 0 & 0 & 0 \\ 0 & 0 & 0 & 0 & 0 & L & 0 & 0 & 0 & 0 \\ 0 & 0 & 0 & 0 & 0 & 0 & L & 0 & 0 & 0 \\ 0 & 0 & 0 & 0 & 0 & 0 & 0 & L & 0 & 0 \\ 0 & 0 & 0 & 0 & 0 & 0 & 0 & 0 & L & 0 \\ 0 & 0 & 0 & 0 & 0 & 0 & 0 & 0 & 0 & L \end{bmatrix}; \quad b = \begin{bmatrix} c_{1,2} \\ c_{1,3} \\ c_{1,4} \\ c_{1,5} \\ c_{2,5} \\ c_{3,2} \\ c_{3,4} \\ c_{3,5} \\ c_{4,2} \\ c_{4,5} \end{bmatrix},$$

where L = lamda .

For the structure of the network with bandwidth of its communications channels, presented in Fig. 2, a diagonal matrix of metrics channels has the form:

$$H = \begin{bmatrix} h_{1,1} & 0 & 0 & 0 & 0 & 0 & 0 & 0 & 0 & 0 \\ 0 & h_{1,1} & 0 & 0 & 0 & 0 & 0 & 0 & 0 & 0 \\ 0 & 0 & h_{1,1} & 0 & 0 & 0 & 0 & 0 & 0 & 0 \\ 0 & 0 & 0 & h_{1,1} & 0 & 0 & 0 & 0 & 0 & 0 \\ 0 & 0 & 0 & 0 & h_{1,1} & 0 & 0 & 0 & 0 & 0 \\ 0 & 0 & 0 & 0 & 0 & h_{1,1} & 0 & 0 & 0 & 0 \\ 0 & 0 & 0 & 0 & 0 & 0 & h_{1,1} & 0 & 0 & 0 \\ 0 & 0 & 0 & 0 & 0 & 0 & 0 & h_{1,1} & 0 & 0 \\ 0 & 0 & 0 & 0 & 0 & 0 & 0 & 0 & h_{1,1} & 0 \\ 0 & 0 & 0 & 0 & 0 & 0 & 0 & 0 & 0 & h_{1,1} \end{bmatrix},$$

where $h_{1,1} = 10^7/250/4$.

$H = \mathrm{diag}(f)$, that is, there are metrics of communication channels on the main diagonal matrix H (8).

In accordance with the original data intensity of incoming traffic at r = 250 all the ways except for 3, 5 and 7 will be used. Thus through 2, 3 and 4 node passes on 33,3(3)% transmitted traffic - with an intensity 83,3 (3). Thus, for 2, 3 and 4 node energy consumption is distributed evenly. This ratio will not change with a decrease in intensity incoming traffic. By increasing the number of nodes involved repeaters for multipath routing incoming traffic will be equally shared between all RNs. Thus, for the example of considered life expectancy has increased in proportion to the number of WSN nodes involved repeaters, between which the load is redistributed.

V. Conclusion

The studies have shown that if the role of nodes is dynamically changed and rebuilt the topology of the network, we can bring the network to lifetime of TD. This may increase the lifetime due to the fact that most of the

time, each of the nodes will be in the role of TD. In addition the set of concurrent RNs cyclically follow each other. Decisions on how to rebuild the topology of the network are taken by a coordinator.

Also the author solved the problem of multipath routing in view of redressing the imbalance of power consumption. To achieve maximizing network lifetime it is necessary to find the maximum number of independent sets of routers. In solving the optimization problem of quadratic programming a uniform load between the transit nodes is obtained and hence their energy consumption will be the same.

REFERENCES

[1] Y. Chen. Energy-balancing multipath routing protocol for wireless sensor networks [Text]: proc. of the 3rd intern. conf. / Y. Chen, N. Nasser // Quality of service in heterogeneous wired/wireless networks QShine '06. 2006. Vol. 21. P. 245–249. doi: 10.1145/1185373.1185401.

[2] S.G. Efremov. Modeling the lifetime of dynamically reconfigurable sensor networks with mobile Stock: dis. … Candidate of Technical Sciences: 05.13.18 / Efremov Sergey G.. – M., 2012. – p. 143.

[3] Tariq Hussain Yahya. Methods to improve the quality of monitoring in sensor networks: dis. ... Candidate of Technical Sciences: 05.12.02 "Telecommunication systems and networks"/ Tariq Hussain Yahya;. – H., 2013. P. 166.

Shostko Igor Svetoslavovich, Professor, Doctor of Technical Sciences, Associate Professor, Department of telecommunication systems, Kharkov National University of Radio Electronics. Research interests: ultra-wideband signals in radio engineering and telecommunication systems. Address: Kharkov, Lenin av, 14, Department of TCS, KNURE. Phone: (057) 702-13-20, E-mail: igor-shostko@yandex.ru

Kulia Julia Eduardovna, PhD student, Department of Telecommunication systems, Kharkov National University of Radio Electronics. Research interests: wireless sensor networks, telecommunication systems. Address: Kharkov, Lenin av, 14, Department of TCS, KNURE. Phone: 063-47-22-773, e-mail: sosedka.27@mail.ru

Optimum Sum Codes, that Effectively Detect the Errors of Low Multiplicities

Valery Sapozhnikov, Vladimir Sapozhnikov, Dmitry Efanov, Vyacheslav Dmitriev, Maria Cherepanova

Automation and Remote Control on Railways Department,
Petersburg State Transport University, Russian Federation

***Abstract* – The article provides the method of formation of the sum code with minimum total number of undetectable errors. The code, suggested by authors, has the same number of check bits, as a classic Berger code, but also has a better detection ability, particularly within the area of low multiplicity errors in data vectors. New sum code allows to develop concurrent error detection (CED) systems of logic units of automation and computer devices with low equipment redundancy and a high percentage of error detection in controlled blocks.**

I. Introduction

Sum codes are often used for data transmission and processing systems, as well as for design of reliable systems of automation and computer devices [1-9]. One of the examples of application of sum codes is a concurrent error detection (CED) system of arithmetical-logical units, that make a part of any modern systems of automation control [10-14].

The CED system structure is presented in Fig. 1. There, the initial arithmetical-logical unit $F(x)$, that realizes the system of operational Boolean functions $f_1(x)$, $f_2(x)$, …, $f_m(x)$, is equipped with the special control equipment. The control equipment includes the reference logic block $G(x)$, calculating the values of test functions $g_1(x)$, $g_2(x)$, …, $g_k(x)$, and the self-checking checker, that registers the conformance of the values of operational and test functions at any given time. This conformance is established at the CED system design stage and usually determined according to the rules of formation of preselected sum code. So the block $F(x)$ outputs are matched with the data vector of length m, and the block $G(x)$ outputs – with the check vector of length k. Those significant parameters of the CED system as detection ability and equipment redundancy are substantially depend on the rules of code formation, and the latter, in its turn, effects the power consumption, processing speed, testability and other characteristics of built discrete system [15,16].

The structure, shown in Fig. 1, in practice is built under condition of 100% detection of single faults [1,17]. By the reason of separate implementation of the blocks $F(x)$, $G(x)$ and checker at any given time the fault can occur only in one element of CED system. The reference logic block faults distort the values of test functions, that is registered by the checker. The checker, as the watchdog in CED system, is built as a self-checking device and thus detects its own faults at leas in one input set [1]. The CED system task is to provide the detection of single faults in block $F(x)$, when the internal configuration of links between logic elements within it can result in occurrence of distortions of different multiplicities in the values of output vector. Therefore, it is possible to consider the characteristics of sum code based on error detection in data vectors, studying by this the features of the CED system itself.

Different sum codes have different characteristics of error detection in data vectors and allow to build systems with various technical specifications. This paper is dedicated to the study of sum codes, that have minimum total number of undetectable errors in data vectors, as well as decreased number of double undetectable errors in comparison with classic sum codes.

II. Analysis of Berger codes and sum codes with weighted transitions properties for error detection in data vectors

Classic sum code, or Berger code [18], is built based on the following principle: data vector weight r (the sum of one data bits), and then the obtained value is presented in binary form and recorded into the bits of the check vector. The number of check bits in Berger code is calculated using the formula: $k = \lceil \log_2(m+1) \rceil$ (notation $\lceil ... \rceil$ is an integer, upward to the calculating value). Hereafter referred the Berger code to as $S(m,k)$-code.

In $S(m,k)$-code the same check vector corresponds to all data vectors with the same weight. For this value r is C_m^r of data vectors. With increasing of r the number of data vectors, corresponding to the same check vector, increases with its maximum at $\frac{m}{2}$ for the even m and at $\frac{m-1}{2}$ for the odd m, and then grows away. Such distribution of data vectors between the check vectors results in the fact, that $S(m,k)$-code does not detect significantly large amount of errors in data vectors. For example, $S(5,3)$-code does not detect 220 errors in data vectors, that forms 22.18% of all possible errors in data vectors (i.e. this code does not detect slightly less than one fourth of errors in data vectors). With low value of detection ability all $S(m,k)$-codes also have low efficiency of low multiplicities error detection – these codes do not detect 50% of double errors, 37.5% of quadruple errors, 31.25% six-fold errors, etc. [19].

Manuscript received January 18, 2015.

Valery Sapozhnikov is with the Petersburg State Transport University, Automation and Remote Control on Railways Department, Russian Federation.

Vladimir Sapozhnikov is with the Petersburg State Transport University, Automation and Remote Control on Railways Department, RF.

Dmitry Efanov is with the Petersburg State Transport University, Automation and Remote Control on Railways Department, RF (corresponding author to provide e-mail: mitriche@yandex.ru).

Vyacheslav Dmitriev is with the Petersburg State Transport University, Automation and Remote Control on Railways Department, RF.

Maria Cherepanova is with the Petersburg State Transport University, Automation and Remote Control on Railways Department, RF.

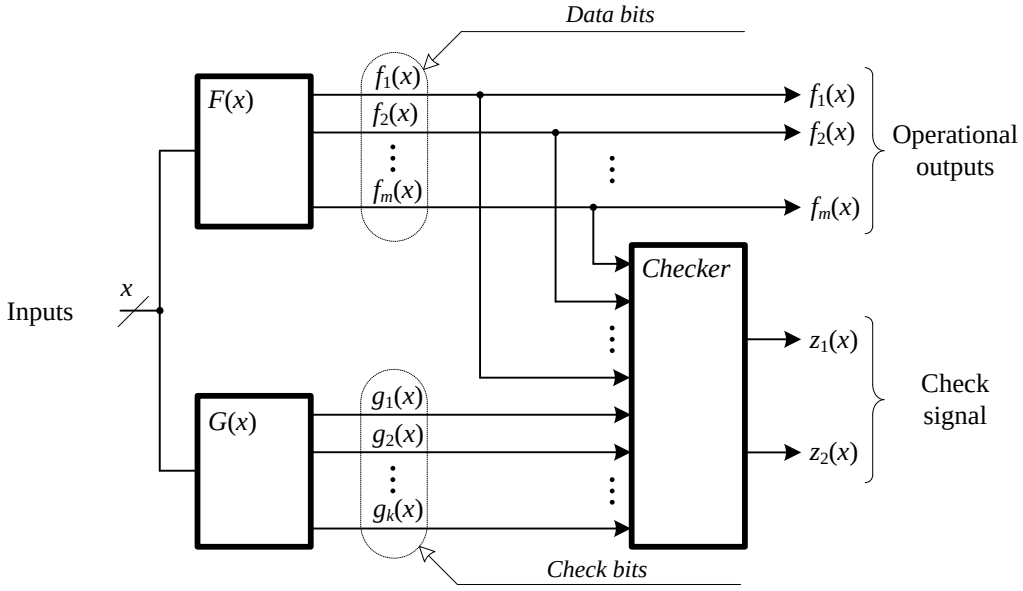

Fig. 1. CED system structure

So the problem of increasing the detection abiliity arises, which includes the detection ability within the area of low multiplicity errors, on condition of keeping the number of check bits in the code. Practically speaking, for example, in CED systems the solution of this problem will allow to detect the bigger number of single faults of controlled logic unit without increasing the equipment redundancy.

In [20] the term of an optimum separable code by the criterion of minimum number of undetectable errors for the specified values of m and k was introduced. The optimum code has a uniform distribution of all 2^m data vectors among 2^k check vectors and does not detect

$$N_{m,k}^{\min} = 2^m\left(2^{m-k}-1\right), \quad (1)$$

errors in data vectors. For instance, the optimum code, where m=5 and k=3, has $N_{5,3}^{\min} = 2^5\left(2^{5-3}-1\right) = 32\cdot 3 = 96$ undetectable errors, i.e. 2.29 times less than S(5,3)-code. The same paper suggests the method for improving the $S(m,k)$-codes characteristics for error detection in data vectors without sacrificing the number of check bits. This method is based on transformation of each Berger code word in its check part using the specific algorithm. This algorithm implicates the determination of the vector weight to the modulus $M = 2^{\lceil \log_2(m+1)\rceil - 1}$ and using the correction factor, equals to modulo two sum of values of some data vector bits. Modified Berger codes, at an average, detect twice as many errors in data vectors as classic $S(m,k)$-codes, however, they are not the optimum codes. In [21-23] there is a suggestion of the line of modified Berger codes, that are obtained by establishing the modulus for data vector weight determination, selected from the set $M \in \left\{2;4;...;2^{\lceil \log_2(m+1)\rceil - 2}\right\}$. These codes have decreased number of check bits in comparison with Berger codes. Modular-modified Berger codes with its m and k values are also not an optimum (excluding the code, where M=2, that has 2 check bits).

Optimum sum code with the same number of check bits as Berger code, can be built by alteration of the algorithm of formation of the sum code with weighted transitions [24-26]:

Algorithm 1. *Check vectors obtaining for sum code with weighted transitions:*

1. Data vector bits are considered, that have the adjacent positions.

2. Each transition from the bit to the bit it is assigned the weight ratio from the positive integers (1, 2, …, m–1), starting from the lower order bit.

3. The sum of so called active transitions (transition between the bit is called active, if the modulo two sum of the values of adjacent bits equals 1) is calculated.

4. Obtained value is presented in binary form and recorded in check vector.

Let us set the sum code with weighted transitions as $WT(m,k)$-code.

$WT(m,k)$-code detects bigger number of errors in data vectors, than $S(m,k)$-code, and however it has the increased number of check bits. This number is equals $k = \left\lceil \log_2 \frac{m(m-1)}{2} \right\rceil$. The increased number of check bits in $WT(m,k)$-code in comparison with $S(m,k)$-code results in increase of complexity of control equipment in CED system (see Fig. 1). Besides, the check bits of $WT(m,k)$-code are used ineffectively – $WT(m,k)$-codes are not optimum codes [27]. Optimum code are obtained by using the following algorithm of formation.

Algorithm 2. *Check vectors obtaining for modified sum code with weighted transitions:*

1. The steps 1 – 3 of Algorithm 1 are carried out.

2. The modulus $M = 2^{\lceil \log_2(m+1)\rceil}$ value is established (this is the modulus of Berger code).

3. The sum V of so called active transitions is calculated.

4. The least non-negative residue of V value for established modulus is calculated: $W = (V) \bmod M$.

5. The number W is presented in binary form and recorded in check vector.

To demonstrate the operation of algorithm of formation of modified sum code with weighted transitions or $WTM(m,k)$-code, let us use the example of $WT8(5,3)$-code formation. Table I presents the weight ratios of each transition between the bits of data vector, and Table 2 presents all

code words of *WT*8(5,3)-code. For instance, in <00101> data vector transitions are considered active between the bits x_1 and x_2, x_2 and x_3, x_3 and x_4. To obtain V value it is necessary to sum up the weight ratios of these transitions: $V=w_{1,2}+w_{2,3}+w_{3,4}=1+2+3=6$. The least non-negative residue of V equals to $W=(6)\text{mod}8=6$, that in binary form is presented as <110>.

TABLE I
WEIGHT RATIOS OF TRANSITIONS IN DATA VECTOR

$w_{4,5}$	$w_{3,4}$	$w_{2,3}$	$w_{1,2}$
4	3	2	1

By analyzing Table II, it is not too difficult to notice that V values for data vectors, equidistant form the middle of the table (these vectors have opposite values of similar bits), are equal. At that the number of repeating V values is unequal (Table III). This results in the irregularity in the distribution of data vectors of *WT*(*m*,*k*)-code among the check vectors (within the test groups). Implementing the modification of *WT*(*m*,*k*)-code under Algorithm 2, this disadvantage is eliminated, because the calculation is made up to the value $M-1=7$: $(8)\text{mod}8=0$, $(9)\text{mod}8=1$ и $(10)\text{mod}8=2$.

TABLE II
CODE WORDS OF *WT*8(5,3)-CODE

№	Data vector bits					V	$W=(V)\text{mod}8$	Check vector bits		
	x_5	x_4	x_3	x_2	x_1			y_3	y_2	y_1
0	0	0	0	0	0	0	0	0	0	0
1	0	0	0	0	1	1	1	0	0	1
2	0	0	0	1	0	3	3	0	1	1
3	0	0	0	1	1	2	2	0	1	0
4	0	0	1	0	0	5	5	1	0	1
5	0	0	1	0	1	6	6	1	1	0
6	0	0	1	1	0	4	4	1	0	0
7	0	0	1	1	1	3	3	0	1	1
8	0	1	0	0	0	7	7	1	1	1
9	0	1	0	0	1	8	0	0	0	0
10	0	1	0	1	0	10	2	0	1	0
11	0	1	0	1	1	9	1	0	0	1
12	0	1	1	0	0	6	6	1	1	0
13	0	1	1	0	1	7	7	1	1	1
14	0	1	1	1	0	5	5	1	0	1
15	0	1	1	1	1	4	4	1	0	0
16	1	0	0	0	0	4	4	1	0	0
17	1	0	0	0	1	5	5	1	0	1
18	1	0	0	1	0	7	7	1	1	1
19	1	0	0	1	1	6	6	1	1	0
20	1	0	1	0	0	9	1	0	0	1
21	1	0	1	0	1	10	2	0	1	0
22	1	0	1	1	0	8	0	0	0	0
23	1	0	1	1	1	7	7	1	1	1
24	1	1	0	0	0	3	3	0	1	1
25	1	1	0	0	1	4	4	1	0	0
26	1	1	0	1	0	6	6	1	1	0
27	1	1	0	1	1	5	5	1	0	1
28	1	1	1	0	0	2	2	0	1	0
29	1	1	1	0	1	3	3	0	1	1
30	1	1	1	1	0	1	1	0	0	1
31	1	1	1	1	1	0	0	0	0	0

TABLE III
DISTRIBUTION OF V VALUES FOR WT8(5,3)-CODE FORMATION

V										
0	1	2	3	4	5	6	7	8	9	10
0	1	2	3	4	5	6	7	8	9	10
			3	4	5	6	7			
			3	4	5	6	7			

Table IV provides the distribution of data vectors within the test groups for the *WT*8(5,3)-code of interest. Within each test group there are 4 data vectors. What is more, in virtue of the equality of V values for equidistant from the middle of Table II data vectors within each test group there are always two data vectors minimum, that differ from each other in all bits. This induces the undetectable errors of maximum multiplicity $d=m$ in *WT*8(5,3)-code. Undetectable errors of lower multiplicities appear in *WT*8(5,3)-codes in case of distortions, that transfer data vectors of one test group into data vectors, not-equidistant from the middle of Table II. This type of distribution of data vectors among the test groups remains unchanged and for all *WTM*(*m*,*k*)-codes. The only exclusion is *WTM*(*m*,*k*)-codes with the number of data bits $m=2^t$ (t=1, 2, …). For these codes there is no filling the last test group, because the number of data bits is that the value $W=2^k-1$ does not form. Actually, where m=4, for example, maximum data vector weight is $W=w_{1,2}+w_{2,3}+w_{3,4}=1+2+3=6$.

Apropos *WTM*(*m*,*k*)-codes with data vectors lengths $m\neq 2^t$ (t=1, 2, …), it should be noticed that within each test group there are transitions for them similar by multiplicity. These transitions determine the number of distortions with different multiplicity within each test group. For example, Fig. 2 shows the graph of all possible transitions within <111> test group of *WT*8(5,3)-code.

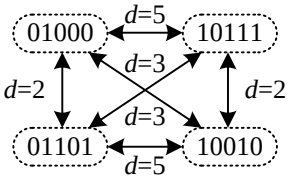

Fig. 2. Transitions within <111> test group of *WT*8(5,3)-code

The total number of undetectable errors in *WTM*(*m*,*k*)-codes is obtained by multiplying the number of errors within one test group by M.

Table V5 provides the distribution of undetectable errors in data vectors of *WTM*(*m*,*k*)-codes for several m values. Analysis of such table allowed to establish the features of a new class of sum codes based on error detection in data vectors:

- any *WTM*(*m*,*k*)-code detects 100% of single distortions (is a fault-tolerant code);
- *WTM*(*m*,*k*)-codes with data vector lengths $m\neq 2^t$ (t=1, 2, …) are optimum;
- *WTM*(*m*,*k*)-codes with data vector lengths $m=2^t$ (t=1, 2, …) are close to optimum, but not such codes;
- *WTM*(*m*,*k*)-codes with even values of m detect 100% of errors of odd multiplicities in data vectors (any Berger codes have this feature);
- *WTM*(*m*,*k*)-codes detect 100% of errors of multiplicity $d=m-1$ in data vectors;
- *WTM*(*m*,*k*)-codes do not detect 100% of errors of maximum multiplicity $d=m$ in data vectors;
- the number of undetectable errors of each multiplicity (as well as the total number of undetectable errors) is multiple of modulus M.

The properties of *WTM*(*m*,*k*)-codes are explained by the rules of its formation. For example, fault-tolerance is explained by the fact, that for weight ratios the sequence of positive integers from 1 to *m*–1 is used, and modulus for residue determination is always bigger than the maximum transition weight in data vector: $w_{m-1,m}=m-1$, $M = 2^{\lceil \log_2 (m+1) \rceil}$ and $M>m-1$. If modulus *M* will be equal to the weight of transition between the highest bits $w_{m,m-1}$, so the residue of this value would be 0: $(w_{m-1,m}) \bmod M = (M) \bmod M = 0$. And this would mean that even with activation of transition the weight values in total sum *W* would always be 0, and the bit would be uncontrolled.

TABLE IV
DISTRIBUTION OF DATA VECTORS OF *WT*8(5,3)-CODE WITHIN TEST GROUPS

W=(*V*)mod8							
0	1	2	3	4	5	6	7
Check vector							
000	**001**	**010**	**011**	**100**	**101**	**110**	**111**
00000	00001	00011	00010	00110	00100	00101	01000
01001	01011	01010	00111	01111	01110	01100	01101
10110	10100	10101	11000	10000	10001	10011	10010
11111	11110	11000	11101	11001	11011	11010	10111

TABLE V
DISTRIBUTION OF UNDETECTABLE ERRORS IN DATA VECTORS OF SOME *WTM*(*M*,*K*)-CODES

m	*k*	*M*	Distribution of undetectable errors by multiplicities, $N_{m,d}$												N_m
			1	2	3	4	5	6	7	8	9	10	11	12	
2	2	4	0	4											4
3	2	4	0	0	8										8
4	3	8	0	8	0	16									24
5	3	8	0	32	32	0	32								96
6	3	8	0	192	0	192	0	64							448
7	3	8	0	448	448	448	448	0	128						1920
8	4	16	0	832	0	1936	0	832	0	256					3856
9	4	16	0	2304	1280	4096	4096	1280	2304	0	512				15872
10	4	16	0	7680	0	24064	0	24064	0	7680	0	1024			64512
11	4	16	0	17408	7424	58496	45696	45696	58496	7424	17408	0	2048		260096
12	4	16	0	44032	0	242688	0	466944	0	242688	0	44032	0	4096	1044480

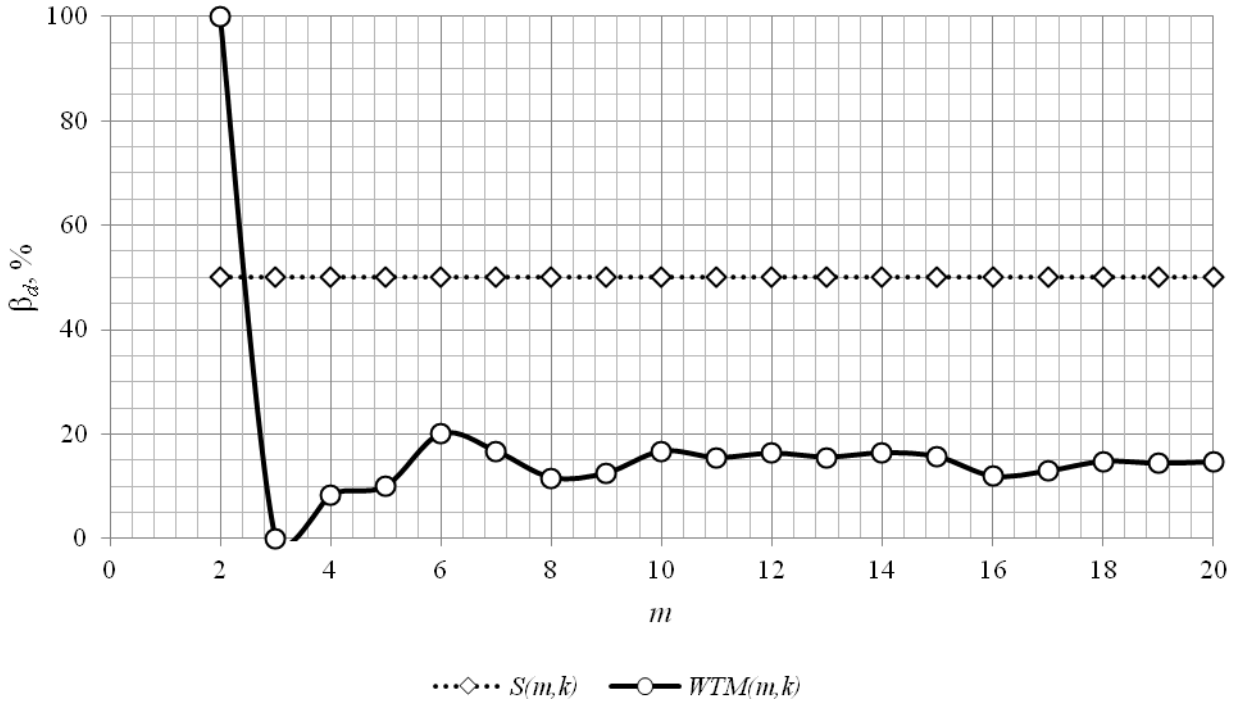

Fig. 3. Part of double undetectable errors in total number of double errors in *S*(*m*,*k*) and *WTM*(*m*,*k*)-codes

Fig. 3 gives the comparison of *WTM*(*m*,*k*)-codes and *S*(*m*,*k*)-codes by its ability of detection of double errors in data vectors – there is a function of the number of double undetectable errors in data vectors to the total number of double errors in data vectors (β_d) by the data vector length. Based on Fig. 3 it follows that *WTM*(*m*,*k*)-codes more than twice as effective in double errors detection, as *S*(*m*,*k*)-codes. Such improvement is true and for errors of any even multiplicities (Table VI). Diagrams of Fig. 4 show the function of η_m, which equals to the number of undetectable errors of given multiplicity in Berger codes and in weight-based codes of interest, to the data vector length *m*. The value η_m demonstrates what fold decrease the number of undetectable errors of given multiplicity in *WTM*(*m*,*k*)-codes in comparison with *S*(*m*,*k*)-codes with the specified *m* value.

For odd *m* values the efficiency of detection of errors of even multiplicities in *WTM*(*m*,*k*)-codes, in comparison with *m*±1, increases, that happens due to the presence of errors of odd multiplicities within the class of undetectable errors in codes with odd *m* values.

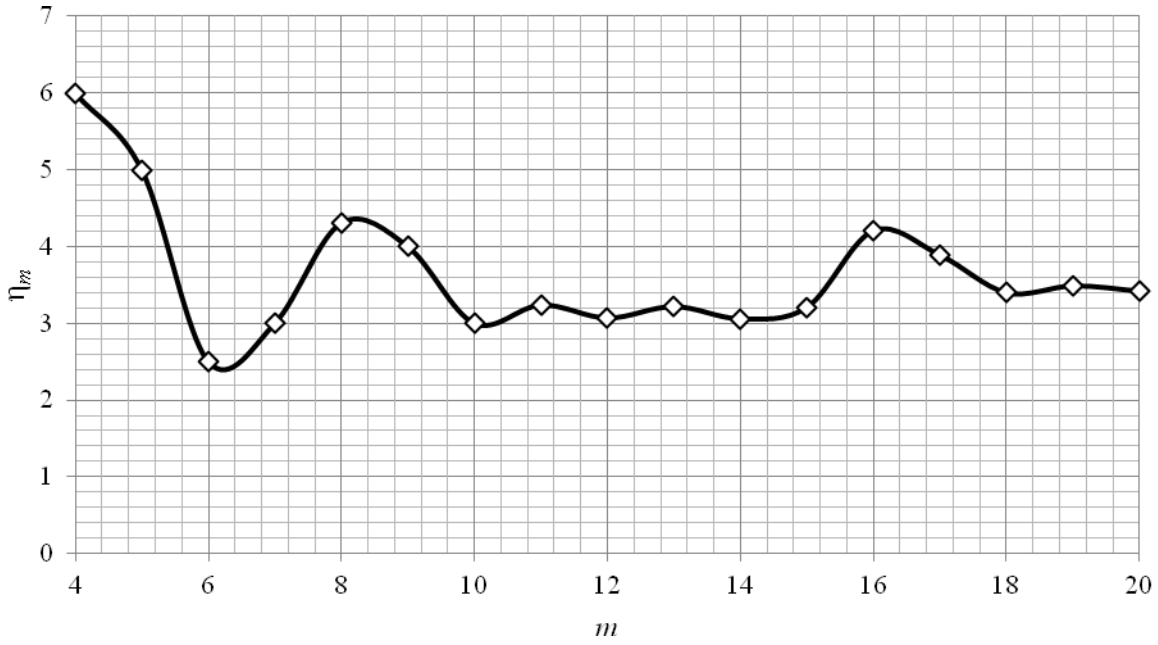

Fig. 4. Improving the characteristic of double errors detection of *WTM*(*m*,*k*)-codes in comparison with *S*(*m*,*k*)-codes

TABLE VI
VALUE BD FOR EACH MULTIPLICITY FOR CLASSIC AND WEIGHT-BASED SUM CODES

m	Part of undetectable errors of multiplicity *d* in total number of errors of given multiplicity, %																			
	1	**2**	3	4	5	6	7	8	9	10	11	12	13	14	15	16	17	18	19	20
WTM(*m*,*k*)-code																				
2	0	**100**																		
3	0	**0**	100																	
4	0	**8.33**	0	100																
5	0	**10**	10	0	100															
6	0	**20**	0	20	0	100														
7	0	**16.67**	10	10	16.67	0	100													
8	0	**11.61**	0	10.8	0	11.61	0	100												
9	0	**12.5**	2.98	6.35	6.35	2.98	12.5	0	100											
10	0	**16.67**	0	11.19	0	11.19	0	16.67	0	100										
11	0	**15.45**	2.2	8.66	4.83	4.83	8.66	2.2	15.45	0	100									
12	0	**16.29**	0	11.97	0	12.34	0	11.97	0	16.29	0	100								
13	0	**15.54**	2.05	8.89	4.75	6.54	6.54	4.75	8.89	2.05	15.54	0	100							
14	0	**16.35**	0	12.76	0	12.27	0	12.27	0	12.76	0	16.35	0	100						
15	0	**15.6**	3.1	9.23	4.26	7.32	5.79	5.79	7.32	4.26	9.23	3.1	15.6	0	100					
16	0	**11.88**	0	6.61	0	6.15	0	6.15	0	6.15	0	6.61	0	11.88	0	100				
17	0	**12.87**	0.81	5.65	1.7	4.09	2.49	3.27	3.27	2.49	4.09	1.7	5.65	0.81	12.87	0	100			
18	0	**14.71**	0	7.25	0	6.26	0	6.15	0	6.15	0	6.26	0	7.25	0	14.71	0	100		
19	0	**14.33**	0.68	6.47	1.46	4.5	2.2	3.61	2.9	2.9	3.61	2.2	4.5	1.46	6.47	0.68	14.33	0	100	
20	0	**14.61**	0	7.47	0	6.43	0	6.2	0	6.16	0	6.2	0	6.43	0	7.47	0	14.61	0	100
S(*m*,*k*)-code																				
2÷20	0	**50**	0	37.5	0	31.25	0	27.34	0	24.61	0	22.56	0	20.95	0	19.64	0	18.55	0	17.62

III. Conclusion

This paper suggests the method for formation of a sum code with minimum total number of undetectable errors in data vectors. Moreover, this new sum code more effectively detects the errors of low multiplicities in data vectors, than the classic Berger code. These advantages of *WTM*(*m*,*k*)-code can be considered while CED systems design with 100% detection of single faults in controlled logic units.

References

[1] E.S. Sogomonyan, and E.V. Slabakov "Self-Checking Devices and Fault-Tolerant Systems" (in Russ.), Moscow: Radio & Communication, 1989, 208 p.

[2] S.J. Piestrak "Design of Self-Testing Checkers for Unidirectional Error Detecting Codes", Wrocław: Oficyna Wydawnicza Politechniki Wrocławskiej, 1995, 111 p.

[3] Y.-Y. Guo, J.-C. Lo, and C. Metra "Fast and Area-Time Efficient Berger Code Checkers", *Workshop on Defect and Fault-Tolerance in VLSI Systems*, 1997, October 20-22, pp. 110-118.

[4] A.Yu. Matrosova, I. Levin, and S.A. Ostanin "Self-Checking Synchronous FSM Network Design with Low Overhead", *VLSI Design*. – 2000. – Vol. 11. – Issue 1. – Pp. 47-58.

[5] A. Matrosova, I. Levin, and S. Ostanin "Survivable Self-Checking Sequential Circuits", *Proc. of 2001 IEEE International Symposium on Defect and Fault Tolerance in VLSI Systems* (DFT 2001), Oct. 24-26, San Francisco, CA, 2001, 395-402 pp.

[6] L-T. Wang, C.E. Stroud, and N.A. Touba "System-on-Chip Test Architectures: Nanometer Design for Testability", Morgan Kaufmann Publishers, 2008, 856 p.

[7] R. Ubar, J. Raik, and H.-T. Vierhaus "Design and Test Technology for Dependable Systems-on-Chip (Premier Reference Source)", Information Science Reference, Hershey – New York, IGI Global, 2011, 578 p.

[8] A.H. Abdulhadi, and A.H. Maamar "Self Checking Register File Using Berger Code", *6th WSEAS International Conference on Circuits, Systems, Control & Signal Processing*, 2007, Cairo, Egypt, December 29-31, pp. 62-68.

[9] P. Srihari "Sum Codes: A Binary Channel Coding Scheme", *International Journal of Computer Science And Technology*, 2014, Vol. 5, Issue 1, pp. 60-64.

[10] N.K. Jha, and S. Wang "Design and Synthesis of Self-Checking VLSI Circuits", *IEEE Trans. Computer-Aided Design*, 1993, Vol. 12, Issue 6, pp. 878-887.

[11] S.S. Gorshe, and B. Bose "A Self-Checking ALU Design with Efficient Codes", *Proceedings of 14th VLSI Test Symposium*, Princeton, NJ, USA, 1996, pp. 157-161.

[12] M. Nicolaidis, and Y. Zorian "On-Line Testing for VLSI – A Compendium of Approaches", *Journal of Electronic Testing: Theory and Applications*, 1998, vol. 12, issue 1-2, pp. 7-20.

[13] O. Potin, Ch. Dufaza, and Ch. Landrault "A New Scheme for Off-Line and On-Line Testing With ABC And Berger Encoding", *Proc. 4th IEEE Int. On-line Testing Workshop*, Italia, Capri, 1998, 71-75.

[14] D. Das, and N.A. Touba "Weight-Based Codes and Their Application to Concurrent Error Detection of Multilevel Circuits", *Proc. 17th IEEE Test Symposium*, USA, California, 1999, pp. 370-376.

[15] V.V. Sapozhnikov, and Vl.V. Sapozhnikov "Self-Checking Discrete Devices" (in Russ.), St. Petersburg: Energoatomizdat, 1992, pp. 224.

[16] L.D. Cheremisinova "Logical Synthesis of Combinational KMOP Circuits Considering the Power Dissipation" (in Russ.), *Bulletin of Tomsk State University. Management, Computer Engineering and Informatics*, 2014, Issue 3, pp. 89-98.

[17] P.P. Parkhomenko, and E.S. Sogomonyan "Basics of Technical Diagnostics (Optimization of Diagnostic Algorithms and Equipment)" (in Russ.), Moscow: Energoatomizdat, 1981, pp. 320.

[18] J.M. Berger "A Note on Error Detection Codes for Asymmetric Channels", *Information and Control*, 1961, vol. 4, issue 1, pp. 68-73.

[19] D.V. Efanov, V.V. Sapozhnikov, and Vl.V. Sapozhnikov "On Sum Code Properties in Functional Control Circuits", *Automation and Remote Control*, 2010, vol. 71, issue 6, pp. 1117-1123.

[20] A.A. Blyudov, D.V. Efanov, V.V. Sapozhnikov, and Vl.V. Sapozhnikov "Formation of the Berger Modified Code with Minimum Number of Undetectable Errors of Informational Bits" (in Russ.)", *Electronic Modeling*, 2012, vol. 34, issue 6, pp. 17-29.

[21] A.A. Blyudov, D.V. Efanov, V.V. Sapozhnikov, and Vl.V. Sapozhnikov "Sum codes for organization of control of combinational circuits", *Automation and Remote Control*, 2013, vol. 74, issue 6, pp. 1020-1028.

[22] D. Efanov, V. Sapozhnikov, Vl. Sapozhnikov, and A. Blyudov "On the Problem of Selection of Sum Code for Combinational Circuit Test Organization", Proceedings of 11th IEEE East-West Design & Test Symposium (EWDTS`2013), Rostov-on-Don, Russia, September 27-30, 2013, pp. 261-266.

[23] A.A. Blyudov, D.V. Efanov, V.V. Sapozhnikov, and Vl.V. Sapozhnikov "On Codes with Summation of Unit Bits In Concurrent Error Detection Systems", *Automation and Remote Control*, 2014, vol. 75, issue 8, pp. 1460-1470.

[24] V.V. Saposhnikov, and Vl.V. Saposhnikov "New Code for Fault Detection in Logic Circuits", *Proc. 4th Int. Conf. on Unconventional Electromechanical and Electrical Systems*, St. Petersburg, Russia, June 21-24, 1999, pp. 693-696.

[25] V. Mehov, V. Saposhnikov, Vl. Sapozhnikov, and D. Urganskov "Concurrent Error Detection Based on New Code with Modulo Weighted Transitions between Information Bits", *Proc. of 7th IEEE East-West Design&Test Workshop (EWDTW`2007)*, Erevan, Armenia, September 25-30, 2007, pp. 21-26.

[26] V.B. Mekhov, V.V. Saposhnikov, and Vl.V. Saposhnikov "Checking of Combinational Circuits Basing on Modification Sum Codes", *Automation and Remote Control*, 2008, vol. 69, issue 8, pp. 1411-1422.

[27] V.V. Sapozhnikov, Vl.V. Sapozhnikov, D.V. Efanov, and V.V. Dmitriev "Properties Of Sum Codes With Weighted Transitions With Direct Sequence Of Weight Ratios (in Russ.)", *Computer Science and Control Systems*, 2014, issue 4, pp. 77-88.

Conductivity of Multi-Component Electron Gas

N.N. Chernyshov
Kharkov National University of Radio Electronics
Ukraine

***Abstract* - The 2D semimetal consisting of heavy holes and light electrons is studied. The consideration is based on the assumption that electrons are quantized by magnetic field while holes remain classical. We assume also that the interaction between components is weak and the conversion between components is absent. The kinetic equation for holes colliding with quantized electrons is utilized. It has been stated that the inter-component friction and corresponding correction to the dissipative conductivity σ_{xx} do not vanish at zero temperature due to degeneracy of the Landau levels. This correction arises when the Fermi level crosses the Landau level. The limits of kinetic equation applicability were found. We also study the situation of kinetic memory when particles repeatedly return to their meeting points.**

***Key words:* electron system, magnetic field, limit, kinetic equation, oscillator and distribution function.**

I. Introduction

Since the discovery of quantum Hall effect, the problem of 2D electron system in strong magnetic field has attracted big attention. It was generally accepted that the most interesting thing is the low-temperature limit when all inelastic processes are frozen out and the system can be treated as the electron-impurity one. Here we concentrate our consideration on the case of semimetal with coexist-ing electrons and holes. Such systems based on 2D layers were obtained and have been intensively studied for the recent years [1, 2]. The specificity of semimetal is the presence of electron-hole scattering. Due to large density of the second com-ponent this process can be comparable with the impurity scattering. Usually, in the Fermi system at T=0 the in-terparticle scattering disappears and the friction between components gives temperature additions T^2 to the transport coefficients [3]. This is not the case in the system with a degenerate ground state, in particular, caused by the Landau quantization. In such a system the scattering redistributes particles within the degenerate state that needs no energy transfer [4].

II. Problem formulation

We consider a 2D semimetal with q_e equivalent electron valleys and q_h equivalent hole valleys centered in points $\mathbf{p}_{e,i}$ and $\mathbf{p}_{h,i}$, correspondingly. The conduction bands with energy spectra $(\mathbf{p} - \mathbf{p}_{e,i})^2/2m_e$ overlaps with the valence bands $E_q - \varepsilon_{\mathbf{p}-\mathbf{p}h,i}$, $\varepsilon_{\mathbf{p}} = p^2/2m_h$ ($E_q > 0$). The hole mass m_h is assumed to be much larger than the electron mass m_e. The distances between electron and hole extrema $|\mathbf{p}_{h,i} - \mathbf{p}_{e,j}|$ are supposed to be large to suppress the electron-hole conversion. At the same time, the scattering between electrons and holes changing the momenta near extrema are permitted. Without the loss of generality, further we shall count the momenta from the band extrema and replace $\mathbf{p} - \mathbf{p}_{h,j} \to \mathbf{p}$, $\mathbf{p} - \mathbf{p}_{e,i} \to \mathbf{p}$.

The system is placed in a moderately strong magnetic field, such that the electrons are quantized, while holes stay classical. In other words, the number of filled hole Landau levels $N_h + 1$ is large, while the analogical electron number $N_e + 1$ has the order of unity. We shall consider the low-temperature limit when the electron transitions occur within the same Landau level and transitions between different electron Landau levels are forbidden. The energy conservation permits this process only when the Landau level is partially filled, i.e. in a state of compressible Landau liquid [5].

We shall neglect the rearrangement of the energy spectrum caused by the interaction between electrons and electrons with holes. The Landau levels widening will be also neglected. The interaction of quantized gas with a classical one is an unusual situation. The kinetics of holes can be described by a classical kinetic equation, while electrons need a quantum description. In accordance with above-mentioned, we shall use the states in crossed electric and magnetic fields $\psi_{n,k}(r) = e^{iky}\varphi_n((x - X_k)/a)/\sqrt{aL_y}$, where φ_n are normalized oscillator functions, L_y is the normalizing length of the system in y-direction, $X_k = X_k^{(0)} - v_d/\omega_e$, $X_k^{(0)} = -a^2k$ is the coordinate of the center of cyclotron motion, $v_d = c[\mathbf{E}, \mathbf{H}]/H^2$ is the drift velocity, $a = c/eH$ is the magnetic length, $\omega_e = eH/m_ec$ is the electron cyclotron frequency, $-e$ is the electron charge; we set $\hbar = 1$ and will restore the dimensionality in the final expressions. The corresponding energy is presented by $\varepsilon_{n,k} = \omega_e(n + 1/2) + eEX_k$.

III. Dissipative conductivity

The transmission of the momentum between electrons and holes is determined by the scattering processes. The collision term in the kinetic equation for holes in the Born approximation reads [6]

$$\hat{I}_{he}\{f_{\mathbf{p}}\} = \frac{2\pi}{S^2}2q_e\sum_{\mathbf{p}',\mathbf{q},\gamma,\gamma'}|u_{\mathbf{q}}|^2\delta_{\mathbf{p}',\mathbf{p}+\mathbf{q}}|J_{\gamma',\gamma}(\mathbf{q})|^2\delta(\varepsilon_{\mathbf{p}'} - \varepsilon_{\mathbf{p}} + \varepsilon_{\gamma'} - \varepsilon_{\gamma})\times$$
$$\times\left[f_{\mathbf{p}}(1-f_{\mathbf{p}'})\varphi_{\gamma}(1-\varphi_{\gamma'}) - f_{\mathbf{p}'}(1-f_{\mathbf{p}})\varphi_{\gamma'}(1-\varphi_{\gamma})\right]. \quad (1)$$

Here $u_{\mathbf{q}}$ is the Fourier transform of potential of interaction between electron and hole, S is the system area

$$\begin{cases} J_{\gamma',\gamma}(\mathbf{q}) = \langle\gamma'|e^{iqr}|\gamma\rangle; \\ \gamma = (n,k);\ \gamma' = (n',k'); \\ \varepsilon_p = p^2/2m_h, \end{cases} \quad (2)$$

Manuscript received March 3, 2015.

Nikolay Chernyshov is with the Kharkov National University of Radio Electronics, Department of Microelectronics, Electronic Valves and Devices, Ukraine, e-mail: chernyshov@kture.kharkov.ua.

is the hole energy (m_h is the hole effective mass). Due to the uniformity of the space the quantity φ_γ does not depend on the wave vector and coincides with the equilibrium distribution function. At zero temperature all factors $\varphi_{n'}(1-\varphi_n)\equiv 0$, excluding the contribution with $n = n^- = N_e$, where N_e is the number of the last partially filled Landau level. The quantities N_e and $\varphi N_e \equiv \nu$ can be expressed via the electron density n_e as $N_e = [n_e\pi a^2/q_e]$, $\nu = \{n_e\pi a^2/q_e\}$ (square and figure brackets mean the integer and fractional parts). We shall expand the collision term with respect to weak non-equilibrium, assuming that the electric field and the deviation of distribution function from equilibrium are small [7].

$$\hat{I}_{he}\{f_{\mathbf{p}}\} = \frac{4\pi q_e}{S^2}\sum_{\mathbf{p}',n,k} R_n(|\mathbf{p}-\mathbf{p}'|)\varphi_n^{(0)}\left(1-\varphi_n^{(0)}\right)\times$$
$$\times\left[\delta(\varepsilon_{\mathbf{p}}-\varepsilon_{\mathbf{p}'})(\delta f_{\mathbf{p}}-\delta f_{\mathbf{p}'})+\delta'(\varepsilon_{\mathbf{p}}-\varepsilon_{\mathbf{p}'})\times\right. \quad (3)$$
$$\left.\times eEa^2(p'_y-p_y)\left(f_{\mathbf{p}}^{(0)}-f_{\mathbf{p}'}^{(0)}\right)\right].$$

Here $\delta f_{\mathbf{p}}$ is linear in E correction to the hole distribution function, $f_{\mathbf{p}}^{(0)}, \varphi_n^{(0)}$ are equilibrium distribution functions of holes and electrons,

$$R_n(q) = |u_q|^2 L_n^2(q^2a^2/2)e^{-q^2a^2/2}, \quad (4)$$

L_n are the Laguerre polynomials. The function $R_n(q)$ has a characteristic size in q-space 1/s. The parameter S is determined by the largest of sizes of potential L and wave functions of electrons a 2(n + 1). In the coordinate space, S corresponds to the typical impact parameter for scattering. Let us consider the hole transport. The kinetic equation for the nonequlibrium correction to the distribution function $\delta f_{\mathbf{p}}$ reads

$$e\mathbf{E}\frac{\partial f_{\mathbf{p}}^{(0)}}{\partial \mathbf{p}} + \omega_h[\mathbf{p},\mathbf{h}]\frac{\partial \delta f_{\mathbf{p}}}{\partial \mathbf{p}} = \hat{I}_{he}\{f_{\mathbf{p}}\}, \quad (5)$$

were $\omega_h = eH/m_hc, \mathbf{h} = \mathbf{H}/H$.

IV. Finite Landau level width

The crucial point for the previous consideration, in particular, for temperature-independent contribution of e-h scattering to the dissipative conductivity is the presence of the Landau levels degeneracy. There are different sources of the Landau levels broadening. One source is the scattering of electrons on holes. The rate of this scattering γ_{eh} can be calculated summing the probability of scattering $W_{\gamma'}$ over the finite states. The result is [8]

$$\gamma_{eh} = \frac{m_h^2 q_h T}{\pi^2}\int_0^{2p_{F,h}} dq \frac{R_N^2(q)}{\sqrt{4p_{F,h}^2-q^2}}. \quad (6)$$

Like D_e the width γ_{eh} vanishes with the temperature, while the hole damping γ_{eh} vanishes with the temperature, while the hole damping γ_{he} stays finite at $T\to 0$.

The smallness of the Landau level width as compared with the temperature is the sufficient condition for the neglect of width. Estimations give $\gamma_{eh}/T \sim m_he^4/(\hbar^2\chi^2E_{F,h})$. The latter parameter is small if the holes are weakly interacting; this demand is supposed in the present study. In particular, the condition $m_he^4/(\hbar^2\chi^2E_{F,h}) << 1$ does not permit to consider the limit $m_h\to\infty$ when the holes become equivalent to immobile impurities. On the other hand, γ_{eh} may be omitted at a low enough T as compared with temperature independent Landau level width γ_i caused by the potential fluctuations. For a long-range potential γ_i is proportional to the amplitude of potential. For developed fluctuations the self consistent Born approximation gives the width of the Landau levels proportional to $\sqrt{n_i}$ (n_i is the impurity concentration) and the potential of individual impurity. The exception is the short-range impurities with $\delta-$like potential for which the part of the Landau level states $1/\pi a^2 - n_i$ remains degenerate if $1/\pi a^2 > n_i$, while n_i states form a band of localized states with a finite width. In the case of the Landau level with a finite width γ_i, the interparticle scattering depends on the radio of the temperature T to the width. If $T << \gamma_i$, the e-h scattering is suppressed and if $T >> \gamma_i$, the scattering does not notice the width. Thus, all the previous consideration of e-h scattering remains valid for intermediate temperature $\hbar\omega > T$. In the dissipative conductivity the scattering processes affect quantized electrons in a parallel manner. One can sum up the contributions to electron σ_{xx} conductivity caused by impurity scattering and electron-hole processes. According to [9], the contribution to electron dissipative current caused by short-range impurity scattering is

$$(\sigma_{xx})_{ei} = \frac{q_e e^2}{\pi^2\hbar}(N_e+1/2)(1-\mu^2). \quad (7)$$

The reduced distance between the Fermi level and the Landau level with number N_e, $\mu = \left(\varepsilon_{F,e}-(N_e+1/2)\omega_e\right)/\gamma N$, is connected with the quantity ν by the equation

$$\nu = \frac{1}{2\pi}\left(\pi + 2\mu\sqrt{1-\mu^2} + 2\arcsin\mu\right). \quad (8)$$

In the case of short-range impurities with small concentration $n_i << 1/\pi\alpha^2$, the absence of widening leads to the validity of the results obtained in the previous section up to zero temperature. In a wider range $n_i < 1/\pi\alpha^2$ the scattering rate $1/\tau_{he}$ should be corrected by the factor $1-n_i\pi\alpha^2$ reflecting the fraction of degenerate states. If the long-range potential fluctuation case is realized the degeneracy disappears. In the absence of e-h scattering, the model of adiabatic transport is valid when electron cyclotron centers are drifting along the lines of constant potential. Without the external field only one infinite fractal level line of the fluctuating potential corresponding to the percolation threshold exists. In the presence of the finite electric field, this level line decays to independent infinite entangled lines going across the external electric

field. The drift does not depend on the charge of particles: the velocities and trajectories of the cyclotron centers of quantized electrons and classical holes are same [10]. The dissipative conductivity of electrons vanishes, while the Hall conductivity changes stepwise between quantized Ne^2/h values. In the lack of degeneracy, the temperature independent e-h scattering also disappears.

V. Conclusion

We have studied the influence of electron-hole interaction on transport in the system where electrons are quantized and holes are not. In these conditions, the second type of carriers plays its role as an additional (or exceptional) channel of scattering. Weak electron-hole interaction can be considered in the Born approximation, despite the degeneracy of the Landau levels, in contrast to the impurity mechanism which is not perturbative in the quantizing magnetic field, even for a weak potential. The scattering of holes on quantized non-interacting electrons occurs if, and only if, the Landau level is partially filled. The chaotization results from the random distribution of electrons in the momentum space, and corresponding entropy at zero temperature remains finite. The scattering of holes can be considered by means of kinetic equation approxima-tion when the Fermi level is near the center of the Lan-dau levels; the kinetic approximation loses applicability apart from the center; on the far wings the holes become localized.

References

[1] Blokh M.D., Magarill L.I. Theory of photogalvanic effect on free carriers // PTG, vol. 22, №8, 1980, pp. 2279-2284 (in Russian).

[2] Chernyshov N.N. Theory of transfer phenomena in an electric field for crystals without an inversion centre // Physical surface engineering, vol. 10, №1, NPTC, Kharkov, 2012, pp. 96-101 (in Russian).

[3] Chernyshov N.N. Photogalvanic effect in crystals without a centre of inversion in view of electron-hole interaction /All- Ukrainian collected volume // Radiotechnika, № 177, KhNURE, 2014, pp. 94-97. (in Russian)

[4] Chernyshov N.N., Slipchenko N.I., Tsymbal A.M., Umyarov K.T, Lukianenko V.L. The photogalvanic effect within spin resonance in quantizing magnetic field // Physical surface engineering, vol. 11, №4, NPTC, Kharkov, 2013, pp. 427-430.

[5] Chern Y.F., Dobrovolska M., et al. Interference of electric-dipole and magnetic-dipole interactions in conduction-electron-spin resonance in InSb // Phys. Rev. B., vol. 32, 1985, pp. 890-902.

[6] Gantmakher V.F., Levinson Y. B.. Sov. Phys. // JETP 47, 1978, 133 p.

[7] Adams E.N., Holstein T.D.. J. Phys. Chem. Solids 10, 1959, 254 p.

[8] Ando T., Uemura Y.. J. Phys. Soc. Jpn 36, 1974, 959 p.

[9] Baskin E.M., L.I. Magarill. Sov. Phys. // JETP 48, 1978, 365 p.

[10] Fogler M., Perel V., B. Shklovskii, Phys. Rev. B 56, 1997, 6823 p.

Nikolay Chernyshov is with the Kharkov National University of Radio Electronics, Department of Microelectronics and Electronic Valves and Devices, Ukraine,
e-mail: chernyshov@kture.kharkov.ua

Secure Multipath Routing Algorithm with Optimal Balancing Message Fragments in MANET

Oleksandra S. Yeremenko, Ali Salem Ali

***Abstract*—This paper is devoted to the proposition of the algorithm of secure multipath routing with optimal balancing message fragments number in MANET. The work considered the concept of the threshold secret sharing scheme in relation to secure routing using non-overlapping paths for the message fragments transmission. Based on the analysis of disadvantages of existing mechanism SPREAD, it was proposed to improve the fragments allocation model, which had been reduced to the optimal balancing of message fragments number transmitted over the non-overlapping paths. Several optimality criteria were suggested as to the solution of balancing problem using Shamir`s scheme with or without redundancy. In the comparative analysis it was justified to use optimality criterion in practice, providing, on the one hand, minimization of dynamically managed upper bound number of fragments transmitted over separate non-overlapping paths in the network, and on the other hand – adaptation to security parameters (probability of compromise) of individual network elements: nodes, links and paths. Numerical examples of models with different optimality criteria of the solutions obtained, and their comparative analysis were presented. Within the proposed algorithm it is suggested to use the model under which the minimum number of fragments is transmitted by the worst path in terms of the probability of compromise, whereas their maximum number - by the best path.**

***Keywords*—Secure routing, MANET, probability of compromise, number of fragments balancing, non-overlapping paths.**

I. Introduction

MOBILE self-organizing networks MANET (Mobile Ad Hoc Network) is widely used nowadays in various applications as it was shown by the analysis. In accordance with the principles of its construction MANET is a complex organizational and technical system, which includes distributed in a certain area mobile nodes with the role of the structural and functional adaptation to signal interference situation, number and content of the supported services, requirements to Quality of Service and security level of transmitted data. Along with the objectives of guaranteeing Quality of Service in the MANET design and operation the key challenge is to ensure information security of the data transmitted by the network [1].

Compared to wired networks ensuring of information security in MANET is associated with the detection and prevention of many existing vulnerabilities and attacks [2]. Firstly, wireless channels are more susceptible to attacks such as passive listening (eavesdropping), active interference of signals and jamming. Secondly, the majority of routing protocols in MANET imply trusted interaction between participating nodes for packet transmission. Dependence on such interaction makes data more vulnerable to unauthorized access, data substitution, and attacks such as "Denial of Service" (DoS). Thirdly, the absence of fixed infrastructure and centralized management makes it difficult to apply many of the traditional solutions to ensure information security.

II. Threshold Message Sharing Mechanism

One of the approaches of ensuring the specified level of information security in communication networks is the implementation of SPREAD mechanism [3, 4], based on the multipath message routing after its fragmentation to parts in accordance with the Shamir`s scheme [3-5] (fig. 1). As a result of using SPREAD mechanism it is possible to reduce the probability of compromise of the transmitted message, because it complicates the adversary`s task: it must compromise not only one path that passed undivided message, but all paths transmitting its fragments. A message is compromised in case of unauthorized access to its content, i.e. in order to compromise the message, transmitted using SPREAD mechanism, all the paths used to deliver message fragments must be compromised. Thus, the fact of a compromised path is adversary access to all message fragments, transmitted over this path.

It should be noted that probability of compromise of individual path depends on the number of nodes and links it consists of and their security parameters, i.e. each element of the path (node, link) can be compromised with a certain probability. In general, various paths used to transmit the

Manuscript received March 12, 2015.

Oleksandra Yeremenko is with Kharkiv National University of Radio Electronics. Faculty of Telecommunications and Instrumentation, Department of Telecommunication Systems, Kharkiv, Ukraine (corresponding author to provide phone/fax: +38057-702-13-20; e-mail: alexere@ukr.net)

Ali Salem Ali is with Al Iraqi University, Network Engineering Department, Adhamiya, Baghdad, Iraq (e-mail: Alialbander2004@yahoo.com).

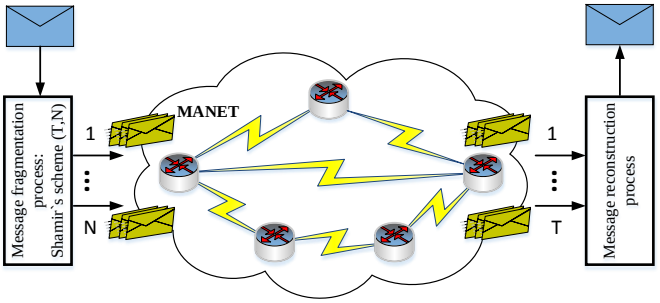

Fig. 1. Message fragmentation according to Shamir`s scheme.

message fragments obtained in accordance with the Shamir`s scheme [3-5] can have different values of the probability of compromise. Unfortunately, under the well-known mathematical models [3, 4] devoted to realization of SPREAD in message fragments allocation over the non-overlapping paths security parameters (such as the probability of compromise) of these are not taken into account explicitly. Thus, the actual problem seems related to the improvement of the mathematical model of secure routing message transmitted over the network based on the optimal allocation of its fragments over non-overlapping paths resulting from the use of applying Shamir`s scheme, and comprehensive address to the security parameters of available paths.

III. Secure Routing Models

Within the model let it be assumed that the following inputs are known:

- S_{msg} and D_{msg} – sender and receiver of a transmitted message;
- M – number of used non-overlapping paths in routing message fragments;
- (T, N) – Shamir`s scheme parameters, where $N$ – total number of fragments, obtained by applying the Shamir`s scheme; T – minimum number of fragments ($T \le N$) needed for the message reconstruction;
- p_i^j – probability of compromise j-th element (node, link) of i-th path;
- M_i – number of elements in the i-th path that can be compromised;
- γ_P – acceptable probability of compromise of message in the network.

In addition, the following parameters should be introduced in the model description:

- n_i – number of fragments, transmitted over the i-th path ($i = \overline{1, M}$);
- P_{msg} – probability of compromise for the whole message during its transmission by fragments over the network.

It is assumed that the sender and the receiver are trusted, i.e. probability of compromise of the sender and receiver nodes is equal to zero. Furthermore, within the proposed solution (as in [3-5]) it is supposed that if the element (node, link) is compromised, all fragments transmitted through the element will also be compromised. Then the probability of compromise of the i-th path consisting of the M_i elements can be calculated by the expression

$$p_i = 1-(1-p_i^1)(1-p_i^2)\dots(1-p_i^{M_i}) = 1-\prod_{j=1}^{M_i}(1-p_i^j). \quad (1)$$

Besides, during the calculation of the control variables n_i ($i = \overline{1, M}$) regulating the allocation of the message fragments over the non-overlapping paths the following condition [2-4] must be met:

$$N = \sum_{i=1}^{M} n_i . \quad (2)$$

In the case of Shamir`s scheme with redundancy when $T < N$ the condition below must be satisfied

$$N - n_i < T , (i = \overline{1, M}). \quad (3)$$

while when $T = N$ the following conditions must be met in the non-redundant sharing scheme

$$1 \le n_i \le T-1 , (i = \overline{1, M}). \quad (4)$$

Condition (4) ensures that in the case of compromising all the paths except i-th path an adversary cannot reconstruct the whole message.

One of the main conditions to be satisfied within the secure routing is that the probability of compromise of the message transmitted over the network must not exceed a specified acceptable value

$$P_{msg} \le \gamma_P . \quad (5)$$

For example, the probability of compromise of a message divided to the N fragments using Shamir`s scheme with parameters (N, N) transmitted over the M paths determined by the expression

$$P_{msg} = \prod_{i=1}^{M} p_i . \quad (6)$$

Satisfaction of condition (5) in accordance with expressions (1) and (6) must be provided during the pre-solution of the problem of calculation of the set of non-overlapping paths in the network. Model 1 may use expressions (1)-(6) proposed in works [3, 4]. Model 1 can be modified due to its disadvantages in relation to optimality of allocation message fragments over the transmission paths.

Model 2 includes constraint conditions (1), (2), (4)-(6) but uses as a criterion of optimal allocation fragments number over the non-overlapping paths the minimum of objective function

$$J = \sum_{i=1}^{M} p_i n_i , \quad (7),$$

which ensures secure routing over the network when the maximum number of message fragments will be sent over the path with the minimum probability of compromise. Conversely over the path with the highest probability of

compromise will be transmitted the minimum number of message fragments.

Model 3 can be described by the following terms. To ensure the optimal balancing of transmitted message fragments over multiple non-overlapping paths to the structure of improved model additional conditions are introduced:

$$n_i \le \beta \ \ (i = \overline{1, M}), \tag{8}$$

where β is a dynamically managed upper bound number of fragments transmitted over separate non-overlapping paths in the network.

Then, as a criterion for optimal solution for the allocation of the number of transmitted message fragments over non-overlapping paths it is reasonable to choose the minimum of the following objective function

$$J = \beta + \sum_{i=1}^{M} p_i n_i \ . \tag{9}$$

Minimization of equation (9) should be carried out under the conditions of constraint equations (2) and (8), thus reducing by the value β maximum number of fragments transmitted in each of the selected paths. Introduction to the object function (9) the term $\sum_{i=1}^{M} p_i n_i$ is aimed at achieving the following objective: if the total number of fragments N is not a multiple of paths number M, then the greater number of fragments will be transmitted over the best path in terms of the probability of compromise. This is the main advantage of the proposed solution and difference from the existing models [3-5].

Model 4 is represented by constraint conditions (1), (2), (5), (6), but the objective function below was chosen as optimality criterion

$$J = \sum_{i=1}^{M} (p_i n_i)^2 \ , \tag{10}$$

which is an extension of the expression (7).

IV. Comparative Analysis of Secure Routing Models

Comparative analysis of solving a problem of allocation message fragments over the non-overlapping paths of four models with different optimality criterions was performed.

Features of the models and proposed solutions (Model 1 ÷ Model 4) will be demonstrated by the following example. Suppose that a pair of nodes, a sender and a receiver, is given, and there are three non-overlapping paths available with different number of elements, nodes and links, between them (fig. 2). Within the example it is agreed that just links can be compromised, which is fair enough for MANET. For the purpose of calculations the following will be assumed:

- for the message fragmentation two cases of Shamir`s scheme are used: (10, 10) without redundancy, and (8, 10) with redundancy;
- the probability of compromise for communication links in accordance with their numbering and belonging to non-overlapping paths in MANET (fig. 2) takes the following values: $p_1^1 = 0{,}5$; $p_1^2 = 0{,}6$; $p_2^1 = 0{,}75$; $p_3^1 = 0{,}45$; $p_3^2 = 0{,}1$; $p_3^3 = 0{,}2$.

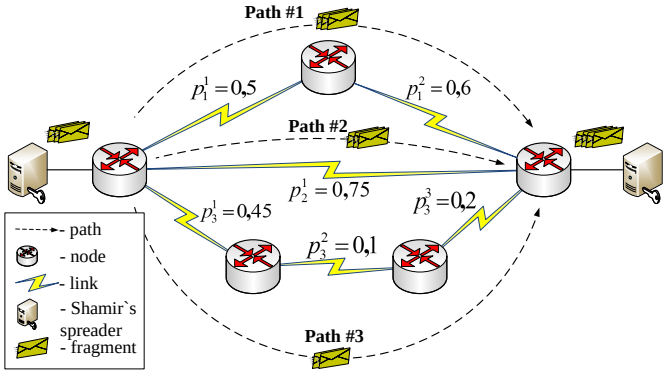

Fig. 2. Initial structure of MANET.

In accordance with expression (1) the following values of the probability of compromise for every path were calculated: $p_1 = 0{,}8$; $p_2 = 0{,}75$; $p_3 = 0{,}604$.

Table 1 shows the valid solutions of the problem of message fragments allocation over the non-overlapping paths obtained through the use of the previously described models.

Consider the case of using the Shamir`s scheme without redundancy, for example, (10, 10). the analysis of calculation results and the comparison of the obtained values of message fragments number allocated over the different paths showed that all four models can give satisfactory solutions. This can be explained by the fact that for compromising the whole message all three paths should be compromised. However, the best models are Model 3 and Model 4, since they imply adaptation to security parameters (Table 1), when the maximum number of message fragments is transmitted over the best path in terms of probability of compromise.

While using Model 1 (Table 1) one of the possible solutions of message fragments allocation over non-overlapping paths is when the maximum number of fragments ($n_1 = 8$)will be transmitted by the worst path in terms of probability of compromise ($p_1 = 0{,}8$), which is a disadvantage of this model.

TABLE I
Comparison of Existing Model and Improved Models of Message Fragments Allocation with Optimal Balancing

Model #	Number of message fragments in path depending on the allocation method			
	Model 1	Model 2	Model 3	Model 4
Path #	Shamir`s scheme (10, 10)			
1	8	1	2	3
2	1	1	4	3
3	1	8	4	4
Path #	Shamir`s scheme (8, 10)			
1	4	1	2	3
2	3	1	4	3
3	3	8	4	4

According to Model 2 using Shamir`s scheme (10, 10) message fragments allocation over the network paths showed

that the maximum number of fragments ($n_3 = 8$)passed over the best in terms of probability of compromise path ($p_3 = 0{,}604$), and their minimum number ($n_1 = 1$) was transmitted in the worst case ($p_1 = 0{,}8$).

Consider the case of using the Shamir`s scheme with redundancy, for example, (8, 10). The best solutions were provided by Model 1 and Model 4, because for compromising the whole message all three paths should be compromised. While in Model 2 the adversary needs to compromise just one path for the reconstruction of the transmitted message ($n_3 = 8$, $T = 8$), and in Model 3 two paths should be compromised ($n_2 = 4$, $n_3 = 4$, $T = 8$).

Model 1 with redundancy based on conditions (1)-(3), (5), (6 provides quite a good solution in terms of optimal allocation of message fragments over non-overlapping paths (Table 1). From the practical viewpoint it is desirable that the process of fragments allocation over the network paths must be balanced to make adversary`s tasks as complicated as possible.

Model 4, based on constraint conditions (1), (2), (5), (6) and the optimality criterion (10), gives the best solution compared to all four models. Using this model it is possible to provide on the one hand the optimal balancing of message fragments transmitted over separate non-overlapping paths in the network, and on the other hand – adaptation to security parameters (probability of compromise) of individual network elements: links and paths. In this case the minimum number of fragments ($n_1 = 3$) is transmitted by the worst path in terms of the probability of compromise, andtheir maximum number ($n_3 = 4$) is transmitted by the best one (Table 1). Therefore, the solution obtained by Model 4 is more preferable because of its ability to adapt to the security parameters of network paths.

V. Conclusion

Thus, the algorithm for secure multipath routing with optimal balancing message fragments in MANET includes the following steps:

1. Analysis of MANET architecture (number of network elements, Quality of Service and security requirements, signal-noise conditions etc).
2. Calculation of the set of non-overlapping paths between given sender and receiver nodes in consequence of condition (5).
3. Fragmentation of transmitted message according to selected Shamir`s scheme with or without redundancy.
4. Optimal allocation of the message fragments over the set of non-overlapping paths based on the model including expressions (1), (2), (5), (6) and optimality criterion (10).

Disadvantages of existing solutions consist in the fact that the process of allocation of message fragments over the non-overlapping paths is not balanced and doesn't provide adaptation of the obtained solutions to security parameters of network elements. Therefore, within the existing models [3-5] it may occur with the fragments allocation that the worst path in terms of the probability of compromise will transmit the maximum number of fragments. Nevertheless, the proposed model procedure for allocation of the transmitted message fragments over the non-overlapping paths is more adapted to security parameters (for example, the probability of compromise) of the individual network elements: nodes, links, and paths. This can be confirmed by the numerical results, when the minimum number of fragments is transmitted by the worst path in terms of the probability of compromise, and their the maximum number is passed by the best one.

The suggested algorithm may be used in practice within secure multipath routing with optimal balancing of message fragments transmitted over the non-overlapping paths. That is due to the fact that one of the key problems in operation of mobile self-organizing networks is ensuring of information security for data transmission through communicational links which in turn are the most vulnerable in MANET.

References

[1] *RFC 2501. Mobile Ad hoc Networking (MANET): Routing Protocol Performance Issues and Evaluation Considerations*. 1999.

[2] *ITU-T X-805. Security architecture for systems providing end-to-end communications*. 2003.

[3] W. Lou, W. Liu, Y. Fang, "SPREAD: Enhancing Data Confidentiality in Mobile Ad Hoc Networks", *INFOCOM 2004, Twenty-third Annual Joint Conference of the IEEE Computer and Communications Societies, IEEE*, Vol. 4, 2004, pp. 2404-2413.

[4] W. Lou, Y. Kwon, "H-SPREAD: A Hybrid Multipath Scheme for Secure and Reliable Data Collection in Wireless Sensor Networks", *Vehicular Technology, IEEE Transactions on*, Vol. 55, Issue 4, 2006, pp. 1320-1330.

[5] S. Alouneh, A. En-Nouaary, A. Agarwal, "A Multiple LSPs Approach to Secure Data in MPLS Networks", *Journal of Networks*, Vol. 2, Issue 4, 2007, pp. 51-58.

Oleksandra S. Yeremenko received her Ph.D. in Telecommunication Systems and Networks from the Kharkiv National University of Radio Electronics (2008) and academic rank of Senior Researcher (2012). She joined the Department of Telecommunication Systems at the Kharkiv National University of Radio Electronics as a senior research assistant in 2007. She has been an associate professor of the Department of Telecommunication Systems since 2011. Her current research interests are NGN, TCP/IP, Network Security, and Fault-Tolerant Routing.

Ali Salem Ali received his B.Sc. in Computer Science from the Al-ma`amoon University, Baghdad, Iraq (2005) and M.Sc. from the National Technical University Kharkiv Polytechnic Institute (2008). He received his Ph.D. in Telecommunication Systems and Networks from the Kharkiv National University of Radio Electronics (2012). He joined the Network Engineering Department at the Al Iraqi University (Iraq, Baghdad, Adhamiya) as a Teacher in 2012. His current research interests are in the area of Network Protocols and Routing.

Parameter Identification of Competitive Diffusion of Nanoporous Particles Media Using Gradient Method and the Heviside's Operational Method

M. Petryk

SoftWare Egeneering Departement,Ternopil Ivan Pulu'y National Technical University

Abstract **– The identification of competitive diffusion parameters in heterogeneous nanoporous materials is analyzed. Solutions to the direct and inverse problems are basing on the Heaviside's operational method and gradient method are obtained. New procedures for identification of diffusion coefficients for co-diffusing components (benzene and hexane) in intra- and intercrystallite spaces are implemented using high-speed gradient methods and mathematical diffusion models as well as the NMR spectra of the adsorbed mass distribution of each component in the zeolite bed. The gradient of the residual functional is obtained basing on optimal control theory. These diffusion coefficients are obtained as a function of time for different positions along the bed. Benzene and hexane concentrations in the inter- and intracrystallite spaces for every position in the bed and for different adsorption times are calculated.**

Key words: **mathematical model, competitive diffusion, direct end inverse boundary problems, functional identification, gradient method, Heviside's operational method, nanoporous media.**

I. Introduction

New theoretical developments in system analysis and mathematical modeling constitute the basis for information technologies of the control of research experiment and the analysis of the state of complex physical objects. The latter include multicomponent systems of competitive mass transfer in nanoporous media; studying their kinetics is an important problem of the modern nanophysics and nanodiffusion.

Nanoporous media widely used in various branches of industry (medicine, petrochemistry, catalysis, partition of liquids and gases) consist of porous structure particles with different physical and chemical (including diffusion) properties. Nanoporous media is a multilevel system of pores with two most important subsystems (spaces): system of micropores and nanopores with high adsorption capacity and low diffusion penetration rate (intraparticle space) and system of macropores and cavities among particles with low capacity and high penetration rate (interparticle space) [1–4].

The numerous studies in this domain concerned molecular transport of isolated substances in a porous medium, where mass transfer was mainly considered on a macrolevel without significant influence of micro- and nanotransfer in particles [1–8], which is a limiting and governing factor of the general kinetics. The major problems of intermolecular interactions, based on the Langmuir–Hinshelwood principle [4], which take place in real systems of diffusion "competition"(competitive diffusion of two and more substances) are not investigated.

Identifying of kinetic transfer parameters that determine the rate of the process at macro- and microlevels and the conditions of their equilibrium is an important scientific problem, which arises along with determining the concentration and gradient fields for each diffusing substance.

II. The Objective And Investigation Tasks

The objective of the work is the development of highly efficient and high-speed parameter identification methods of competitive diffusion of gases in the catalytic media of nanoporous particles taking into account the complex of limiting physical factors of inner transfer kinetics.

The following taskes are stated:

- to stady theoretically the competitive diffusion in media of particles (crystallites) of nanoporous structure, the mechanisms of mass transfer in the system «itercrystallite space-nanoporous particles", intereactions and flow of micro- and macrotransfer, equilibrium conditions,
- basing on the optimal control theory developed for multicomponent distributed systems to state and to interpret the direct and conjugate coefficient identification problems on the basis of functional (residual, error), to implement the gradient procedure of parameter identification;
- to justifay mathematically and to construct analytical solutions of direct and conjugate problems using the Heviside's operational method,
- to implement the technology of transfer parameter identification on the basis of obtaining explicit expressions of gradients residual functional, identification and modeling, to define the distributions of the diffusion kinetic parameters.

Manuscript received February 7, 2015.

Petryk M. is with the Ternopil National Technical University named after Ivan Pulu'y. Address: 56 rue Ruska, 46001 Ternopil, Tél. 38 035 2 25 64 96 ; Fax 38 035 2 25 49 83, e-mail:: Mykhaylo_Petryk@tu.edu.te.ua ; SoftEng@utc.fr

III. MATHEMATICAL MODEL OF COMPETITIVE DIFFUSION IN MICROPOROUS SOLIDS

The model presented is similar to the biporous model [6, 7, 15, 16]. We consider a system of complex competitive mass transfers between two diffusing components (benzene and hexane) in a heterogeneous medium (crystallite bed) with crystallites of nanoporous structure. The diffusion process involves two types of mass transfer: diffusion in the macropores (intercrystallite space), and diffusion in the micropores of crystallites (intracrystallite space).

A cylindrical bed of zeolite crystallites, assumed to be spherical (radius R), is exposed to a constant concentration of adsorbate in the gas phase (Fig. 1). One face of this bed is permeable to the two gases. In this case one can consider that diffusion of the two gases is axial in the macropores of the intercrystallite space (z direction along the height, l, of the bed) and radial in the micropores of the zeolite. We have made the following assumptions: (i) during the evolution of the system towards equilibrium there is a concentration gradient in the macropores and/or in the micropores; (ii) the effect of heat is negligible; (iii) diffusion occurs in the Henry's law region of the adsorption isotherm; (iv) all crystallites are spherical and have the same radius R; (v) the crystallite bed is uniformly packed.

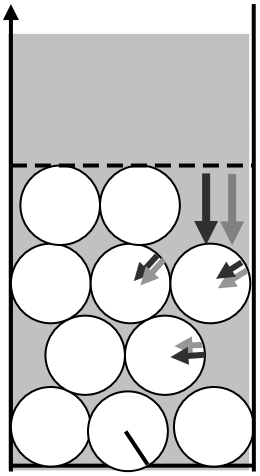

Fig. 1. Schema of diffusion competitive in nanoporous particles media

The coefficients of competitive diffusion in intracrystallite space D_{intra_s} and intercrystallite space D_{intra_s}, $s=\overline{1,2}$ (s = 1 for benzene and s = 2 for hexane) being unknown, the mathematical model of gas diffusion kinetics in the zeolite bed is defined in domains: $\Omega_T = (0,T)\times\Omega,\ \Omega = (0,1)$ by the solutions of the system of differential equations (with dimensionless coordinates defined in the nomenclature) [5, 8]:

$$\frac{\partial C_s(t,Z)}{\partial t} = \frac{D_{inter_s}}{l^2}\frac{\partial^2 C_s}{\partial Z^2} - e_{inter} K_s \frac{D_{intra_s}}{R^2}\left(\frac{\partial Q_s}{\partial X}\right)_{X=1}, \quad (1)$$

$$\frac{\partial Q_s(t,X,Z)}{\partial t} = \frac{D_{intra_s}}{R^2}\left(\frac{\partial^2 Q_s}{\partial X^2} + \frac{2}{X}\frac{\partial Q_s}{\partial X}\right). \quad (2)$$

Initial conditions

$$C_s(t=0,Z)=0;\ \ Q_s(t=0,X,Z)=0;\ X\in(0,1),\ Z\in\Omega, \quad (3)$$

boundary conditions for coordinate Z:

$$C_s(t,1)=1,\ \frac{\partial C_s}{\partial Z}(t,Z=0)=0,\ t\in(0,T); \quad (4)$$

boundary conditions at itch point $(Z,t)\subset\Omega_T$ for concentrations Q_s for particle radius X :

$$\frac{\partial}{\partial X}Q_s(t,X=0,Z)=0 \text{ (symmetry condition)}, \quad (5)$$

$$Q_s(t,X=1,Z)=C_s(t,Z) \text{ (equilibrium condition)},\ t\in(0,T),\ Z\in\Omega; \quad (6)$$

additional condition (*experimental data*):

$$\left[C_s(t,Z)+\bar{Q}_s(t,Z)\right]\Big|_\gamma = M_s(t,Z)\Big|_\gamma,\ s=\overline{1,2};\gamma\in\Omega,\ t\in(0,T). \quad (7)$$

The problem of the calculation (1)–(7) is: to find unknown functions $D_{intra_s}\in\Omega_T$, $D_{inter_s}\in\Omega_T$ ($D_{intra_s}>0$, $D_{inter_s}>0$, $s=\overline{1,2}$), when absorbed masses $C_s(t,Z)+\bar{Q}_s(t,Z)$ satisfy the condition (7) for every point $\gamma\subset\Omega$ [16, 17].

Here:

$$e_{inter}=\frac{\varepsilon_{inter}c_s}{\varepsilon_{inter}c_s+(1-\varepsilon_{inter})q_s}\approx\frac{\varepsilon_{inter}}{(1-\varepsilon_{inter})K_s};\ e_{intra}=1-e_{inter},\ K_s=\frac{q_{s_\infty}}{c_{s_\infty}},$$

$\bar{Q}_s(t,Z)=\int_0^1 Q_s(t,X,Z)X\,dX$ - average concentration of adsorbed component s ($s=\overline{1,2}$) in micropores; $M_s(t,Z)\big|_\gamma$ - experimental distribution of absorbed mass in macro- and micropores) at $\gamma\subset\Omega$ (results of NMR data) [8].

IV. MATHEMATICAL JUSTIFICATION OF THE IDENTIFICATION PROBLEM SOLVABILITY

The identification of diffusion coefficients D_{intra_s} and D_{inter_s} is a complex mathematical problem. In general, it is not possible to obtain a correct statement of the problem of calculation of diffusion coefficients (1) - (7) and to construct a unique analytical solution, because of the complexity of taking into account all the physical parameters (variation of temperature or pressure, crystallite structures, non-linearity of Langmuir isotherms, etc.), as well as the insufficient number of reliable experimental data, measurement errors and other factors.

Therefore, according to the principle of Tikhonov [12], later developed by Lions [13] and Sergienko and Deineka [17], the same problems of identification of diffusion coefficients require the specification of the model solution with each iteration step, by minimizing the difference between the calculated values and the experimental data.

The method proposed is a generalization of the identification approaches presented in [7, 15, 16]; it allows to reduce the number of iterations to 2-3 of magnitude for each specification cycle. It can also be used to identify parameters for more complicated adsorption systems and to identify three or more parameters simultaneously.

The solution of the problem of calculation of diffusion coefficients (1) - (7) is reduced to the problem of minimizing the functional of the difference (9) between the model solution and the experimental data, the solution being refined incrementally by means of a special regularisation procedure which uses fast, high-performance gradient methods [13, 14, 17].

Gradient methods of diffusion coefficients identification based on a Lagrange functional of residuals (target, error, etc.) have found practical application in the work of Lions [13] (problems of thermoelasticity), later developed by Alifanov (calculation of temperature fields for plane apparatus elements) [14], then by Sergienko, Deineka, Petryk, and Fraissard (problems of hydromechanics, of filtration, of adsorption, etc.) [17, 15, 16].

Gradient method of identification. According to [17, 16] and using the error minimization gradient method for identification of competitive diffusion coefficients for intracrystallite space D_{intra_s} and intercrystallite space D_{inter_s} of the s-th diffusing component, we obtain the iteration expression for the $n+1$-th identification step:

$$D^{n+1}_{intra_s}(t)=D^{n}_{intra_s}(t)-\nabla J^{n}_{D_{intra_s}}(t)\frac{\left[E^{n}_{s}\left(D^{n}_{intra_s},D^{n}_{inter_s};t,\gamma\right)\right]^2}{\left\|\nabla J^{n}_{D_{intra_s}}(t)\right\|^2+\left\|\nabla J^{n}_{D_{inter_s}}(t)\right\|^2},$$

$$D^{n+1}_{inter_s}(t)=D^{n}_{inter_s}(t)-\nabla J^{n}_{D_{inter_s}}(t)\frac{\left[E^{n}_{s}\left(D^{n}_{intra_s},D^{n}_{inter_s};t,\gamma\right)\right]^2}{\left\|\nabla J^{n}_{D_{intra_s}}(t)\right\|^2+\left\|\nabla J^{n}_{D_{inter_s}}(t)\right\|^2}, \quad (8)$$

where $J\left(D_{inter_s},D_{intra_s}\right)$ - the error functional (residual), which describes the deviation of the model solution from the experimental data on $\gamma\in\Omega$ written as:

$$J(D_{inter_s},D_{intra_s})=\frac{1}{2}\int_0^T\left[C_s(t,Z,D_{inter_s},D_{intra_s})+\bar{Q}_s(t,Z,D_{inter_s},D_{intra_s})-M_s(t)\right]^2_{\gamma}dt, \quad (9)$$

where $\nabla J^{n}_{D_{intra_s}}(t)$, $\nabla J^{n}_{D_{intra_s}}(t)$ - the gradients of the error functional $J\left(D_{inter_s},D_{intra_s}\right)$,

$$\left\|\nabla J^{n}_{D_{intra_s}}(t)\right\|^2=\int_0^T\left[\nabla J^{n}_{D_{intra_s}}(t)\right]^2dt,\ \left\|\nabla J^{n}_{D_{inter_s}}(t)\right\|^2=\int_0^T\left[\nabla J^{n}_{D_{inter_s}}(t)\right]^2dt,$$

$$E^{n}_{s}(t)=C_s(D^{n}_{intra_s},D^{n}_{inter_s};t,\gamma)+\bar{Q}_s(D^{n}_{intra_s},D^{n}_{inter_s};t,\gamma)-M_s(t).$$

V. Analytical Solution Of Direct Problem

The solution C_s, Q_s of the direct problem (1)-(6) was obtained by the procedure described in [6] using the Heaviside's operational method:

$$C_s(t,Z)=1+2\pi\left(\frac{R}{l}\right)^2\frac{D_{inter_s}}{D_{intra_s}}\sum_{n=1}^{\infty}\sum_{k=1}^{\infty}\Phi(\beta_{kn},Z)\exp\left(-\frac{D_{intra_{s1}}}{R^2}\beta^2_{kn}t\right).$$

$$N_s(t,X,Z)=1+2\pi\left(\frac{R}{l}\right)^2\frac{D_{inter_s}}{D_{intra_s}}\sum_{n=1}^{\infty}\sum_{k=1}^{\infty}\Phi(\beta_{kn},Z)\frac{\sin(\beta_{kn}X)}{\sin(\beta_{kn})}\times \times\exp\left(-\frac{D_{intra_s}}{R^2}\beta^2_{kn}t\right), \quad (10)$$

$$\Phi(\beta_{kn},Z)=\frac{(2n-1)\cos\left(\frac{2n-1}{2}\pi Z\right)}{(-1)^n\beta^2_{kn}\left[\frac{3}{e_{inter}}\left(\frac{1}{\sin^2(\beta_{kn})}-\frac{ctg(\beta_{kn})}{\beta_{kn}}\right)+2\right]},$$

were β_{kn} - roots of transcendent equations

$$\frac{3}{e_{inter}}\frac{l^2}{R^2}\frac{D_{inttra_s}}{D_{inter_s}}\left(\frac{e_{inter}}{3}\beta^2-\beta ctg\beta+1\right)=\frac{2n-1}{2}\pi,\quad n,k=\overline{1,\infty}.$$

VI. Identification Metods Of Competitive Diffusion In Microporous Solids

According to [17] the identification procedure of coefficients diffusion (8) requires a special calculation technology of gradients $\nabla J^{n}_{D_{intra_s}}(t)$, $\nabla J^{n}_{D_{inter_s}}(t)$ of functional residual (9), which is a major determinant components of regularization formulas (8). This leads to the problem of unconditional optimization of Lagrange extended functional [13, 17]

$$\Phi\left(D_{inter_s},D_{intra_s}\right)=J_s+I_{s_1}+I_{s_2}, \quad (11)$$

here I_{s_1}, I_{s_2} - the components, accounted of specificity of basic equations of direct problem (1)-(6):

$$I_{s_1}=\int_0^T\int_0^1\phi_s(t,Z)\left(\frac{\partial C_s}{\partial t}-\frac{D_{inter_s}}{l^2}\frac{\partial^2 C_s}{\partial Z^2}+e_{inter}K_s\frac{D_{intra_s}}{R^2}\frac{\partial Q_s}{\partial X}_{X=1}\right)dZdt,$$

$$I_{s_2}=\int_0^T\int_0^1\int_0^1\psi_s(t,Z)\left(\frac{\partial Q_s(t,X,Z)}{\partial t}-\frac{D_{intra_s}}{R^2}\left(\frac{\partial^2}{\partial X^2}+\frac{2}{X}\frac{\partial}{\partial X}\right)Q_s\right)XdXdZdt,$$

here J_s - residual functional (9), ϕ_s,ψ_s, $_{s,=\overline{1,2}}$ – unknown factors of Lagrange, to be determined from the condition of stationary of the functional $\Phi(D_{inter_s},D_{intra_s})$ [8, 14]:

$$\Delta\Phi(D_{inter_s},D_{intra_s})\equiv\Delta J_s+\Delta I_{s_1}+\Delta I_{s_2}=0. \quad (12)$$

The calculation of components in eq. (A.4) is carried out assuming that the values D_{inter_s}, D_{intra_s} received increments ΔD_{inter_s}, ΔD_{intra_s}. As a result, the concentration $C_s(t,Z)$ will change into some increment $\Delta C_s(t,Z)$ and the concentration $Q_s(t,X,Z)$ well change into increment $\Delta Q_s(t,X,Z)$, $s=\overline{1,2}$.

VII. Conjugate Problem

The calculation result of functional increments $\Delta J_s, \Delta J_{s_1}, \Delta J_{s_2}$ in (A.4) (using the integration by parts, by the initial and boundary conditions of direct problem (1)-(6), equating outside integral members and the inside integral components with the same increments $\Delta C_s(t,Z)$ and $Q_s(t,X,Z)$ to zero) leads to solving the additional conjugate problem of determining the unknown Lagrange factors ϕ_s, ψ_s of functional (11):

$$\frac{\partial \phi_s(t,Z)}{\partial t}+\frac{D_{inter_s}}{l^2}\frac{\partial^2 \phi_s}{\partial Z^2}+e_{inter}K_s\frac{D_{intra_s}}{R^2}\frac{\partial \psi_s}{\partial X}\Big|_{X=1}=E_s^n(t)\delta(Z-\gamma) \quad (13)$$

$$\frac{\partial \psi_s(t,X,Z)}{\partial t}+\frac{D_{intra_s}}{R^2}\left(\frac{\partial^2}{\partial X^2}+\frac{2}{X}\frac{\partial}{\partial X}\right)\psi_s=E_s^n(t)\delta(Z-\gamma). \quad (14)$$

$$\phi_s(t,Z)_{|t=T}=0;\ \psi_s(t,X,Z)_{|t=T}=0 \text{ (conditions at } t=T) \quad (15)$$

$$\frac{\partial}{\partial Z}\phi_s(t,0)=0,\ \phi_s(t,1)=0, \quad (16)$$

here $E_s^n(t)=C_s(D_{intra_s}^n, D_{inter_s}^n;t,\gamma)+\bar{Q}_s(D_{intra_s}^n, D_{inter_s}^n;t,\gamma)-M_s(t)$, $\delta(Z-\gamma)$ - function of Dirac [6].

We have obtained solution ϕ_s, ψ_s of conjugate problem (13)-(16) by the procedure described in [6] using the operational method of the Heaviside's.

VIII. Relationship Between Direct And Conjugate Problem

Substituting in the initial direct problem (1) - (6) instead D_{inter_s}, D_{intra_s} and $C_s(t,Z)$, $Q_s(t,X,Z)$ the corresponding values with increments $D_{inter_s}+\Delta D_{inter_s}$, $D_{intra_s}+\Delta D_{intra_s}$ and $C_s(t,Z)+\Delta C_s(t,Z)$, $Q_s(t,X,Z)+\Delta Q_s(t,X,Z)$, and subtracting with the transformed equations and conditions of the problem the relevant components of the equations of problem (1) - (6) and neglecting terms of the second order of smallness, we obtain basic equations of the direct problem (1)-(6) in terms of increments $\Delta C_s(t,Z)$ and $\Delta Q_s(t,X,Z)$, $s=\overline{1,2}$ in the operator form :

$$Lw_s(t,X,Z)=X_s,\ w_s\in(0,1)\cup\Omega_T, \quad (17)$$

Similarly we record the system of he basic equations of conjugate boundary problem (13)-(16) in operator form:

$$L^*\Psi_s(t,X,Z)=E_s(t)\delta(Z-\gamma),\ \Psi_s\subset(0,1)U\Omega_T, \quad (18)$$

$$=L=\begin{bmatrix}\frac{\partial}{\partial t}-\frac{\partial}{\partial Z}\left(D_{inter_s}\frac{\partial}{\partial Z}\right) & e_{inter}\frac{D_{intra_s}}{R}\frac{\partial}{\partial X}\Big|_{X=1}\\ 0 & \frac{\partial}{\partial t}-\frac{D_{intra_s}}{R^2}\left(\frac{\partial^2}{\partial X^2}+\frac{2}{X}\frac{\partial}{\partial X}\right)\end{bmatrix},$$

$$=L^*=\begin{bmatrix}\frac{\partial}{\partial t}+\frac{\partial}{\partial Z}\left(D_{inter_s}\frac{\partial}{\partial Z}\right) & e_{inter}\frac{D_{intra_s}}{R^2}\frac{\partial}{\partial X}\Big|_{X=1}\\ 0 & \frac{\partial}{\partial t}+\frac{D_{intra_s}}{R^2}\left(\frac{\partial^2}{\partial X^2}+\frac{2}{X}\frac{\partial}{\partial X}\right)\end{bmatrix}$$

$$w_s(t,X,Z)=\begin{bmatrix}\Delta C_s(t,Z)\\ \Delta Q_s(t,X,Z)\end{bmatrix},\ \Psi_s(t,X,Z)=\begin{bmatrix}\phi_s(t,Z)\\ \psi_s(t,X,Z)\end{bmatrix},$$

$$X_s(t,X,Z)=\begin{bmatrix}\frac{\partial}{\partial Z}\left(\Delta D_{inter_s}\frac{\partial}{\partial Z}C_s\right)-e_{inter}\frac{\Delta D_{intra_s}}{R^2}\frac{\partial}{\partial X}Q_s\Big|_{X=1}\\ \frac{\Delta D_{intra_s}}{R^2}\left(\frac{\partial^2}{\partial X^2}+\frac{2}{X}\frac{\partial}{\partial X}\right)Q_s(t,X,Z)\end{bmatrix}, \quad (19)$$

here L^* - conjugate Lagrange operator to operator L.

IX. Obtaining The Residual Functional Increment Formula

Increment calculated of residual functional (9), neglecting terms of the second order of smallness, has the view

$$\Delta J_s(D_{inter_s}, D_{intra_s})=\int_0^T\int_0^1 E_s(t)\Delta C_s\delta(Z-\gamma)dZd\tau+\int_0^T\int_0^1\int_0^1 E_s(t)\delta(Z-\gamma)\Delta Q_s XdXdZdt.$$

Using the change of variable $w_s=L^{-1}X_s$, here L^{-1} - inverse operator to operator L, we obtain

$$\Delta J_s\left(D_{intra_s}, D_{inter_s}\right)=\int_0^T\int_0^1 L^{-1}X_{s_1}(t,Z)E_s(t)\delta(Z-\gamma)dZdt+ \\ +\int_0^T\int_0^1\int_0^1 L^{-1}X_{s_2}(t,X,Z)E_s(t)\delta(Z-\gamma)XdXdZdt \quad (20)$$

Defining the scalar product

$$\left(Lw_s(t,X,Z),\Psi_s(t,X,Z)\right)=\begin{bmatrix}\iint_{\Omega_T} L\Delta C_s(t,Z)\phi_s(t,Z)dZdt\\ \iiint_{(0,R)\cup\Omega_T} L\Delta Q_s(t,X,Z)(t,X,Z)\psi_s(t,X,Z)XdXdZdt\end{bmatrix}v, \quad (21)$$

and taking into account (A.20) the identity of Lagrange [13, 17]

$$\left(Lw_s(t,X,Z),\Psi_s(t,X,Z)\right)=\left(w_s(t,X,Z),L^*\Psi_s(t,X,Z)\right)v \quad (22)$$

and the equality $L^{-1*}\left[E_s(t)\delta(Z-\gamma)\right]=\Psi_s$, we obtain the increment of residual functional expressed by the solution of conjugate

problem and the vector of right parts of equations system (19):

$$\Delta J_s(D_{inter_s}, D_{intra_s}) = \left(\Psi_s(t,X,Z),\ X_s(t,X,Z)\right), \qquad (23)$$

here $\phi_s(t,Z)$ and $\psi_s(t,X,Z)$ belong to $\bar{\Omega}_T$ and $[0,1] \cup \bar{\Omega}_T$ respectively, L^{-1*} - conjugate operator to inverse operator L^{-1}, Ψ_s - solution vector of conjugate problem (13)-(16).

Revealing in equation (23) the components $X_s(t,X,Z)$ taking in account the equality (19), we come to the important formula, which establishes the relationship between the direct problem (1) - (6) and the conjugate problem (13) - (16) and which makes it possible to obtain explicit analytical expressions of components of the residual functional gradient

$$\Delta J_s(D_{intra_s}, D_{inter_s}) = \left(\phi_s, \frac{\partial}{\partial Z}\left(\Delta D_{inter_s} \frac{\partial}{\partial Z} C_s\right) - e_{inter} \frac{\Delta D_{intra_s}}{R^2} \frac{\partial}{\partial X} Q_s\Big|_{X=1}\right) + \left(\psi_s, \frac{\Delta D_{intra_s}}{R^2}\left(\frac{\partial^2}{\partial X^2} + \frac{2}{X}\frac{\partial}{\partial X}\right) Q_s\right). \qquad (24)$$

Analytical expressions of the gradients of the residual functional. Differentiating expression (24), by ΔD_{intra_s} and ΔD_{inter_s} respectively, and the opening of scalar products according to (21), we obtain the required analytical expressions for the gradient of the residual functional respectively to the components necessary of diffusion coefficients as functions for time in intracrystalite space and intercrystalite space respectively:

$$\nabla J_{D_{intra_s}}(t) = -\frac{e_{inter}}{R^2} \int_0^1 \frac{\partial}{\partial X} Q_s(t,X,Z)\phi_s(t,Z)dZ + \frac{1}{R^2} \int_0^1 \int_0^1 \left(\frac{\partial^2}{\partial X^2} + \frac{2}{X}\frac{\partial}{\partial X}\right) Q_s(t,X,Z)\psi_s(t,X,Z)XdXdZ, \qquad (25)$$

$$\nabla J_{D_{inter_s}}(t) = \int_0^1 \frac{\partial^2 C_s(t,Z)}{\partial Z^2}\phi_s(t,Z)dZ. \qquad (26)$$

The formulas of gradients $\nabla J^n_{D_{intra_s}}(t)$, $\nabla J^n_{D_{intra_s}}(t)$ include analytical expressions of direct problem solutions (1) - (6). It provides high performance of computing process, avoiding a large number of inner loop iterations by using exact analytical methods.

Another advantage of the formulas (8) is that it is possible to identify the unknown kinetic parameters as a function of time $(D_{intra_s}(t), D_{inter_s}(t))$ and other coordinates. It provides the possibility of internal diffusion kinetics in intracrystallite space and intercrystallite space and get an overall vision of the whole process.

X. Numerical Simulation And Analysis: Competitive Diffusion Coefficients, Concentration Profiles In Itercrystallite Space And Intracrystaliyte Space

The benzene and hexane intracrystallite diffusion coefficients D_{intra_1} and D_{intra_2} are presented in Figure 2 as functions of time for the five coordinates positions: 6, 8, 10, 12, 14 mm, defined now from the top of the bed. The curves for benzene D_{intra_1} (Fig. 2a) are pseudo exponentials. D_{intra_1} decreases from 9.0 E-12 to about 1.0 E-14 (equilibrium) depending on the position of the crystallite and the time, as well as on the amount of adsorbed gas. The shapes of the variations of D_{intra_2} for hexane are roughly the same, but the diffusion coefficients are higher, from about 9.0 E-11 to 2.0 E-12 (Fig. 2b).

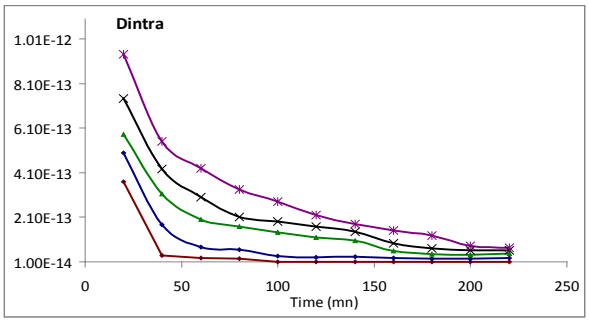

A

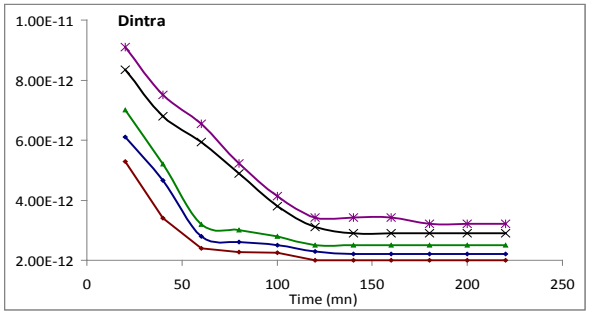

b

Fig. 2. Variation of intracrystallite diffusion coefficients for (a) benzene D_{intra_1} and (b) hexane D_{intra_2} against time at different positions of the bed

6 mm, 8 mm, 10 mm, 12 mm, 14 mm

Figure 3 presents the benzene and hexane diffusion coefficient distributions in intercrystallite space D_{inter_1} and D_{inter_2} as functions of time and for coordinate positions from 6 to 14 mm. These coefficients decrease with time from 6.0 E-6 to 1.0 E-6 (equilibrium) for benzene and from 2.7 E-6 to 1.0 E-5 for hexane, depending on the position in the bed and the increase in the adsorbed concentrations.

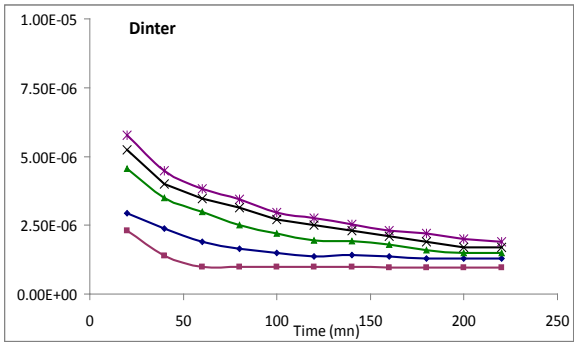

a

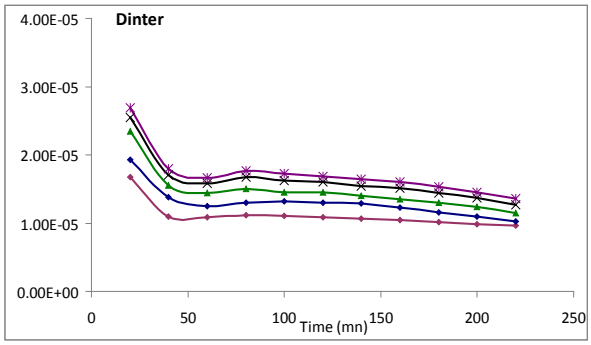

b

Fig. 3. Variation of intercrystallite diffusion coefficients for (a) benzene D_{inter_1} and (b) hexane D_{inter_2}, against time at different positions of the bed

6 mm, 8 mm, 10 mm, 12 mm, 14 mm

Figure 4 compares calculated and experimental curves for the total mass of benzene and hexane in the catalytic bed.

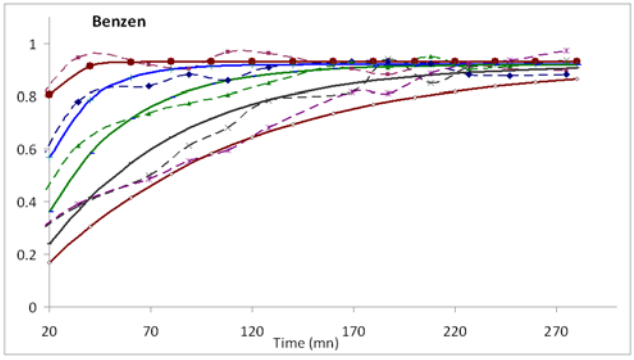

a

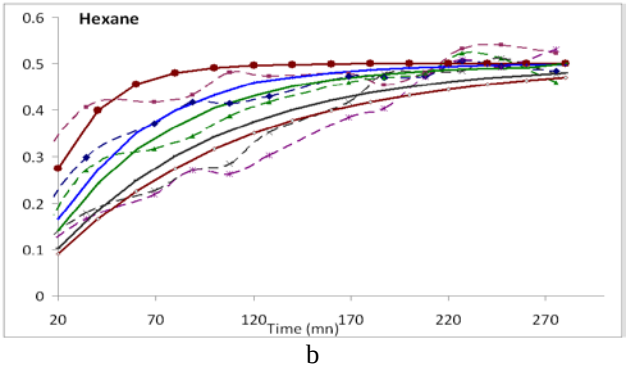

b

Fig. 4. Concentration of (a) benzene and (b) hexane *versus* time at different positions of the catalytic bed: *dotted* - experimental curves, *continuous* – model curves

6 mm, 8 mm, 10 mm, 12 mm, 14 mm

As it can be seen from the graphs (Fig. 4a), the distributions of the total adsorbed mass of benzene are in good agreement with the experimental distributions for each measurement position. The maximum deviation is generally less than 5%. A similar pattern is observed for hexane (Fig. 4b). Here the greatest differences (6-7%) are for the curves corresponding to positions 6 and 8 mm.

XI. Conclusion

As a result for the first time in a single physical experiment it was possible to probe at every moment the concomitant distribution of several gases co-diffusing in a porous solid and to identify their diffusion parameters.

Scientific novelty. For the first time high-speed efficient methods of diffusion parameters identification have been developed taking advantage of low-consuming high-speed solution of the direct and conjugate problem. The analytic solutions of the direct and conjugate problem, using the Heviside's operational methods have been stated and interpreted. Basing on the theory of the multicomponent systems state control, explicit expressions of residual functional gradient have been obtained, which made possible to implement the efficient identification algorithms, to determine diffusion coefficients distributions.

Practical importance. Application of the developed identification methods makes possible to obtain the diffusion coefficients for both components as the functions of time for different positions along the catalytic bed, which allows to specify the main diffusion flows in intercrystallite space (macro level) and in intracrystallite space (micro level) of nanoporous media and to realize the high-speeds procedures of such dependencies creation.

The prospects of investigation are: generalization of the obtained results on the two-components and multi-components catalytic medias of different configuration; obtaining of the methods and identification algorithms of three and more parameters; development of these methods as to their implementation and application to non-linear models of competitive diffusion, when the diffusion coefficients are considered as the functions of concentrations of the diffused components, and other parameters.

Nomenclature:

c : adsorbate concentration in macropores.

c_∞ : adsorbate equilibrium concentration in macropores.

$C = c/c_\infty$: dimensionless adsorbate concentration in macropores.

D_{inter} : macropore diffusion coefficient, m^2/s

D_{intra} : micropore diffusion coefficient, m^2/s

K : adsorption equilibrium constant

l : bed length, mm.

L: dimensionless bed length (L=1)

M : total uptake at time t.

M_T : total uptake at equilibrium.

q : adsorbate concentration in micropores.

q_∞ : equilibrium adsorbate concentration in micropores.

$Q = q/q_\infty$: dimensionless adsorbate concentration in micropores.

x : distance from crystallite center, mm.

R : mean crystallite radius, mm (we assume that the crystallites are spherical).
X = x/R: dimensionless distance from crystallite center.
z : distance from the bottom of the bed for mathematical simulation, mm.
Z = z/l : dimensionless distance from the bottom of the bed.
e_{inter} – porosity,
T – total duration of diffusion, min.
n - iteration number of identification,
Greek letters
ε_{inter} : bed porosity.

References:

[1] M. Fernandez, J. Kärger, D. Freude, A. Pampel, J.M. van Baten, R. Krishna, Microporous and Mesoporous Materials 105 (2007) 124-131.
[2] L.F. Gladen, M.D. Mantle, A.J. Sederman, Handbook of Heterogeneous Catalysis, 2nd Edition Eds: G. Ertl, H. Knözinger, F. Schüth, J. Weitkamp, Wiley-VCH, Weinheim 2008. 1784 P.
[3] A. A. Lysova, I. V. Koptyu, Chem. Soc. Rev. 39 (2010) 4585-4601.
[4] P. N'Gokoli-Kekele, M.-A. Springuel, J.-J. Bonardet, J.-M. Dereppe, J. Fraissard, Studies in Surface Science and Catalysis 133 (2001) 375-382.
[5] S. Leclerc, G. Trausch, B. Cordier, D. Grandclaude, A. Retournard, J. Fraissard, D. Canet, Magn. Reson. Chem. 44 (2006) 311- 317.
[6] M. Petryk, S. Leclerc, D. Canet, J. Fraissard, Diffusion Fundamentals 4 (2007) 11.1. Online in http://www.diffusion-fundamentals.org
[7] M. Petryk, S. Leclerc, D. Canet, J. Fraissard, Catalysis Today 139 (2008) 234-240.
[8] S. Leclerc, M. Petryk, D. Canet, J. Fraissard, Catalysis Today 187 (2012) 104-107.
[9] R. Krishna, J.M. van Baten, J. Phys. Chem. B 109 (2005) 6386-6396.
[10] C. Fërste, A. Germanus, J. Curger, H. Pfeifer, J. Caro, W. Pilz, A. Zikanova, J. Chem. Eng. Soc., Faraday Trans. 1 83 (1987) 2301-2309.
[11] R. Krishna, J.M. van Baten, Chem. Eng. Journal 140 (2008) 614-620.
[12] A.N. Tikhonov and V.Y. Arsenin. Solutions of Ill-Posed Problems, Washington D.C. : V.H. Winston ; New York : J. Wiley (1977), 288 P.
[13] J.-L. Lions, Perturbations Singulières dans les Problemes aux Limites et en Contrôle Optimal, New York: Springer. Lecture Notes in Math. Ser. 2008 645 P.
[14] O.M. Alifanov, Inverse problems of heat exchange, Moscow: Engineering (1988) 280 P.
[15] V. Deineka, M. Petryk, J. Fraissard, Cybernetics and System Analysis, Springer 47(5) (2011) 705-723.
[16] , M. Petryk, J. Fraissard, J. of Automation and Information Sciences 41(3) (2009) 37-55.
[17] I.V. Sergienko, V.S. Deineka, Optimal Control of Distributed Systems with Conjugation Conditions, New York: Kluwer Academic Publishers (2005) 400 P.

Petryk Mykhaylo, Dr of Sc., Prof., is with the Ternopil National Technical University named after Ivan Pulu'y.
Address: 56 rue Ruska, 46001 Ternopil,
Tél. 38 035 2 25 64 96; Fax 380352254983,
e-mail: Mykhaylo_Petryk@tu.edu.te.ua ;
SoftEng@utc.fr

Quasi-Phi-Functions in Packing Problem of Ellipsoids

A. Pankratov, T. Romanova, O. Khlud

***Abstract* - The paper considers the problem of packing a given collection of ellipsoids of revolution into a rectangular container of minimal volume. Our ellipsoids can be continuos rotated and translated. A class of radical-free quasi-phi-functions is used for an analytical description of non-overlapping and containment constraints. We formulate the packing problem in the form of a nonlinear programming problem and propose a solution strategy, which allow us to search for local optimal packings. The actual search for a local minimum is performed by IPOPT. We provide computational results.**

***Index Terms* – packing, ellipsoids, continuous rotations, non-overlapping, containment, quasi-phi-functions, solution algorithm, nonlinear optimization**

I. Introduction

In this paper we deal with the optimal ellipsoid packing problem, which is a part of operational research and computational geometry. The problem is NP-hard [1] and has multiple applications in modern biology, mineralogy, medicine, materials science, nanotechnology, as well as in the chemical industry, power engineering etc.

Our approach is based on mathematical modeling of relations between ellipsoids and thus reducing the packing problem to a nonlinear optimization problem. To this end a class of quasi-phi-functions [2] is used for analytic description of placement of ellipsoids in a rectangular container taking into account their continuous rotations and translations.

The paper is organized as follows: In Section 2 we formulate the optimal ellipsoid packing problem and give a short review of related works. In Section 3 we define quasi-phi-functions for nonoverlapping and containment constraints. In Section 4 we propose a mathematical model as a continuous nonlinear programming problem by means of quasi-phi-functions and describe a solution strategy. In Section 5 we provide our computational results. Finally we give some conclusions in Section 6.

Manuscript received March 18, 2015

Alexandr V. Pankratov is with the Institute for Problems in Machinery of National Academy of Sciences of Ukraine (Kharkov).

Tatiana E. Romanova is with the Institute for Mechanical Engineering Problems of the National Academy of Sciences of Ukraine (corresponding author to provide e-mail: sherom@kharkov.ua).

Olga M. Khlud is with the Kharkiv National University of Radioelectronics.

II. Problem Formulation

We consider here a packing problem in the following setting**.** Let Ω denote a rectangular domain of length l, width w and height h. All of these dimensions may be variable, or one (two) may be fixed and the other variable. Suppose a set of ellipsoids of revolution, E_i, $i \in \{1, 2, \ldots, n\} = I_n$, is given to be placed in Ω without overlaps. Each ellipsoid E_i is generated by rotation of an ellipse of semi-axes a_i and b_i, $a_i > b_i$, along the axis of revolution *OX*, therefore we assume that third semi-axe is defined as $c_i = b_i$. With each ellipsoid E_i we associate its local coordinate system whose origin coincides with the center of the ellipsoid and the coordinate axes are aligned with the ellipsoid's axes. In that system the ellipsoid is described by parametric equations $x = a_i \cos t_i$, $y = b_i \sin t_i \cos g_i$, $z = b_i \sin t_i \sin g_i$, $0 \le t_i \le 2\pi$, $0 \le g_i \le 2\pi$. We also use a fixed coordinate system attached to the container Ω. The location and orientation of each ellipsoid E_i is defined by a variable vector of its placement parameters (v_i, θ_i). Here $v_i = (x_i, y_i, z_i)$ is a translation vector, $\theta_i = (\theta_i^1, \theta_i^2)$ is a vector of rotation parameters, where θ_i^1, θ_i^2 are appropriate angles from axis OX to OY, from axis OY to OZ in the local coordinate system of ellipsoid E_i. The rotated by angles θ_i^1, θ_i^2 and translated by vector v_i ellipsoid E_i is defined as $E_i(u) = \{p \in R^3 : p = v_i + M(\theta_i) \cdot p^0, \forall p^0 \in E_i^0\}$, where E_i^0 denotes the non-translated and non-rotated ellipsoid E_i, $M(\theta) = M_2(\theta_i^2) \cdot M_1(\theta_i^1)$ is a rotation matrix, where

$$M_1(\theta_i^1) = \begin{pmatrix} \cos\theta_i^1 & -\sin\theta_i^1 & 0 \\ \sin\theta_i^1 & \cos\theta_i^1 & 0 \\ 0 & 0 & 1 \end{pmatrix},$$

$$M_2(\theta_i^2) = \begin{pmatrix} 1 & 0 & 0 \\ 0 & \cos\theta_i^2 & -\sin\theta_i^2 \\ 0 & \sin\theta_i^2 & \cos\theta_i^2 \end{pmatrix}.$$

Packing problem of ellipsoids. Pack the set of ellipsoids E_i, $i \in I_n$, within a rectangular domain

$\Omega = \{(x, y, z) \in R^3 : 0 \le x \le l, 0 \le y \le w, 0 \le z \le h\}$ of minimal volume. If one of the two dimensions (l or w or h) is fixed, we need to minimize the other ones. If all are variable, it is natural to minimize the volume $F = l \cdot w \cdot h$ of the container.

At present, the interest in finding effective solutions for placement problems of ellipsoids is growing rapidly (see, e.g., [4-8]). This is due to a large number of applications and an extreme complexity of methods used to handle many of them.

The remarkable method of the problem of cutting ellipses from a rectangular plate of minimal area was developed by Josef Kallrath and Steffen Rebennack, see [10]. The paper offers a good overview of related publications. For a small number of ellipses they are able to compute a globally optimal solution subject to the finite arithmetic of global solvers at hand. However, for more than 14 ellipsoids none of the nonlinear programming (NLP) solvers available in GAMS can even compute a locally optimal solution. Therefore, the authors of [10] develop polylithic approaches, in which the ellipses are added sequentially in a strip-packing fashion to the rectangle restricted in width but unrestricted in length. The rectangle's area is minimized at each step in a greedy fashion. The sequence in which they add ellipses is random; this adds some GRASP flavor to the approach. The polylithic algorithms allow the authors to compute good solutions for up to 100 ellipses.

Paper [9] studies the problem of placing a given collection of ellipses into a rectangular container of minimal area. Radical free quasi-phi-functions are used to reduce it to a nonlinear programming problem and develop an efficient solution algorithm. The paper provides computational results with local optimal solutions for the problem (up to 120 ellipses).

The present paper proposes an approach, which is capable of handling precise ellipsoids (without approximations) and thus finding an exact local optimal solution. The approach can be considered as some extension of quasi-phi-functions for ellipses, derived in [9], to 3D case.

III. Quasi-phi-functions for nonoverlapping and containment constraints

Quasi-phi-functions for nonoverlapping constraints. Let $E_i(u_i)$ and $E_j(u_j)$ be two ellipsoids of revolution with semi-axes a_i, b_i, c_i and a_j, b_j, c_j.

Then, a quasi-phi-function for $E_i(u_i)$ and $E_j(u_j)$ may be defined as follows

$$\Phi'_{ij}(u_i, u_j, u'_{ij}) = \min\{\chi(\Theta_i, \Theta_j, u'_{ij}), \chi_1^+(u_i, u_j, u'_{ij}), \chi_1^-(u_i, u_j, u'_{ij}), \chi_2^+(u_i, u_j, u'_{ij}), \chi_2^-(u_i, u_j, u'_{ij})\}, \quad (1)$$

where $u'_{ij} = (t_i, g_i, t_j, g_j)$,

$$\chi = -\left\langle N'_i, N'_j \right\rangle = -\alpha'_i\alpha'_j - \beta'_i\beta'_j - \gamma'_i\gamma'_j,\ \Theta_i = (\theta_i^1, \theta_i^2),$$

$$(\alpha'_i, \beta'_i, \gamma'_i) = M(\Theta_i)\cdot(\alpha_i, \beta_i, \gamma_i)^T,$$

$$\alpha_i = \frac{\cos t_i}{a_i},\ \beta_i = \frac{\sin t_i \cos g_i}{b_i},\ \gamma_i = \frac{\sin t_i \sin g_i}{b_i},$$

$$\Theta_j = (\theta_j^1, \theta_j^2),\ (\alpha'_j, \beta'_j, \gamma'_j) = M(\Theta_j)\cdot(\alpha_j, \beta_j, \gamma_j)^T,$$

$$\alpha_j = \frac{\cos t_j}{a_j},\ \beta_j = \frac{\sin t_j \cos g_j}{b_j},\ \gamma_j = \frac{\sin t_j \sin g_j}{b_j},$$

$$\chi_k^+ = \alpha'_i(x_{jk}^+ - x_i) + \beta'_i(y_{jk}^+ - y_i) + \gamma'_i(z_{jk}^+ - z_i) - 1,$$

$$\chi_k^- = \alpha'_i(x_{jk}^- - x_i) + \beta'_i(y_{jk}^- - y_i) + \gamma'_i(z_{jk}^- - z_i) - 1,$$

$(x_{jk}^+, y_{jk}^+, z_{jk}^+)$ are coordinates of point q_{jk}^+ and $(x_{jk}^-, y_{jk}^-, z_{jk}^-)$ are coordinates of point q_{jk}^-, $k = 1, 2$ (see Fig.1).

We derive q_{jk}^+ and q_{jk}^- as follows:

$$(x_{j2}^+, y_{j2}^+, z_{j2}^+) = v_j + M(\Theta_j)M_2(g_j)(a_j \cos t_j, b_j \sin t_j, \sqrt{2}a_j)^T,$$

$$(x_{j2}^-, y_{j2}^-, z_{j2}^-) = v_j + M(\Theta_j)M_2(g_j)(a_j \cos t_j, b_j \sin t_j, -\sqrt{2}a_j)^T,$$

$$(x_{j1}^+, y_{j1}^+, z_{j1}^+) = v_j + M(\Theta_j)M_2(g_j)(x_j^+, y_j^+, 0)^T,$$

$$(x_{j1}^-, y_{j1}^-, z_{j1}^-) = v_j + M(\Theta_j)M_2(g_j)(x_j^-, y_j^-, 0)^T,$$

$$(x_j^+, y_j^+) = (\alpha_j^t, \beta_j^t) + \eta(-\beta_j^t, \alpha_j^t),$$

$$(x_j^-, y_j^-) = (\alpha_j^t, \beta_j^t) - \eta(-\beta_j^t, \alpha_j^t),$$

$$(\alpha_j^t, \beta_j^t) = M_1(t_j)(a_j, 0)^T,\ \eta = \sqrt{2}(a_j)^2.$$

Thus a nonoverlapping constraint, i.e. $\operatorname{int} E_i(u_i) \cap \operatorname{int} E_j(u_j) = \varnothing$, can be defined as $\Phi'_{ij}(u_i, u_j, u'_{ij}) \ge 0$, where Φ'_{ij} is a quasi-phi-function of ellipsoids $E_i(u_i)$ and $E_j(u_j)$ given by (1).

Quasi-phi-functions for containment constraints. Let vertices of our rectangular container $\Omega = \{(x, y, z) \in R^3 : 0 \le x \le l, 0 \le y \le w, 0 \le z \le h\}$ be given as follows: $\{v_i, i = 1, \ldots, 8\} = \{(0, w, 0), (l, w, 0), (l, 0, 0), (0, 0, 0), (0, w, h), (l, w, h), (l, 0, h), (0, 0, h)\}$.

And let $E_i(u_i)$ be ellipsoid of revolution with semi-axes a_i, b_i and $c_i = b_i$, $a_i > b_i$, $i = 1, 2\ldots, n$.

Then a quasi-phi-function for $E_i(u_i)$ and object $\Omega^* = R^3 \setminus \operatorname{int}\Omega$ may be defined in the form

$$\Phi'_i(u_i, u'_i) = \min\{\varphi_{i1}(u), \varphi_{i2}(u), \varphi_{i3}(u)\}, \quad (2)$$

where $(u_i, u'_i) \in R^{11}$, $u'_i = (t'_{i1}, t'_{i2}, t'_{i3}, g'_{i1}, g'_{i2}, g'_{i3})$, $0 \le t'_{ik} \le 2\pi$, $0 \le g'_{ik} \le 2\pi$,

$$\varphi_{i1}(u) = \min\{\varphi_{11}^i(v_1), \varphi_{11}^i(v_2), \varphi_{11}^i(v_3), \varphi_{11}^i(v_4), \varphi_{12}^i(v_5), \varphi_{12}^i(v_6), \varphi_{12}^i(v_7), \varphi_{12}^i(v_8)\},$$

$$\varphi_{i2}(u) = \min\{\varphi_{21}^i(v_1), \varphi_{21}^i(v_4), \varphi_{21}^i(v_5), \varphi_{21}^i(v_8), \varphi_{22}^i(v_2), \varphi_{22}^i(v_3), \varphi_{22}^i(v_6), \varphi_{22}^i(v_7)\},$$

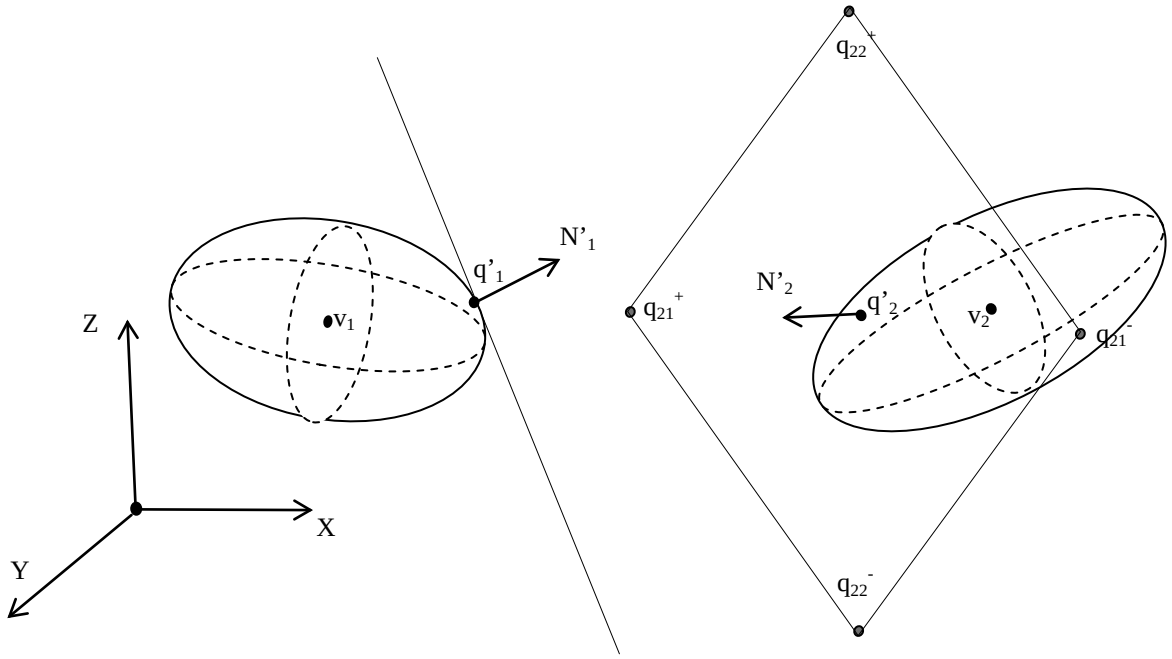

Fig. 1 Illustration to construction of a quasi-phi-function for two ellipsoids $E_1(u_1)$ and $E_2(u_2)$

$$\varphi_{i3}(u) = \min\{\varphi^i_{31}(v_1), \varphi^i_{31}(v_2), \varphi^i_{31}(v_5), \varphi^i_{31}(v_6), \varphi^i_{32}(v_3), \varphi^i_{32}(v_4), \varphi^i_{32}(v_7), \varphi^i_{32}(v_8)\},$$

$$\varphi^i_{k1} = A_{ik}x + B_{ik}y + C_{ik}z + D_{ik} - 1,$$

$$\varphi^i_{k2} = -A_{ik}x - B_{ik}y - C_{ik}z - D_{ik} - 1,$$

$$(A_{ik}, B_{ik}, C_{ik}) = M(\Theta_i)(a_i \cos t_{ik}, b_i \sin t_{ik} \cos g_{ik}, b_i \sin t_{ik} \sin g_{ik})^T,$$

$$D_{ik} = -A_{ik}x_i - B_{ik}y_i - C_{ik}z_i,\ k = 1, 2, 3.$$

Thus, a containment constraint, i.e. $E_i(u_i) \subset \Omega \Leftrightarrow \operatorname{int} E_i(u_i) \cap \Omega^* = \varnothing$, can be defined as $\Phi'_i(u_i, u'_i) \geq 0$, where Φ'_{ij} is a quasi-phi-function for $E_i(u_i)$ and Ω^* given by (2).

IV. Mathematical Model And Solution Strategy

The vector $u \in R^\sigma$ of all our variables can be described as follows: $u = (l, w, h, u_1, u_2, \ldots, u_n, \tau)$, where (l, w, h) denote the variable dimensions of the rectangular container Ω and $u_i = (v_i, \theta_i)$ is the vector of placement parameters for the ellipsoid E_i, $i \in I_n$, where $v_i = (x_i, y_i, z_i)$, $\theta_i = (\theta_i^1, \theta_i^2)$. The vector τ denotes the vector of extra variables (for our quasi-phi-functions), defined as follows:

$$\tau = (t^1_1, g^1_1, t^1_2, g^1_2, \ldots, t^m_1, g^m_1, t^m_2, g^m_2, t'^1_1, g'^1_1, t'^1_2, g'^1_2, t'^1_3, g'^1_3, \ldots, t'^n_1, g'^n_1, t'^n_2, g'^n_2, t'^n_3, g'^n_3),$$

where $t^k_1, g^k_1, t^k_2, g^k_2$ are extra variables for the *k*-th pair of ellipsoids, $k = 1, \ldots, m$, $m = \frac{(n-1)n}{2}$, and t'^i_1, g'^i_1, t'^i_2, g'^i_2, t'^i_3, g'^i_3, are extra variables for each ellipsoid E_i, $i \in I_n$. Lastly, R^σ denotes the σ-dimensional Euclidean space, where $\sigma = 3 + 5n + 2n(n-1) + 6n = 2n^2 + 9n + 3$ is the number of the problem variables.

A mathematical model of the basic packing problem may now be stated in the following form:

$$\min_{u \in W \subset R^\sigma} F(u), \quad (3)$$

$$W = \{u \in R^\sigma : \Phi'_{ij} \geq 0, \Phi'_i \geq 0, i = 1, 2, \ldots, n, j = 1, 2, \ldots, n, j > i\}, \quad (4)$$

where $F(u) = l \cdot w \cdot h$, Φ'_{ij} is a quasi-phi-function (1) defined for the pair of ellipsoids E_i and E_j, (to hold *nonoverlapping* constraint), Φ'_i is a quasi-phi-function (2) defined for an ellipsoid E_i and the object Ω^* (to hold the *containment* constraint).

Our constrained optimization problem (3)-(4) is a continuous nonlinear programming problem.

We propose the following solution strategy for the problem, which involves three major stages:

1)First we generate a number of random starting points.

2)Then starting from each point obtained at Step 1 we search for a local minimum of the objective function *F*(u) of problem (3)-(4).

3)Lastly, we choose the best local minimum from those found at Step 2. This is our best solution of the problem (3)-(4).

V. Computational results

Here we present a number of Instances to demonstrate the efficiency of our quasi-phi-functions. We have run our experiments on an AMD Athlon 64 X2 5200+ computer. We search for 100 local minima to each of Instances. The actual search for a local minimum is performed by IPOPT proposed in [11], which is available at an open access

noncommercial software depository (https://projects.coin-or.org/Ipopt) .

We consider a collection of ellipsoids: $\{E_i, i = 1, .., 12\} = \{(a_i, b_i, c_i), i = 1, 2, ..., 12\}$ = {(5, 4, 4), (7, 5, 5), (6, 5, 5), (4, 3, 3), (5.5, 4.5, 4.5), (7.5, 5.5, 5.5), (6.5, 5.5, 5.5), (4.5, 3.5, 3.5), (5.3, 4.3, 4.3), (7.3, 5.3, 5.3), (6.3, 5.3, 5.3), (4.3, 3.3, 3.3)}.

Instance E2. Local optimal placement of ellipsoids $\{E_i, i = 1, 2\}$ is shown in Figure 2,a. Container has volume $F^* = 2192.513985$ and sizes $(l^*, w^*, h^*) = (10.000000, 10.006950, 21.909912)$. Average time per one local minimum is 2.09 sec.

Instance E3. Local optimal placement of ellipsoids $\{E_i, i = 1, 2, 3\}$ is shown in Figure 2,b. Container has volume $F^* = 3385.008834$ and sizes $(l^*, w^*, h^*) = (10.000000, 33.797139, 10.015667)$. Average time per one local minimum is 5.89 sec**.**

Instance E4. Local optimal placement of ellipsoids $\{E_i, i = 1, ..., 4\}$ is shown in Figure 2,c. Container has volume $F^* = 3539.283378$ and sizes $(l^*, w^*, h^*) = (18.273863, 10.014451, 19.340061)$. Average time per one local minimum is 22.76 sec.

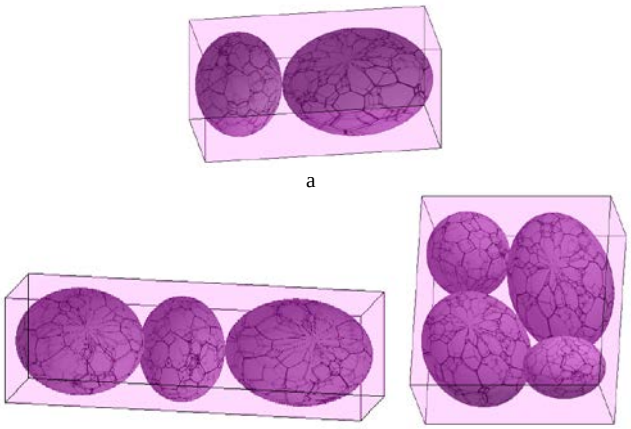

a

b c

Fig. 2. Local optimal placement of ellipsoids in Instances: a – E2, b – E3, c – E4

Instance E5. Local optimal placement of ellipsoids $\{E_i, i = 1, ..., 5\}$ is shown in Figure 3,a. Container has volume $F^* = 4347.434370$ and sizes $(l^*, w^*, h^*) = (24.366822, 10.000252, 17.841164)$. Average time per one local minimum is 60.71 sec**.**

Instance E6. Local optimal placement of ellipsoids $\{E_i, i = 1, ..., 6\}$ is shown in Figure 3,b. Container has volume $F^* = 6312.236870$ and sizes $(l^*, w^*, h^*) = (27.244026, 11.000291, 21.062399)$. Average time per one local minimum is 126.02 sec**.**

Instance E7. Local optimal placement of ellipsoids $\{E_i, i = 1, ..., 7\}$ is shown in Figure 3,c. Container has volume $F^* = 7687.512942$ and sizes $(l^*, w^*, h^*) = (18.960443, 19.723184, 20.557029)$. Average time per one local minimum is 222.36 sec**.**

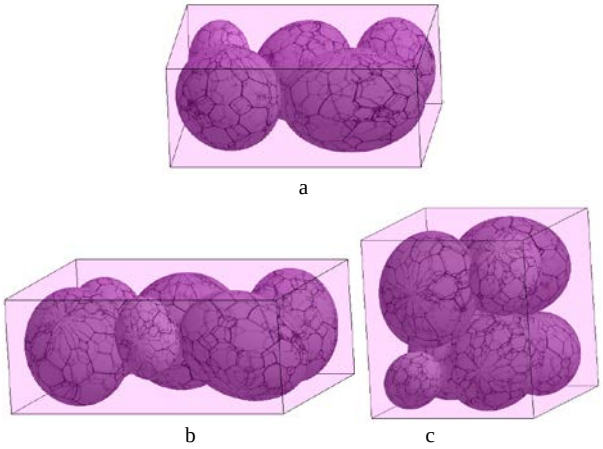

a

b c

Fig. 3. Local optimal placement of ellipsoids in Instances: a – E5, b – E6, c – E7

Instance E8. Local optimal placement of ellipsoids $\{E_i, i = 1, ..., 8\}$ is shown in Figure 4a. Container has volume $F^* = 7998.224794$ and sizes $(l^*, w^*, h^*) = (20.223526, 19.919118, 19.854851)$. Average time per one local minimum is 359.88 sec**.**

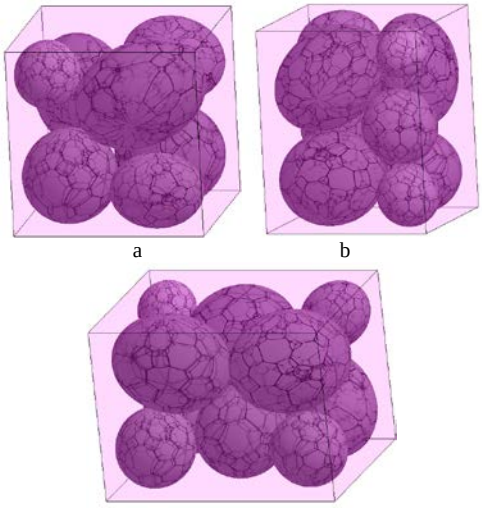

a b

c

Fig. 4. Local optimal placement of ellipsoids in Instances: a – E8, b – E9, c – E10

Instance E9. Local optimal placement of ellipsoids $\{E_i, i = 1, ..., 9\}$ is shown in Figure 4b. Container has volume $F^* = 8524.765214$ and $(l^*, w^*, h^*) = (19.365765, 18.695366, 23.545819)$. Average time per one local minimum is 369.42 sec**.**

Instance E10. Local optimal placement of ellipsoids $\{E_i, i = 1, ..., 10\}$ is shown in Figure 4c. Container has

volume $F^* = 10263.381559$ and sizes $(l^*, w^*, h^*) = (25.780036, 18.893787, 21.071135)$. Average time per one local minimum is 371.23**.**

Instance E11. Local optimal placement of ellipsoids $\{E_i, i = 1, \ldots, 11\}$ is shown in Figure 5a. Container has volume $F^* = 11860.716557$ and sizes $(l^*, w^*, h^*) = (21.945274, 27.902451, 19.369908)$. Average time per one local minimum is 445.95 sec**.**

Instance E12. Local optimal placement of ellipsoids $\{E_i, i = 1, \ldots, 12\}$ is shown in Figure 5b. Container has volume $F^* = 11768.260385$ and sizes $(l^*, w^*, h^*) = (19.327419\ 19.558038\ 31.132438)$. Average time per one local minimum is 836.70 sec.

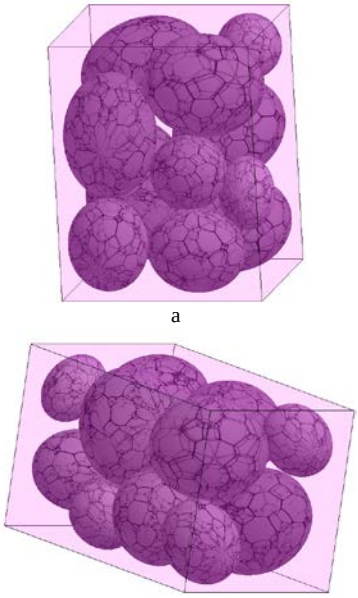

a

b

Fig. 5. Local optimal placement of ellipsoids in Instances: a − E11, b −E12

VI. CONCLUSIONS

We developed here an *exact* continuous NLP model of the placement problem of ellipsoids, using quasi-phi-functions. The use of quasi-phi-functions allows us to handle ellipsoids which can be continuously rotated and translated, but there is a price to pay: now the optimization has to be performed over a larger set of parameters, including the extra variables, besides placement parameters of ellipsoids. The model can be realized by the current state-of-the art local or global solvers. We are working on the improvement of our algorithms to generate feasible starting points, as well as, to reduce our problem dimension in local optimisation procedures, based on the paper [9]. We expect that efficiency of our algorithms will be increased in the future.

REFERENCES

[1] Stojan Ju.G., Pankratov A.V., Romanova T.E., Chernov N.I. Kvazi-phi-funkcii dlja matematicheskogo modelirovanija otnoshenij geometricheskih ob'ektov// Dopovidi NAN Ukraïni. – 2014. – T.9. – C. 49-54 (in Russian).

[2] Chazelle, B., Edelsbrunner, H., Guibas, L.J.: The complexity of cutting complexes. Discrete & Computational Geometry. 4(2), 139-81 (1989).

[3] A. Donev, I. Cisse, D. Sachs, E.A. Variano, F.H. Stillinger, R. Connelly, S. Torquato, M. Chaikin. Improving the density of jammed disordered packings using ellipsoids/ Science. – 2004. – Vol. 303 No 5660. – P. 990-993.

[4] W. Man, A. Donev, F.H. Stillinger, M.T. Sullivan, W.B. Russel, D. Heeger, S. Inati, S. Torquato, P.M. Chaikin. Experiments on random packings of ellipsoids/ Phys Rev Lett. – 2005. – Vol. 94(19).

[5] W. X. Xu, H. S. Chen, Z. Lv. An overlapping detection algorithm for random sequential packing of elliptical particles / Physica. – 2011. – Vol. 390. – P. 2452-2467.

[6] W. Wang, J. Wang, M.-S. Kim. An algebraic condition for the separation of two ellipsoids. Computer Aided Geometric Design. – 2001. – Vol. 18. – P. 531-539.

[7] Y. Choi, J. Chang, W. Wang, G. Elber. Continuous Collision Detection for Ellipsoids / Visualization and Computer Graphics. – 2008. – Vol. 15, Issue 2. – P. 311-325.

[8] C. Uhler, S. J. Wright. Packing Ellipsoids with Overlap. SIAM Review, 55(4):671-706, – 2013.

[9] Chernov N, Stoyan Y, Pankratov A and Romanova T. Quasi-phi-functions and optimal packing of ellipses submitted to Journal of Global Optimization (2014).

[10] Josef Kallrath and Steffen Rebennack, "Cutting Ellipsoids from Area-Minimizing Rectangles" Journal of Global Optimization, 2013. DOI10.1007/s10898-013-0125-3

[11] Wachter, A., Biegler, L. T.: On the implementation of an interior-point filter line-search algorithm for large-scale nonlinear programming. Mathematical Programming.106, 1, 25-57 (2006)

Alexandr V. Pankratov received Doctor of Technical Sciences degree in Mathematical Modeling and Computational Methods (2013) from Institute for Problems in Machinery of National Academy of Sciences of Ukraine (Kharkov). From 2013 he is a senior researcher at the Department of Mathematical Modeling and Optimal Design, Institute for Mechanical Engineering Problems of the National Academy of Sciences of Ukraine. His current research interests include mathematical modeling, operational research, computational geometry, optimisation, packing, cutting and covering.

Tatiana E. Romanova received Doctor of Technical Sciences degree in Mathematical Modeling and Computational Methods (2003) from Institute of Cybernetics of the National Academy of Sciences of Ukraine (Kiev). From 2002 he is a senior researcher at the Department of Mathematical Modeling and Optimal Design, Institute for Mechanical Engineering Problems of the National Academy of Sciences of Ukraine. From 2005 she is a professor at the Department of Applied Mathematics, Kharkiv National University of Radioelectronics. Her current research interests include mathematical modeling, operational research, computational geometry, optimisation, packing, cutting and covering.

Olga M. Khlud received Bachelor's degree in System Analysis (2014) from Kharkiv National University of Radioelectronics. She is an undergraduate at the Kharkiv National University of Radioelectronics. Her current research interests include mathematical modeling, operational research, packing and cutting.

Preparation of Papers for IEEE TRANSACTIONS and JOURNALS

First A. Author, Second B. Author, Jr., and Third C. Author, *Member, IEEE*

***Abstract*—These instructions give you guidelines for preparing papers for IEEE TRANSACTIONS and JOURNALS. Use this document as a template if you are using Microsoft *Word* 6.0 or later. Otherwise, use this document as an instruction set. The electronic file of your paper will be formatted further at IEEE. Define all symbols used in the abstract. Do not cite references in the abstract. Do not delete the blank line immediately above the abstract; it sets the footnote at the bottom of this column.**

***Index Terms*—About four key words or phrases in alphabetical order, separated by commas. For a list of suggested keywords, send a blank e-mail to keywords@ieee.org or visit** http://www.ieee.org/organizations/pubs/ani_prod/keywrd98.txt

I. INTRODUCTION

THIS document is a template for Microsoft *Word* versions 6.0 or later. If you are reading a paper or PDF version of this document, please download the electronic file, TRANS-JOUR.DOC, from the IEEE Web site at http://www.ieee.org/web/publications/authors/transjnl/index.html so you can use it to prepare your manuscript. If you would prefer to use LATEX, download IEEE's LATEX style and sample files from the same Web page. Use these LATEX files for formatting, but please follow the instructions in TRANS-JOUR.DOC or TRANS-JOUR.PDF.

If your paper is intended for a *conference,* please contact your conference editor concerning acceptable word processor formats for your particular conference.

When you open TRANS-JOUR.DOC, select "Page Layout" from the "View" menu in the menu bar (View | Page Layout), which allows you to see the footnotes. Then, type over sections of TRANS-JOUR.DOC or cut and paste from another document and use markup styles. The pull-down style menu is at the left of the Formatting Toolbar at the top of your *Word* window (for example, the style at this point in the document is "Text"). Highlight a section that you want to designate with a certain style, then select the appropriate name on the style menu. The style will adjust your fonts and line spacing. **Do not change the font sizes or line spacing to squeeze more text into a limited number of pages.** Use italics for emphasis; do not underline.

To insert images in *Word,* position the cursor at the insertion point and either use Insert | Picture | From File or copy the image to the Windows clipboard and then Edit | Paste Special | Picture (with "float over text" unchecked).

IEEE will do the final formatting of your paper. If your paper is intended for a conference, please observe the conference page limits.

II. PROCEDURE FOR PAPER SUBMISSION

A. Review Stage

Please check with your editor on whether to submit your manuscript as hard copy or electronically for review. If hard copy, submit photocopies such that only one column appears per page. This will give your referees plenty of room to write comments. Send the number of copies specified by your editor (typically four). If submitted electronically, find out if your editor prefers submissions on disk or as e-mail attachments.

If you want to submit your file with one column electronically, please do the following:

--First, click on the View menu and choose Print Layout.

--Second, place your cursor in the first paragraph. Go to the Format menu, choose Columns, choose one column Layout, and choose "apply to whole document" from the dropdown menu.

--Third, click and drag the right margin bar to just over 4 inches in width.

Manuscript received November 8, 2011. (Write the date on which you submitted your paper for review.) This work was supported in part by the U.S. Department of Commerce under Grant BS123456 (sponsor and financial support acknowledgment goes here). Paper titles should be written in uppercase and lowercase letters, not all uppercase. Avoid writing long formulas with subscripts in the title; short formulas that identify the elements are fine (e.g., "Nd–Fe–B"). Do not write "(Invited)" in the title. Full names of authors are preferred in the author field, but are not required. Put a space between authors' initials.

F. A. Author is with the National Institute of Standards and Technology, Boulder, CO 80305 USA (corresponding author to provide phone: 303-555-5555; fax: 303-555-5555; e-mail: author@ boulder.nist.gov).

S. B. Author, Jr., was with Rice University, Houston, TX 77005 USA. He is now with the Department of Physics, Colorado State University, Fort Collins, CO 80523 USA (e-mail: author@lamar.colostate.edu).

T. C. Author is with the Electrical Engineering Department, University of Colorado, Boulder, CO 80309 USA, on leave from the National Research Institute for Metals, Tsukuba, Japan (e-mail: author@nrim.go.jp).

The graphics will stay in the "second" column, but you can drag them to the first column. Make the graphic wider to push out any text that may try to fill in next to the graphic.

B. Final Stage

When you submit your final version (after your paper has been accepted), print it in two-column format, including figures and tables. You must also send your final manuscript on a disk, via e-mail, or through a Web manuscript submission system as directed by the society contact. You may use *Zip* or CD-ROM disks for large files, or compress files using *Compress, Pkzip, Stuffit,* or *Gzip.*

Also, send a sheet of paper or PDF with complete contact information for all authors. Include full mailing addresses, telephone numbers, fax numbers, and e-mail addresses. This information will be used to send each author a complimentary copy of the journal in which the paper appears. In addition, designate one author as the "corresponding author." This is the author to whom proofs of the paper will be sent. Proofs are sent to the corresponding author only.

C. Figures

Format and save your graphic images using a suitable graphics processing program that will allow you to create the images as PostScript (PS), Encapsulated PostScript (EPS), or Tagged Image File Format (TIFF), sizes them, and adjusts the resolution settings. If you created your source files in one of the following you will be able to submit the graphics without converting to a PS, EPS, or TIFF file: Microsoft Word, Microsoft PowerPoint, Microsoft Excel, or Portable Document Format (PDF).

D. Electronic Image Files (Optional)

Import your source files in one of the following: Microsoft Word, Microsoft PowerPoint, Microsoft Excel, or Portable Document Format (PDF); you will be able to submit the graphics without converting to a PS, EPS, or TIFF files. Image quality is very important to how yours graphics will reproduce. Even though we can accept graphics in many formats, we cannot improve your graphics if they are poor quality when we receive them. If your graphic looks low in quality on your printer or monitor, please keep in mind that cannot improve the quality after submission.

If you are importing your graphics into this Word template, please use the following steps:

Under the option EDIT select PASTE SPECIAL. A dialog box will open, select paste picture, then click OK. Your figure should now be in the Word Document.

If you are preparing images in TIFF, EPS, or PS format, note the following. High-contrast line figures and tables should be prepared with 600 dpi resolution and saved with no compression, 1 bit per pixel (monochrome), with file names in the form of "fig3.tif" or "table1.tif."

Photographs and grayscale figures should be prepared with 300 dpi resolution and saved with no compression, 8 bits per pixel (grayscale).

Sizing of Graphics

Most charts graphs and tables are one column wide (3 1/2 inches or 21 picas) or two-column width (7 1/16 inches, 43 picas wide). We recommend that you avoid sizing figures less than one column wide, as extreme enlargements may distort your images and result in poor reproduction. Therefore, it is better if the image is slightly larger, as a minor reduction in size should not have an adverse affect the quality of the image.

Size of Author Photographs

The final printed size of an author photograph is exactly 1 inch wide by 1 1/4 inches long (6 picas × 7 1/2 picas). Please ensure that the author photographs you submit are proportioned similarly. If the author's photograph does not appear at the end of the paper, then please size it so that it is proportional to the standard size of 1 9/16 inches wide by 2 inches long (9 1/2 picas × 12 picas). JPEG files are only accepted for author photos.

How to create a PostScript File

First, download a PostScript printer driver from http://www.adobe.com/support/downloads/pdrvwin.htm (for Windows) or from http://www.adobe.com/support/downloads/ pdrvmac.htm (for Macintosh) and install the "Generic PostScript Printer" definition. In *Word,* paste your figure into a new document. Print to a file using the PostScript printer driver. File names should be of the form "fig5.ps." Use Open Type fonts when creating your figures, if possible. A listing of the acceptable fonts are as follows: Open Type Fonts: Times Roman, Helvetica, Helvetica Narrow, Courier, Symbol, Palatino, Avant Garde, Bookman, Zapf Chancery, Zapf Dingbats, and New Century Schoolbook.

Print Color Graphics Requirements

IEEE accepts color graphics in the following formats: EPS, PS, TIFF, Word, PowerPoint, Excel, and PDF. The resolution of a RGB color TIFF file should be 400 dpi.

When sending color graphics, please supply a high quality hard copy or PDF proof of each image. If we cannot achieve a satisfactory color match using the electronic version of your files, we will have your hard copy scanned. Any of the files types you provide will be converted to RGB color EPS files.

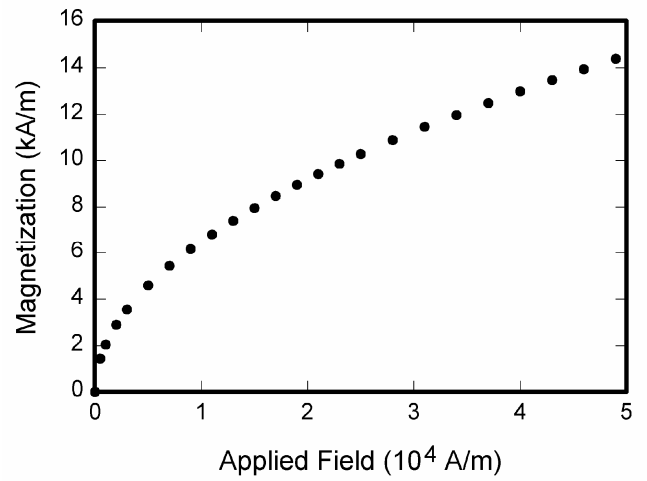

Fig. 1. Magnetization as a function of applied field. Note that "Fig." is abbreviated. There is a period after the figure number, followed by two spaces. It is good practice to explain the significance of the figure in the caption.

Web Color Graphics

IEEE accepts color graphics in the following formats: EPS, PS, TIFF, Word, PowerPoint, Excel, and PDF. The resolution of a RGB color TIFF file should be at least 400 dpi.

Your color graphic will be converted to grayscale if no separate grayscale file is provided. If a graphic is to appear in print as black and white, it should be saved and submitted as a black and white file. If a graphic is to appear in print or on IEEE Xplore in color, it should be submitted as RGB color.

Graphics Checker Tool

The IEEE Graphics Checker Tool enables users to check graphic files. The tool will check journal article graphic files against a set of rules for compliance with IEEE requirements. These requirements are designed to ensure sufficient image quality so they will look acceptable in print. After receiving a graphic or a set of graphics, the tool will check the files against a set of rules. A report will then be e-mailed listing each graphic and whether it met or failed to meet the requirements. If the file fails, a description of why and instructions on how to correct the problem will be sent. The IEEE Graphics Checker Tool is available at http://graphicsqc.ieee.org/

For more Information, contact the IEEE Graphics H-E-L-P Desk by e-mail at graphics@ieee.org. You will then receive an e-mail response and sometimes a request for a sample graphic for us to check.

E. Copyright Form

An IEEE copyright form should accompany your final submission. You can get a .pdf, .html, or .doc version at http://www.ieee.org/copyright. Authors are responsible for obtaining any security clearances.

TABLE I
UNITS FOR MAGNETIC PROPERTIES

Symbol	Quantity	Conversion from Gaussian and CGS EMU to SI [a]
Φ	magnetic flux	1 Mx $\rightarrow 10^{-8}$ Wb = 10^{-8} V·s
B	magnetic flux density, magnetic induction	1 G $\rightarrow 10^{-4}$ T = 10^{-4} Wb/m^2
H	magnetic field strength	1 Oe $\rightarrow 10^3/(4\pi)$ A/m
m	magnetic moment	1 erg/G = 1 emu $\rightarrow 10^{-3}$ A·m^2 = 10^{-3} J/T
M	magnetization	1 erg/(G·cm^3) = 1 emu/cm^3 $\rightarrow 10^3$ A/m
$4\pi M$	magnetization	1 G $\rightarrow 10^3/(4\pi)$ A/m
σ	specific magnetization	1 erg/(G·g) = 1 emu/g $\rightarrow$ 1 A·m^2/kg
j	magnetic dipole moment	1 erg/G = 1 emu $\rightarrow 4\pi \times 10^{-10}$ Wb·m
J	magnetic polarization	1 erg/(G·cm^3) = 1 emu/cm^3 $\rightarrow 4\pi \times 10^{-4}$ T
χ, κ	susceptibility	1 $\rightarrow 4\pi$
χ_ρ	mass susceptibility	1 cm^3/g $\rightarrow 4\pi \times 10^{-3}$ m^3/kg
μ	permeability	1 $\rightarrow 4\pi \times 10^{-7}$ H/m = $4\pi \times 10^{-7}$ Wb/(A·m)
μ_r	relative permeability	$\mu \rightarrow \mu_r$
w, W	energy density	1 erg/cm^3 $\rightarrow 10^{-1}$ J/m^3
N, D	demagnetizing factor	1 $\rightarrow 1/(4\pi)$

Vertical lines are optional in tables. Statements that serve as captions for the entire table do not need footnote letters.

[a]Gaussian units are the same as cgs emu for magnetostatics; Mx = maxwell, G = gauss, Oe = oersted; Wb = weber, V = volt, s = second, T = tesla, m = meter, A = ampere, J = joule, kg = kilogram, H = henry.

III. MATH

If you are using *Word,* use either the Microsoft Equation Editor or the *MathType* add-on (http://www.mathtype.com) for equations in your paper (Insert | Object | Create New | Microsoft Equation *or* MathType Equation). "Float over text" should *not* be selected.

IV. UNITS

Use either SI (MKS) or CGS as primary units. (SI units are strongly encouraged.) English units may be used as secondary units (in parentheses). **This applies to papers in data storage.** For example, write "15 Gb/cm^2 (100 Gb/in^2)." An exception is when English units are used as identifiers in trade, such as "3½-in disk drive." Avoid combining SI and CGS units, such as current in amperes and magnetic field in oersteds. This often leads to confusion because equations do not balance dimensionally. If you must use mixed units, clearly state the units for each quantity in an equation.

The SI unit for magnetic field strength H is A/m. However, if you wish to use units of T, either refer to magnetic flux density B or magnetic field strength symbolized as $\mu_0 H$. Use the center dot to separate compound units, e.g., "A·m^2."

V. Helpful Hints

A. Figures and Tables

Because IEEE will do the final formatting of your paper, you do not need to position figures and tables at the top and bottom of each column. In fact, all figures, figure captions, and tables can be at the end of the paper. Large figures and tables may span both columns. Place figure captions below the figures; place table titles above the tables. If your figure has two parts, include the labels "(a)" and "(b)" as part of the artwork. Please verify that the figures and tables you mention in the text actually exist. **Please do not include captions as part of the figures. Do not put captions in "text boxes" linked to the figures. Do not put borders around the outside of your figures.** Use the abbreviation "Fig." even at the beginning of a sentence. Do not abbreviate "Table." Tables are numbered with Roman numerals.

Color printing of figures is available, but is billed to the authors. Include a note with your final paper indicating that you request and will pay for color printing. Do not use color unless it is necessary for the proper interpretation of your figures. If you want reprints of your color article, the reprint order should be submitted promptly. There is an additional charge for color reprints. **Please note that many IEEE journals now allow an author to publish color figures on Xplore and black and white figures in print. Contact your society representative for specific requirements.**

Figure axis labels are often a source of confusion. Use words rather than symbols. As an example, write the quantity "Magnetization," or "Magnetization *M*," not just "*M*." Put units in parentheses. Do not label axes only with units. As in Fig. 1, for example, write "Magnetization (A/m)" or "Magnetization ($\mathrm{A \cdot m^{-1}}$)," not just "A/m." Do not label axes with a ratio of quantities and units. For example, write "Temperature (K)," not "Temperature/K."

Multipliers can be especially confusing. Write "Magnetization (kA/m)" or "Magnetization (10^3 A/m)." Do not write "Magnetization (A/m) × 1000" because the reader would not know whether the top axis label in Fig. 1 meant 16000 A/m or 0.016 A/m. Figure labels should be legible, approximately 8 to 12 point type.

B. References

Number citations consecutively in square brackets [1]. The sentence punctuation follows the brackets [2]. Multiple references [2], [3] are each numbered with separate brackets [1]–[3]. When citing a section in a book, please give the relevant page numbers [2]. In sentences, refer simply to the reference number, as in [3]. Do not use "Ref. [3]" or "reference [3]" except at the beginning of a sentence: "Reference [3] shows ... ." Please do not use automatic endnotes in *Word*, rather, type the reference list at the end of the paper using the "References" style.

Number footnotes separately in superscripts (Insert | Footnote).[1] Place the actual footnote at the bottom of the column in which it is cited; do not put footnotes in the reference list (endnotes). Use letters for table footnotes (see Table I).

Please note that the references at the end of this document are in the preferred referencing style. Give all authors' names; do not use "*et al*." unless there are six authors or more. Use a space after authors' initials. Papers that have not been published should be cited as "unpublished" [4]. Papers that have been accepted for publication, but not yet specified for an issue should be cited as "to be published" [5]. Papers that have been submitted for publication should be cited as "submitted for publication" [6]. Please give affiliations and addresses for private communications [7].

Capitalize only the first word in a paper title, except for proper nouns and element symbols. For papers published in translation journals, please give the English citation first, followed by the original foreign-language citation [8].

C. Abbreviations and Acronyms

Define abbreviations and acronyms the first time they are used in the text, even after they have already been defined in the abstract. Abbreviations such as IEEE, SI, ac, and dc do not have to be defined. Abbreviations that incorporate periods should not have spaces: write "C.N.R.S.," not "C. N. R. S." Do not use abbreviations in the title unless they are unavoidable (for example, "IEEE" in the title of this article).

D. Equations

Number equations consecutively with equation numbers in parentheses flush with the right margin, as in (1). First use the equation editor to create the equation. Then select the "Equation" markup style. Press the tab key and write the equation number in parentheses. To make your equations more compact, you may use the solidus (/), the exp function, or appropriate exponents. Use parentheses to avoid ambiguities in denominators. Punctuate equations when they are part of a sentence, as in

$$\int_0^{r_2} F(r,\varphi)\, dr\, d\varphi = [\sigma r_2 / (2\mu_0)] \cdot \int_0^{\infty} \exp(-\lambda\,|z_j - z_i|)\, \lambda^{-1} J_1(\lambda r_2)\, J_0(\lambda r_i)\, d\lambda . \quad (1)$$

Be sure that the symbols in your equation have been defined before the equation appears or immediately following. Italicize symbols (*T* might refer to temperature,

[1]It is recommended that footnotes be avoided (except for the unnumbered footnote with the receipt date on the first page). Instead, try to integrate the footnote information into the text.

but T is the unit tesla). Refer to "(1)," not "Eq. (1)" or "equation (1)," except at the beginning of a sentence: "Equation (1) is ... ."

E. Other Recommendations

Use one space after periods and colons. Hyphenate complex modifiers: "zero-field-cooled magnetization." Avoid dangling participles, such as, "Using (1), the potential was calculated." [It is not clear who or what used (1).] Write instead, "The potential was calculated by using (1)," or "Using (1), we calculated the potential."

Use a zero before decimal points: "0.25," not ".25." Use "cm^3," not "cc." Indicate sample dimensions as "0.1 cm × 0.2 cm," not "0.1 × 0.2 cm^2." The abbreviation for "seconds" is "s," not "sec." Do not mix complete spellings and abbreviations of units: use "Wb/m^2" or "webers per square meter," not "webers/m^2." When expressing a range of values, write "7 to 9" or "7-9," not "7~9."

A parenthetical statement at the end of a sentence is punctuated outside of the closing parenthesis (like this). (A parenthetical sentence is punctuated within the parentheses.) In American English, periods and commas are within quotation marks, like "this period." Other punctuation is "outside"! Avoid contractions; for example, write "do not" instead of "don't." The serial comma is preferred: "A, B, and C" instead of "A, B and C."

If you wish, you may write in the first person singular or plural and use the active voice ("I observed that ..." or "We observed that ..." instead of "It was observed that ..."). Remember to check spelling. If your native language is not English, please get a native English-speaking colleague to carefully proofread your paper.

VI. Some Common Mistakes

The word "data" is plural, not singular. The subscript for the permeability of vacuum μ_0 is zero, not a lowercase letter "o." The term for residual magnetization is "remanence"; the adjective is "remanent"; do not write "remnance" or "remnant." Use the word "micrometer" instead of "micron." A graph within a graph is an "inset," not an "insert." The word "alternatively" is preferred to the word "alternately" (unless you really mean something that alternates). Use the word "whereas" instead of "while" (unless you are referring to simultaneous events). Do not use the word "essentially" to mean "approximately" or "effectively." Do not use the word "issue" as a euphemism for "problem." When compositions are not specified, separate chemical symbols by en-dashes; for example, "NiMn" indicates the intermetallic compound $Ni_{0.5}Mn_{0.5}$ whereas "Ni–Mn" indicates an alloy of some composition Ni_xMn_{1-x}.

Be aware of the different meanings of the homophones "affect" (usually a verb) and "effect" (usually a noun), "complement" and "compliment," "discreet" and "discrete," "principal" (e.g., "principal investigator") and "principle" (e.g., "principle of measurement"). Do not confuse "imply" and "infer."

Prefixes such as "non," "sub," "micro," "multi," and "ultra" are not independent words; they should be joined to the words they modify, usually without a hyphen. There is no period after the "et" in the Latin abbreviation "*et al.*" (it is also italicized). The abbreviation "i.e.," means "that is," and the abbreviation "e.g.," means "for example" (these abbreviations are not italicized).

An excellent style manual and source of information for science writers is [9]. A general IEEE style guide and an *Information for Authors* are both available at http://www.ieee.org/web/publications/authors/transjnl/index.html

VII. Editorial Policy

Submission of a manuscript is not required for participation in a conference. Do not submit a reworked version of a paper you have submitted or published elsewhere. Do not publish "preliminary" data or results. The submitting author is responsible for obtaining agreement of all coauthors and any consent required from sponsors before submitting a paper. IEEE Transactions and Journals strongly discourage courtesy authorship. It is the obligation of the authors to cite relevant prior work.

The Transactions and Journals Department does not publish conference records or proceedings. The Transactions does publish papers related to conferences that have been recommended for publication on the basis of peer review. As a matter of convenience and service to the technical community, these topical papers are collected and published in one issue of the Transactions.

At least two reviews are required for every paper submitted. For conference-related papers, the decision to accept or reject a paper is made by the conference editors and publications committee; the recommendations of the referees are advisory only. Undecipherable English is a valid reason for rejection. Authors of rejected papers may revise and resubmit them to the Transactions as regular papers, whereupon they will be reviewed by two new referees.

VIII. Publication Principles

The contents of IEEE Transactions and Journals are peer-reviewed and archival. The Transactions publishes scholarly articles of archival value as well as tutorial expositions and critical reviews of classical subjects and topics of current interest.

Authors should consider the following points:

1) Technical papers submitted for publication must advance the state of knowledge and must cite relevant prior work.
2) The length of a submitted paper should be commensurate with the importance, or appropriate to

the complexity, of the work. For example, an obvious extension of previously published work might not be appropriate for publication or might be adequately treated in just a few pages.

3) Authors must convince both peer reviewers and the editors of the scientific and technical merit of a paper; the standards of proof are higher when extraordinary or unexpected results are reported.
4) Because replication is required for scientific progress, papers submitted for publication must provide sufficient information to allow readers to perform similar experiments or calculations and use the reported results. Although not everything need be disclosed, a paper must contain new, useable, and fully described information. For example, a specimen's chemical composition need not be reported if the main purpose of a paper is to introduce a new measurement technique. Authors should expect to be challenged by reviewers if the results are not supported by adequate data and critical details.
5) Papers that describe ongoing work or announce the latest technical achievement, which are suitable for presentation at a professional conference, may not be appropriate for publication in a TRANSACTIONS or JOURNAL.

IX. CONCLUSION

A conclusion section is not required. Although a conclusion may review the main points of the paper, do not replicate the abstract as the conclusion. A conclusion might elaborate on the importance of the work or suggest applications and extensions.

APPENDIX

Appendixes, if needed, appear before the acknowledgment.

ACKNOWLEDGMENT

The preferred spelling of the word "acknowledgment" in American English is without an "e" after the "g." Use the singular heading even if you have many acknowledgments. Avoid expressions such as "One of us (S.B.A.) would like to thank ... ." Instead, write "F. A. Author thanks ... ." **Sponsor and financial support acknowledgments are placed in the unnumbered footnote on the first page, not here.**

REFERENCES

[1] G. O. Young, "Synthetic structure of industrial plastics (Book style with paper title and editor)," in *Plastics*, 2nd ed. vol. 3, J. Peters, Ed. New York: McGraw-Hill, 1964, pp. 15–64.

[2] W.-K. Chen, *Linear Networks and Systems* (Book style). Belmont, CA: Wadsworth, 1993, pp. 123–135.

[3] H. Poor, *An Introduction to Signal Detection and Estimation*. New York: Springer-Verlag, 1985, ch. 4.

[4] B. Smith, "An approach to graphs of linear forms (Unpublished work style)," unpublished.

[5] E. H. Miller, "A note on reflector arrays (Periodical style—Accepted for publication)," *IEEE Trans. Antennas Propagat.*, to be published.

[6] J. Wang, "Fundamentals of erbium-doped fiber amplifiers arrays (Periodical style—Submitted for publication)," *IEEE J. Quantum Electron.*, submitted for publication.

[7] C. J. Kaufman, Rocky Mountain Research Lab., Boulder, CO, private communication, May 1995.

[8] Y. Yorozu, M. Hirano, K. Oka, and Y. Tagawa, "Electron spectroscopy studies on magneto-optical media and plastic substrate interfaces (Translation Journals style)," *IEEE Transl. J. Magn.Jpn.*, vol. 2, Aug. 1987, pp. 740–741 [*Dig. 9th Annu. Conf. Magnetics* Japan, 1982, p. 301].

[9] M. Young, *The Techincal Writers Handbook.* Mill Valley, CA: University Science, 1989.

[10] J. U. Duncombe, "Infrared navigation—Part I: An assessment of feasibility (Periodical style)," *IEEE Trans. Electron Devices*, vol. ED-11, pp. 34–39, Jan. 1959.

[11] S. Chen, B. Mulgrew, and P. M. Grant, "A clustering technique for digital communications channel equalization using radial basis function networks," *IEEE Trans. Neural Networks*, vol. 4, pp. 570–578, Jul. 1993.

[12] R. W. Lucky, "Automatic equalization for digital communication," *Bell Syst. Tech. J.*, vol. 44, no. 4, pp. 547–588, Apr. 1965.

[13] S. P. Bingulac, "On the compatibility of adaptive controllers (Published Conference Proceedings style)," in *Proc. 4th Annu. Allerton Conf. Circuits and Systems Theory*, New York, 1994, pp. 8–16.

[14] G. R. Faulhaber, "Design of service systems with priority reservation," in *Conf. Rec. 1995 IEEE Int. Conf. Communications,* pp. 3–8.

[15] W. D. Doyle, "Magnetization reversal in films with biaxial anisotropy," in *1987 Proc. INTERMAG Conf.*, pp. 2.2-1–2.2-6.

[16] G. W. Juette and L. E. Zeffanella, "Radio noise currents n short sections on bundle conductors (Presented Conference Paper style)," presented at the IEEE Summer power Meeting, Dallas, TX, Jun. 22–27, 1990, Paper 90 SM 690-0 PWRS.

[17] J. G. Kreifeldt, "An analysis of surface-detected EMG as an amplitude-modulated noise," presented at the 1989 Int. Conf. Medicine and Biological Engineering, Chicago, IL.

[18] J. Williams, "Narrow-band analyzer (Thesis or Dissertation style)," Ph.D. dissertation, Dept. Elect. Eng., Harvard Univ., Cambridge, MA, 1993.

[19] N. Kawasaki, "Parametric study of thermal and chemical nonequilibrium nozzle flow," M.S. thesis, Dept. Electron. Eng., Osaka Univ., Osaka, Japan, 1993.

[20] J. P. Wilkinson, "Nonlinear resonant circuit devices (Patent style)," U.S. Patent 3 624 12, July 16, 1990.

[21] *IEEE Criteria for Class IE Electric Systems* (Standards style), IEEE Standard 308, 1969.

[22] *Letter Symbols for Quantities*, ANSI Standard Y10.5-1968.

[23] R. E. Haskell and C. T. Case, "Transient signal propagation in lossless isotropic plasmas (Report style)," USAF Cambridge Res. Lab., Cambridge, MA Rep. ARCRL-66-234 (II), 1994, vol. 2.

[24] E. E. Reber, R. L. Michell, and C. J. Carter, "Oxygen absorption in the Earth's atmosphere," Aerospace Corp., Los Angeles, CA, Tech. Rep. TR-0200 (420-46)-3, Nov. 1988.

[25] (Handbook style) *Transmission Systems for Communications,* 3rd ed., Western Electric Co., Winston-Salem, NC, 1985, pp. 44–60.

[26] *Motorola Semiconductor Data Manual,* Motorola Semiconductor Products Inc., Phoenix, AZ, 1989.

[27] (Basic Book/Monograph Online Sources) J. K. Author. (year, month, day). *Title* (edition) [Type of medium]. Volume (issue). Available: http://www.(URL)

[28] J. Jones. (1991, May 10). Networks (2nd ed.) [Online]. Available: http://www.atm.com

[29] (Journal Online Sources style) K. Author. (year, month). Title. *Journal* [Type of medium]. Volume(issue), paging if given. Available: http://www.(URL)
[30] R. J. Vidmar. (1992, August). On the use of atmospheric plasmas as electromagnetic reflectors. *IEEE Trans. Plasma Sci.* [Online]. *21(3).* pp. 876–880. Available: http://www.halcyon.com/pub/journals/21ps03-vidmar

First A. Author (M'76–SM'81–F'87) and the other authors may include biographies at the end of regular papers. Biographies are often not included in conference-related papers. This author became a Member (M) of IEEE in 1976, a Senior Member (SM) in 1981, and a Fellow (F) in 1987. The first paragraph may contain a place and/or date of birth (list place, then date). Next, the author's educational background is listed. The degrees should be listed with type of degree in what field, which institution, city, state, and country, and year degree was earned. The author's major field of study should be lower-cased.

The second paragraph uses the pronoun of the person (he or she) and not the author's last name. It lists military and work experience, including summer and fellowship jobs. Job titles are capitalized. The current job must have a location; previous positions may be listed without one. Information concerning previous publications may be included. Try not to list more than three books or published articles. The format for listing publishers of a book within the biography is: title of book (city, state: publisher name, year) similar to a reference. Current and previous research interests end the paragraph.

The third paragraph begins with the author's title and last name (e.g., Dr. Smith, Prof. Jones, Mr. Kajor, Ms. Hunter). List any memberships in professional societies other than the IEEE. Finally, list any awards and work for IEEE committees and publications. If a photograph is provided, the biography will be indented around it. The photograph is placed at the top left of the biography. Personal hobbies will be deleted from the biography.

Camera-ready was prepared in Kharkov National University of Radio Electronics
Approved for publication: 27.03.2015. Format 60×84 1/8.
Relative printer's sheets: 8,2. Circulation: 300 copies.
Published by SPD FL Stepanov V.V.
Lenin Ave, 14, Kharkov, 61166, Ukraine

Рекомендовано Вченою радою Харківського національного
університету радіоелектроніки (протокол № 7 від 27.03.2015)
Підписано до друку 27.03.2015. Формат 60×841/8.
Умов. друк. арк. 8,2. Тираж 300 прим. Ціна договірна.
Віддруковано у ФОП Степанов В.В.
61166, Харків, просп. Леніна, 14.